12-2010

NOVEL CONSTITUTIVELY ACTIVE POINT MUTATIONS IN THE NH2 DOMAIN OF CXCR2 CAPTURE THE RECEPTOR IN DIFFERENT ACTIVATION STATES

Giljun Park
The University of Tennessee, Knoxville, gpark1@utk.edu

To the Graduate Council:

I am submitting herewith a dissertation written by Giljun Park entitled "NOVEL CONSTITUTIVELY ACTIVE POINT MUTATIONS IN THE NH2 DOMAIN OF CXCR2 CAPTURE THE RECEPTOR IN DIFFERENT ACTIVATION STATES." I have examined the final electronic copy of this dissertation for form and content and recommend that it be accepted in partial fulfillment of the requirements for the degree of Doctor of Philosophy, with a major in Microbiology.

Tim E. Sparer, Major Professor

We have read this dissertation and recommend its acceptance:

Jeffrey Becker, Elias Fernandez, Todd Reynolds and Thandi Onami

Accepted for the Council:

Carolyn R. Hodges

Vice Provost and Dean of the Graduate School

(Original signatures are on file with official student records.)

To the Graduate Council:

I am submitting here with a dissertation written by Giljun Park entitled “Novel constitutively active point mutations in the NH2 domain of CXCR2 capture the receptor in different activation states.” I have examined the final electronic copy of this dissertation for form and content and recommend that it be accepted in partial fulfillment of the requirements for the degree of Doctor of Philosophy, with a major in Microbiology.

Tim Sparer

Major Professor

We have read this dissertation
and recommend its acceptance:

Jeffry M. Becker

Thandi Onami

Todd Reynolds

Elias Fernandez

Accepted for the Council:

Carolyn R. Hodges

Vice Provost and Dean of the
Graduate School

(Original signatures are on file with official student records)

NOVEL CONSTITUTIVELY ACTIVE POINT MUTATIONS IN THE NH2 DOMAIN OF CXCR2 CAPTURE THE RECEPTOR IN DIFFERENT ACTIVATION STATES

A Dissertation

Presented for the

Doctor of Philosophy

Degree

The University of Tennessee, Knoxville

Giljun Park

December 2010

DEDICATION

I would like to dedicate this dissertation to my parents, Woong-yeol Park and Kyung-ae Kim, and to my parents in-law, Jin-gun Kim and Jung-ae Park, who stood by me, supported me and pray for me all the times.

I would also like to dedicate this work to my lovely wife, heejung, daughter, Joomin, and son, Joovin for all the support and encouragement they gave me. Without their love, I could never have completed this work.

ACKNOWLEDGEMENT

I am most grateful to Professor Tim Sparer for the privilege and opportunity to work in his laboratory and wish to thank him for the advice and encouragement based on his distinguished scientific insight and knowledge. It was really a great journey to work for such an enthusiastic scientist and real teacher. I am also thankful that he was so patient during the times I was struggling with problems. I am grateful to work for you. I would like to appreciate to my committee members: Dr. Jeffrey Becker, Dr. Elias Fernandez, Dr. Todd Reynolds and Dr. Thandi Onami for their suggestions, critical reviews and guidance during my studies. I also would like to thank to Dr. Tom Masi for his support and valuable ideas on critical decisions throughout these studies.

In addition I wish to thank all my colleagues in Dr. Sparer’s laboratory. They are always kind and warm. I want to thank Dr. Mindy Miller-Kittrell and Dr. Jinho Heo for sharing a wonderful life in the lab for a long time. Also, I want to thank all other Sparerians: Haeryoung Kown, Faith Baumann, Courtney Copeland, and Holly Saito for their help and making me laugh everyday.

Finally I want to thank to my family in Korea, Heejung, Joomin and joovin, and member of Korean church of Knoxville for all the support that they gave me during all these years.

ABSTRACT

Chemokines are structurally and functionally related 8-10 kDa proteins defined by four conserved cysteine residues. They consist of a superfamily of proinflammatory mediators that promote the recruitment of various kinds of leukocytes and other cell types through binding to their respective chemokine receptor, a member of the GPCR family. Abnormal control of this system results in various diseases including tumorigenesis and cancer metastasis. Deregulation can occur when constitutively active mutant (CAM) chemokine receptors are locked in the "on" position. This can lead to cellular transformation/tumorigenesis. A viral CAM receptor, ORF74, that can cause tumors in humans, also has homology to human CXC chemokine receptor 2 (CXCR2), which is a G-protein-coupled receptor (GPCR) expressed on neutrophils, some monocytes, endothelial cells, and some epithelial cells. CXCR2 activation with ELR+ CXC chemokines induces leukocyte migration, trafficking, cellular differentiation, angiogenesis and cellular transformation. Using a high throughput yeast screen we identified a novel point mutation, D9H, in CXCR2, which leads to constitutive activation (CA). Generation of positively charged substitutions, D9K and D9R, and D143V as a positive control resulted in CA CXCR2 with differential levels of cellular transformation. To further investigate how D9 mutations lead to differential CA, we used inhibitors of known signal transduction pathways. Pertusiss toxin (PTX) sensitivity in foci formation assays demonstrated that D9R uses the G_i subunit like WTCXCR2 and D143V, while D9H and D9K do not. All

CA receptors use the JAK pathway based on sensitivity to the inhibitor, AG490. Phosphorylation of PLC-beta 3 and sensitivity to the PLC-beta 3 inhibitor, U73122, implicates that mutant receptors such as D143V, D9H, D9K, and D9R utilize the $G_{q/11}$ subunit. Interestingly, D9R use both G_i and $G_{q/11}$ subunits. All of the CA receptors induced phosphorylation of the epidermal growth factor receptor (EGFR) indicating a transactivation between CXCR2 and EGFR. These data describe two novel and important findings. First, N-terminal CXCR2 controls activation and signaling using multiple G protein subunits to elicit downstream signaling. Second, our work supports the "functional selectivity" model for GPCR activation. That is, mimicking agonist activation, CA CXCR2 receptors have multiple conformational states that lead to differential activation.

TABLE OF CONTENTS

List of Tables

List of Figures

PART I. GENERAL INTRODUCTION

CHAPTER 1. G PROTEIN-COUPLED RECEPTORS

An Overview

Since the structure of the G-protein coupled receptor (GPCR), rhodopsin was crystallized and solved [1] [2], technological advances have expanded the structure and function of GPCR superfamilies. Also, the number of identified GPCRs has grown rapidly and now consists of nearly 1,500 unique full-length members [3-5]. GPCRs are one of the largest and most diverse groups of proteins in the human genome [4, 6]. These proteins can bind to a broad range of exogenous stimuli including light, odor, and taste [6, 7], as well as endogenous ligands including peptides and hormones (e.g. angiotensin, bradykinin, endothelin, and melanocortin), biogenic amines (e.g. adrenaline, dopamine, histamine, and serotonin), nucleosides and nucleotides (e.g. adenosine, adenosine triphosphate, and uridine triphosphate), peptide pheromones (e.g. alpha-factor and a-factor in a variety of fungi), and lipids and eicosanoids (e.g. cannabinoids, leukotrienes, prostaglandins, and thromboxanes) [8] (Table 1 and Figure 1).

GPCRs play an important role as a physical conduit of extracellular signals across the cellular membrane inducing complex biological processes and function through intracellular heterotrimeric G proteins [9-11]. G proteins are comprised of non-identical α (~33-35 kDa), β (~35 kDa), and γ (~15 kDa) subunits [5].

Class: A Rhodopsin-like receptors	
Family I	Olfactory receptors, adenosine receptors, melanocortin receptors, and others
Family II	Biogenic amine receptors
Family III	Vertebrate opsins and neuropeptide receptors
Family IV	Invertebrate opsins
Family V	Chemokine, chemotactic, somatostatin, opioids and others
Family VI	Melatonin receptors and others
Class B: Calcitonin and related receptors	
Family I	Calcitonin and calcitonin-like receptors
Family II	PTH/PTHrP receptors
Family III	Glucagon, secretin receptors and others
Family IV	Latrotoxin receptors and others
Class C: Metabotropic glutamate and related receptors	
Family I	Metabotropic glutamate receptors
Family II	Calcium receptors
Family II	GABAb receptors
Family IV	Putative pheromone receptors
Class D: STE2 pheromone receptors	
Class E: STE3 pheromone receptors	
Class F: cAMP and archaebacterial opsin receptors	

Table 1. Sequence-based groupings within the G-protein-coupled receptors

Abbreviation: PTH, Parathyroid hormone receptor; PTHrP, Parathyroid hormone related peptide receptor; GABAb, γ-Aminobutyric acid receptor
Modified from Flower et al [12].

Figure 1. Classification and diversity of GPCRs.

Class A GPCRs are characterized by several highly conserved amino acids in the TMs and there is usually a disulfide bridge linking extracellular loops 1 and 2. Most of the class A receptors have a palmitoylated cysteine residue in the intracellular C-terminal tail. The binding sites of the endogenous small-molecule hormone ligands of class A GPCRs are located within the 7 TM bundle (A-1, the ligand binding site is indicated in orange). For peptide and glycoprotein hormone receptors (A-2 and A-3, respectively), binding occurs at the N terminus, the extracellular loop segments and the extracellular domains of the TM helices. Class B GPCRs contain a relatively long N-terminal tail (B). The class B receptors show a number of conserved proline residues within the TMs. The majority of class C receptors are characterized by very large N- and C-terminal tails, a disulfide bridge connecting the first and second extracellular loops, together with a very short and well-conserved third intracellular loop (C). A number of the highly conserved residues of class A GPCRs are also strongly conserved in class C GPCRs. The ligand binding site is located in the N-terminal domain, which is composed of the so-called venus flytrap (VFT, gray color filled region) module that shares sequence similarity with bacterial periplasmic amino acid binding proteins. In all class C GPCRs except the GABAb receptor, a cysteine-rich domain (CRD), which contains nine conserved cysteine residues, links the VFT to the 7 TM domain.

Modified from Jacoby et al [13].

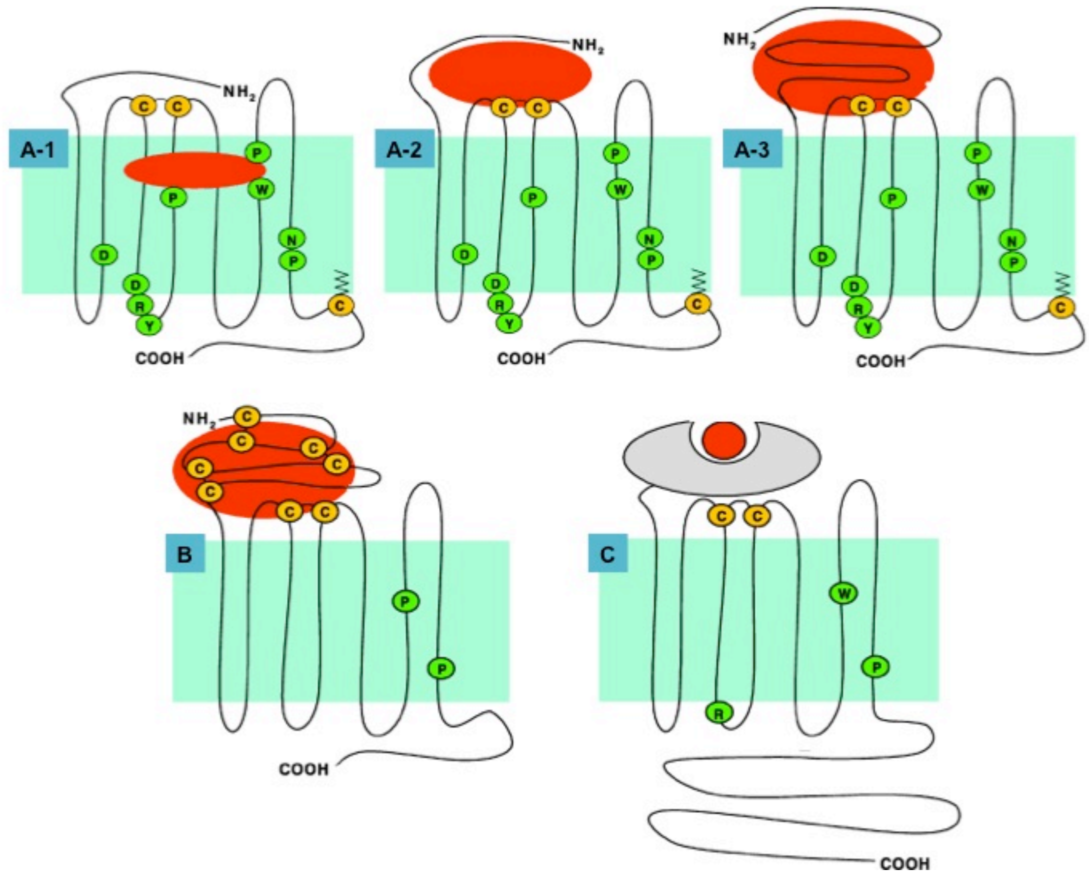
A-1
A-2
A-3
B
C
NH2
COOH
C
D
R
Y
P
W
N

Mammalian G proteins are comprised of one of 17 α-subunits combined with one of 5 β-subunits and one of 12 γ-subunits, which provides an extraordinary combinatorial potential for inducing signal transduction pathways [5, 14] (Table 2).

The common structural features of GPCRs are seven transmembrane (TM)-spanning α-helical domains, an extracellular N-terminus, an intracellular C-terminus, and three loops on each side of the membrane [9]. Interaction of the GPCRs with their ligands causes a conformational alteration, which induces the dissociation of the G protein α-subunit from the GPCR and the βγ-subunit leading to the exchange of GDP with GTP [15, 16]. Activation of the G proteins transmits a signal through effectors, such as adenylyl cyclase and phospholipase Cβ [5] (Table 3).

Because of the high degree of selectivity and sensitivity between GPCRs and their ligands, they function as key modulators for complex biological processes such as neurotransmission, hormone and enzyme release from endocrine and exocrine glands, immune responses, cardiac- and smooth-muscle contraction and blood pressure regulation. Malfunction of GPCR mediated processes can lead to a variety of disorders including cancer development and progression [17-19]. Considering the broad range of GPCR-modulated biological processes, GPCRs are attractive drug targets for pharmaceutical companies. In fact, they are the top target proteins for pharmaceutical discovery programs [20].

Table 2. The class and subunits of heterotrimeric G proteins, gene names and localization in mammalian cells.

G protein	Gene	Localization
Gα-subunits		
1. Gα $_{i/o}$ class		
$G\alpha_{i1}$	*Gnai1*	Widely distributed
$G\alpha_{i2}$	*Gnai2*	Ubiquitous
$G\alpha_{i3}$	*Gnai3*	Widely distributed
$G\alpha_{o}$	*Gnao*	Neuronal, neuroendocrine
$G\alpha_{z}$	*Gnaz*	Neuronal, platelets
$G\alpha_{gust}$	*Gnag*	Taste cells, brush cells
$G\alpha_{t1}$	*Gnat1*	Retinal rods, taste cels
$G\alpha_{t2}$	*Gnat2*	Retinal cones, stem cells
2. Gα $_{q/11}$ class		
$G\alpha_{q}$	*Gnaq*	Ubiquitous
$G\alpha_{11}$	*Gna11*	Ubiquitous
$G\alpha_{14}$	*Gna14*	Kidney, lung, spleen
$G\alpha_{15/16}$	*Gna15*	Haematopoietic cells
3. Gα $_{s}$ class		
$G\alpha_{s}$	*Gnas*	Ubiquitous
$G\alpha_{s}$XL	*Gnasxl*	Neuroendocrine
$G\alpha_{olf}$	*Gnal*	Olfactory epithelium, brain
4. Gα $_{12/13}$ class		
$G\alpha_{12}$	*Gna12*	Ubiquitous
$G\alpha_{13}$	*Gna13*	Ubiquitous

to be continued on the next page

Table 2-continued. The class and subunits of heterotrimeric G proteins, gene names and localization in mammalian cells.

G protein	Gene	Localization
Gβ-subunits		
Gβ	*Gnb1*	Widely, retinal rods
Gβ2	*Gnb2*	Widely distributed
Gβ3	*Gnb3*	Widely, retinal cones
Gβ4	*Gnb4*	Widely distributed
Gβ5	*Gnb5*	Primarily brain
Gγ-subunits		
Gγ 1, Gγ rod	*Gngt1*	Retinal rods, brain
Gγ 14, Gγ cone	*Gngt2*	Retinal cones, brain
Gγ 2, Gγ 6	*Gng2*	Widely distributed
Gγ 3	*Gng3*	Brain, blood
Gγ 4	*Gng4*	Brain, other tissues
Gγ 5	*Gng5*	Widely distributed
Gγ 7	*Gng7*	Widely distributed
Gγ 8, Gγ 9	*Gng8*	Widely distributed
Gγ 10	*Gng10*	Widely distributed
Gγ 11	*Gng11*	Widely distributed
Gγ 12	*Gng12*	Widely distributed
Gγ 13	*Gng13*	Taste buds

Modified from Malbon [5]

Table 3. Heterotrimeric G-protein subunits and their functions.

G proteins	Effectors	Function
Gα subunits		
$G\alpha_{i1}$	Adenylyl cyclase	Inhibition
$G\alpha_{i2}$	Adenylyl cyclase	Inhibition
$G\alpha_{i3}$	Adenylyl cyclase	Inhibition
$G\alpha_{oAB}$	Adenylyl cyclase	Inhibition
$G\alpha_{z}$	Adenylyl cyclase	Inhibition
$G\alpha_{t1}$	Phosphodiesterase	Activation
$G\alpha_{t2}$	Phosphodiesterase	Activation
$G\alpha_{gust}$	Phosphodiesterase	Activation
$G\alpha_{s}$	Adenynyl cyclase	Stimulation
$G\alpha_{olf}$	Adenynyl cyclase (olfactory)	Stimulation
$G\alpha_{sXL}$	Adenynyl cyclase	Stimulation
$G\alpha_{q}$	Phospholipase Cβ	Stimulation
$G\alpha_{11}$	Phospholipase Cβ	Stimulation
$G\alpha_{14\text{-}16}$	Phospholipase Cβ	Stimulation
$G\alpha_{12}$	Rho guanine nucleotide-exchange factors	Stimulation
$G\alpha_{13}$	Rho guanine nucleotide-exchange factors	Stimulation
Gβ subunits		
$G\beta_{1\text{-}5}$	Adenynyl cyclase	Inhibition
	$Ca^{+}$and K^{+} channel	Stimulation
	Phosphatidylinisitol 3-kinase	Stimulation
	GRK2 and GRK3	Recruitment
	Phospholipase Cβ	Stimulation
Gγ subunits		
$G\gamma_{1\text{-}12}$	Adenynyl cyclase	Inhibition
	$Ca^{+}$and K^{+} channel	Stimulation
	Phosphoinisitol 3-phosphate kinase	Stimulation
	GRK2 and GRK3	Recruitment
	Phospholipase Cβ	Stimulation

Abbreviation: GRK, G-protein receptor kinase. Modified from Malbon [5].

Currently GPCRs are the molecular targets of about 30% of all marketed drugs, 50% of all modern prescription drugs, and 25% of the top-selling drugs [13, 21, 22]. Moreover only approximately 30% of all known GPCRs, mainly in the biogenic amine family (a subfamily of class 1 GPCRs), have been targeted with drugs. However, many novel GPCRs have been reported as 'orphan' receptors because their function and endogenous ligands are still unknown [21, 23, 24]. Research on GPCRs could potentially contribute to our understanding and eventually contribute to the development of treatments for diseases involving GPCRs.

GPCR ACTIVATION

GPCR activation is induced by a variety of ligands [4, 8]. The focus of GPCR research is the identification of the binding domains for ligands using genetic, biochemical, and biophysical techniques. For understanding the structure-function relationship between GPCRs and their ligands, molecular techniques such as site-directed or random mutagenesis, domain swapping, and the use of labeled probes have been used to identify the important residues and domains [25]. The binding sites of endogenous "small-molecule" ligands in family 1 receptors, such as for the retinal chromophore in rhodopsin and catecholamines in the adrenergic receptors have well characterized receptor-binding domains [26-28]. Recent studies on the binding domains of peptide receptors such as the receptors for angiotensin [29-31], parathyroid hormone [32, 33], secretin [34], bradykinin B2 [35, 36], gonadotropin-releasing hormone [37], opioids [38, 39], neurokinin (NK) [40, 41], vasopressin/oxytosin [42-44], cholecystokin/gastrin [45, 46], and neurotensin 1 [47] have been extended into other classes of GPCRs. Although there are some common features among ligands, there are a variety of unique interactions between GPCRs and their cognate ligands. For instance, large ligands, including proteins, bind to extracellular loops, whereas small molecules ligands, such as pharmacological agents, bind within the TM region of GPCRs (Figure 1). Peptides ligands present a combination of the two processes. The peptides primarily bind to the extracellular loops and part of the ligand may penetrate into the transmembrane region at the same time and interact with residues buried within the lipid bilayer [48-51].

Before the crystal structure of ligand-activated human β_2 adrenergic receptor (β_2AR) was solved [52], simplistic models were generated where GPCRs were simple binary switches that could be in either an inactive and active forms. However, GPCRs are no longer considered simple ON/OFF switches. Instead they are more like rheostats that are dynamic and assume many different conformations [53, 54]. Recently, multi-state models suggest that GPCRs spontaneously shift between multiple active and inactive conformations in order to explain their complex GPCR activation states [55, 56]. The 5-HT$_2$-serotonin receptors [57] α_{2A}-adrenoceptors [58], AT$_1$ receptor [59], gonadotropin-releasing hormone receptors [60], μ-opioid receptors [61] and many others have different receptor conformations supporting the multi-state model. Based on the multi-state model, the concept of ‘functional selectivity,’ ‘agonist-directed trafficking’, or ‘biased agonism’ have been used to describe how different ligands for a specific receptor can induce different conformations of the receptor [62]. Recently, the these different terms have been narrowed to either ‘functional selectivity’ or ‘ligand-induced differential signaling’ to describe this phenomenon [63].

In addition to functional selectivity, ‘ligand efficacy’ addresses the complex functional behavior of GPCRs. Ligand efficacy is used to describe the effect of a ligand on the structure and biophysical properties of a receptor [55]. Natural and synthetic ligands can be divided into four different efficacy classes: ‘full agonists’ are able to maximally activate the receptor; ‘partial agonists’ induce submaximal activation even at saturating concentrations; ‘neutral antagonists’ show no effect on signaling activity but can prevent other ligands from binding to the receptor; ‘inverse agonist’ decrease basal or constitutive activity [55].

GPCR Signaling

Initially, G proteins were described as guanine-nucleotide regulatory proteins that functionally link the receptor with effectors. The initial description of G proteins was glucagon stimulation of adenylyl cyclase through the secondary effector cyclic AMP in rat liver cells [64]. The G protein, G_s, was purified and shown to be a heterotrimeric structure, composed of a α, β, and γ subunit [65, 66]. Each of these subunits are comprised of 17 α subunits, 5 β subunits, and 12 γ subunits [5]. The α subunit is GDP-bound and forms a complex with one β subunit and one γ subunit, which functionally dissociate from the βγ complex when it binds GTP. Mostly the α subunit is the active form when it is bound to

GTP and regulates the activity of downstream effectors [15]. Commonly, G proteins are designated by their α subunit, which means the G_s heterotrimeric complex includes $G\alpha_s$; G_q includes $G\alpha_q$; G_i includes $G\alpha_i$; and so on. The four major α subunit subfamilies are $G\alpha_s$, $G\alpha_i$, $G\alpha_q$, and $G\alpha_{12}$. $G\alpha_s$ is activated by a large group of GPCRs and stimulates adenylyl cyclase, which induces the synthesis of cyclic AMP from ATP. In contrast to G_s, $G\alpha_i$ inhibits adenylyl cyclase actitivity. $G\alpha_q$ activates phospholipase Cβ and $G\alpha_{12}$ activates Rho-Guanine-Nucleotide Exchange Factors (GEFs) [5, 67] (Figure 2). Pertussis toxin (PTX) was the first tool for characterizing G-protein-dependent signaling processes. PTX specifically inactivates all members of the $G\alpha_i$ family of G proteins ($G\alpha_{i1}$, $G\alpha_{i2}$, $G\alpha_{i3}$, $G\alpha_{oA}$, $G\alpha_{oB}$, $G\alpha_{t1}$, $G\alpha_{t2}$ and $G\alpha_z$). All other G proteins are insensitive to PTX [67]. PTX catalyses the ADP-ribosylation of a conserved arginine residue (Arg-178 in $G\alpha_{i1}$, Arg-201 in $G\alpha_s$ and Arg-174 in $G\alpha_t$) on Gα proteins resulting in inhibition of both GTPase activity and its interaction with Gβγ (Table 3) [68-70].

In addition to Gα subunits, the Gβγ dimer itself also has an ability to induce signal transduction pathways modulating its own set of effectors, such as phospholipase Cβ, adenylyl cyclase, and K+ channels [71-76] (Table 3).

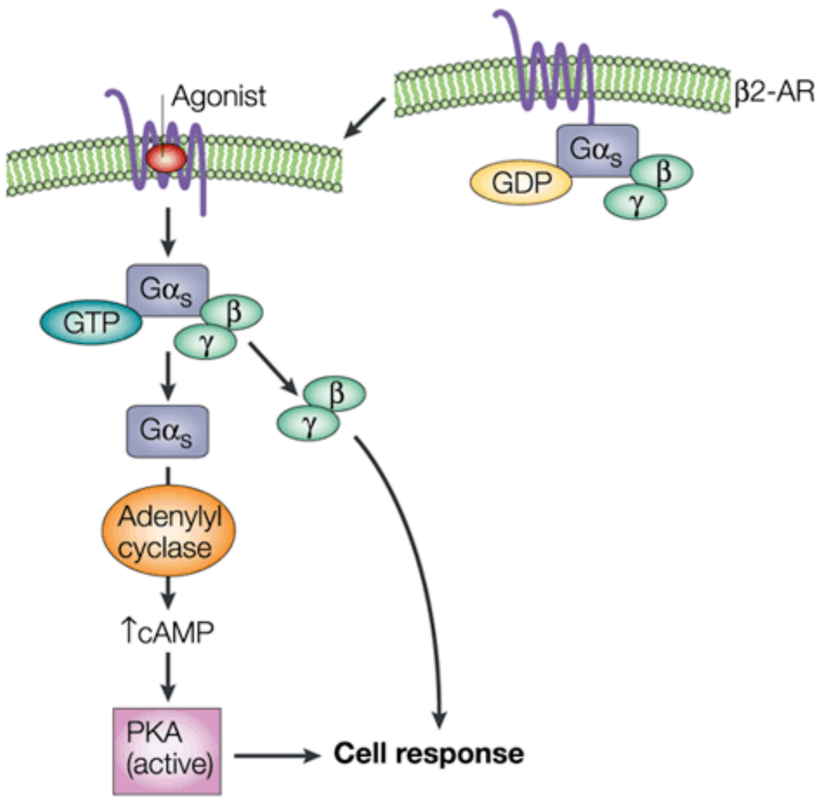

Figure 2. Classical overview of GPCR signal transduction pathways.

Normally GDP are bounded in Gα subunit under the inactive state lacking ligand binding. Ligand binding to the GPCR induces GPCR activation, which causes GDP exchange with GTP and dissociation between Gα and βγ subunit. In the case of the β2 adrenergic receptor, agonist binding leads to receptor activation that induces $G\alpha_s$ activation. This activation stimulates secondary effector, adenylyl cyclase, which induces accumulation of cyclic AMP. The accumulated cyclic AMP activates a serine/threonine kinase, protein kinase A (PKA) activation. PKA activation leads to phosphorylation of various kinases and transcriptional factors. The βγ subunit modulates α subunit independent pathways.

Adapted from Pierce et al [67].

The β and γ subunits form a functional unit that only can be dissociated under denaturing conditions. Even though most β subunits can interact with most γ subunits, not all possible combination of subunits have been identified [4, 77]. β and γ proteins are found in a wide variety of cell types except 1 Gβ and 5 Gγ proteins, which are expressed in selective tissues, such as the brain or taste buds (Table 2). Therefore, overlapping signaling cascades through Gβγ can also increase the complexity of intracellular signaling. To terminate the signal, hydrolysis of GTP to GDP is controlled by the regulator of G protein signaling (RGS) protein leading to reassociation of the heterotrimer and the termination of the activation cycle. The extraordinary combinational complexity of αβγ heterotrimers limits the ability to identify signal transduction pathways induced by G proteins, in spite of technological advances [67].

In addition to the classical G protein signaling pathways an additional layer of complexity has been added to models of GPCR activation. For example, β_2AR shows coupling to both $G\alpha_s$ and $G\alpha_i$ in cardiac myocytes [78] but can also induce a signal transduction cascade through MAP kinase pathways, which is mediated in a G protein-independent manner through β-arrestins [79, 80]. Because of the complexity of theses pathways, specific G protein subunit pairs that function on specific signal transduction pathways have rarely been shown.

Constitutively Active Mutant GPCRs

Ligand-independent GPCR activation that leads to G-protein activation is called constitutive activity [81]. Since the first constitutively active mutants (CAMs) were identified in α1-adrenergic receptor in 1990 [82], CAMs have been identified in almost all classes of GPCRs and are not limited to specific secondary messengers. Because unstimulated wild type GPCRs have differential basal activity from fully inactive to completely active, the exact definition of a CAM remains controversial [83]. The general definition of a CAM is is a receptor that has an increase in basal activity compared to its wild type counterpart without stimulation [81, 83].

GPCR activation requires an alteration of the wild type conformation in order to trigger G protein activation. This activation also induces the activation of other protein involved in signal transduction and receptor trafficking. These include protein kinase A (PKA) and protein kinase C (PKC), or a family of G-protein-coupled receptor kinases (GRKs). Generally GPCR activity is down-regulated with GRK and β-arrestins. In fact, GRK phosphorylation induces binding of arrestin proteins to the receptor and inhibits further interactions between the receptor and the G protein [84-86]. CAM GPCRs mimic, to some degree, the active conformation of the wild type receptor and spontaneously adopt a structure that is able to activate G proteins [81]. Therefore, the position and characteristics of the CAMs potentially provides a snapshot of the structural differences between the inactive and the active states of GPCRs.

Kjelsberge et al [87] suggested the loss of intramolecular interactions induces a gain-of function CAM phenotype implying the existence of structural constraints that maintain the silence of a ligand-free receptor. They described a mutation of Ala293 to any other of the 19 amino acids in the α_{1B}-adrenergic receptor resulted in constitutive activation [87]. Interestingly, a number of GPCRs in family A have been characterized by the conserved motif, D/ERY, at the junction of third TM domain and intracellular loop as the main structural constraint for maintaining the receptor inactivation. Mutation of the first residue of this motif in rhodopsin [88], α_{1B}-adrenergic receptor [89], β_2-adrenergic receptor [90], gonadotropin-releasing hormone receptor [91] M1 muscarinic receptor [92], CXC chemokine receptor 2 (CXCR2) [93] or the lutropin/choriogonadotropin receptor [94] leads to constitutive activation. Two models possibly explain the constitutive activity in these mutants. One model suggests that the mutation might disrupt the constraining interactions of the arginine residues in TM1, 2, and 7 [87, 89, 95]. However another model that is broadly accepted has constitutive activity mediated through the disruption of an ionic interaction between the arginine and the aspartic or glutamic acid of the motif [2, 91, 96]. Alternatively, the D/ERY motif might regulate the active state the CAMs using other mechanisms.

Other domains have been shown to be important for GPCR activation as well. One example is the large ectodomain of the luteinizing hormone receptor [97] or thyroid stimulating hormone receptor [81]. This region constrains the TM region maintaining the inactive state and its deletion leads to constitutive activation. In addition the long C-terminal intracellular domain (more than 350 residues) of the metabotropic glutamate receptor 1 constrains G protein activation. A number of splice variants of the C-terminal domain induce constitutive activity [98]. Interestingly, no CAMs of GPCRs encoding a mutation on N-terminus have been reported except CAM of thyloid stimulating hormone receptor (TSHR) that present a mutation in large N-terminal exodomain [99, 100].

Constitutively Active Mutant Viral GPCRs

Given the flexibility of GPCR signaling and its promiscuous contribution to different physiological processes, it seems obvious that viruses would have evolved proteins to exploit these receptors for their evolutionary advantage. These pirated receptors could function to aid in recognition and infection of permissive cells or for activating host signaling in order to evade immune recognition or aid in replication [101].

Many DNA-viruses, such as Kaposi sarcoma-associated herpesvirus (KSHV), Epstein–Barr virus (EBV), human cytomegalovirus (HCMV), and human herpesvirus 6 and 7 encode GPCRs that have been hijacked from their cellular hosts and rendered constitutively active following mutations in key structural motifs. Several CAM GPCRs have recently been implicated in virally-induced oncogenesis [102]. One example is KSHV, the causative agent of Kaposi’s sarcoma (KS) [103] and primary effusion lymphoma [104]. The KSHV genome encodes a GPCR, ORF74, whose closest homologues are the chemokine receptors CXCR1 and CXCR2 [105]. KSHV ORF74 binds a variety of chemokines, such as CXCL-1, 2, 3, 5, 7, 8, 10 and 12 [106]. Chemokines, such as CXCL-1 and CXCL-8, can further activate ORF74 or function as neutral ligands [107]. Others, such as CXCL-10 and CXCL-12, can inhibit ORF74 signaling functioning as inverse agonists [108]. In addition, KSHV ORF74 induces cellular transformation in NIH3T3 cells and tumorigenesis in nude mice [109]. Furthermore, transgenic mice expressing KSHV-ORF74 develop angioproliferative lesions in multiple organs, which is morphologically identical with KS [110]. These tumors are highly vascularized, contain a spindle cell component, express VEGF-C mRNA, and many of the cells are $CD31^+$ cells. CD31 and VEGF-C expression are typically displayed in KS [111].

KSHV ORF74 signals through G_q based on the accumulation of inositol phosphate from the activation of phospholipase C. In addition KSHV ORF74 is not inhibited by PTX treatment whereas chemokine receptors couple to G_i [112]. KSHV ORF74 stimulates PI3K–AKT/Protein Kinase B (PKB) pathway in endothelial cells, which protects them from apoptosis [113]. Therefore, the survival of KSHV-infected endothelial cells would allow for longer survival and production of the virus. Stimulation of AKT/PKB in KSHV-ORF74-expressing cells is dependent on βγ subunits of the G protein in both PTX-sensitive and -insensitive G proteins [93, 105]. In addition to G-protein mediated signaling, G-protein independent signal transduction was reported. Burger et al showed that KSHV-ORF74 constitutively induces the activation of the JAK-STAT3 pathway [114] (Figure 3).

Figure 3. KSHV-ORF74 induced signal transduction pathways mediated by both Gα_i and Gα_q.

G-proteins, Gαi and Gαq, drive PI3K (red arrow) and PLC-β (blue arrow) dependent intracellular cascades, respectively. In addition Gβγ also induces PI3K mediated signaling. G-protein independent kinase (orange dotted arrow), and JAK-STAT3 (orange arrow), are also induced by ORF74. KSHV ORF74 ligand-independently activates various transcriptional factors. Abbreviations: PLC (Phospholipase C), PKC (Protein kinase C), MEK (Mitogen activated protein kinase kinase), MAPK (Mitogen activated protein kinase), PI3K (Phosphatidylinositol 3-kinases), PKB (Protein kinase B), JAK (Janus activated kinase), STAT3 (Signal transducers and activators of transcription protein), AP-1(Activator protein-1), CREB (cyclic-AMP-response-element-binding-protein), NFAT (Nuclear factor activator of T cells), HIF-1α (Hypoxia-inducible factor-1α).

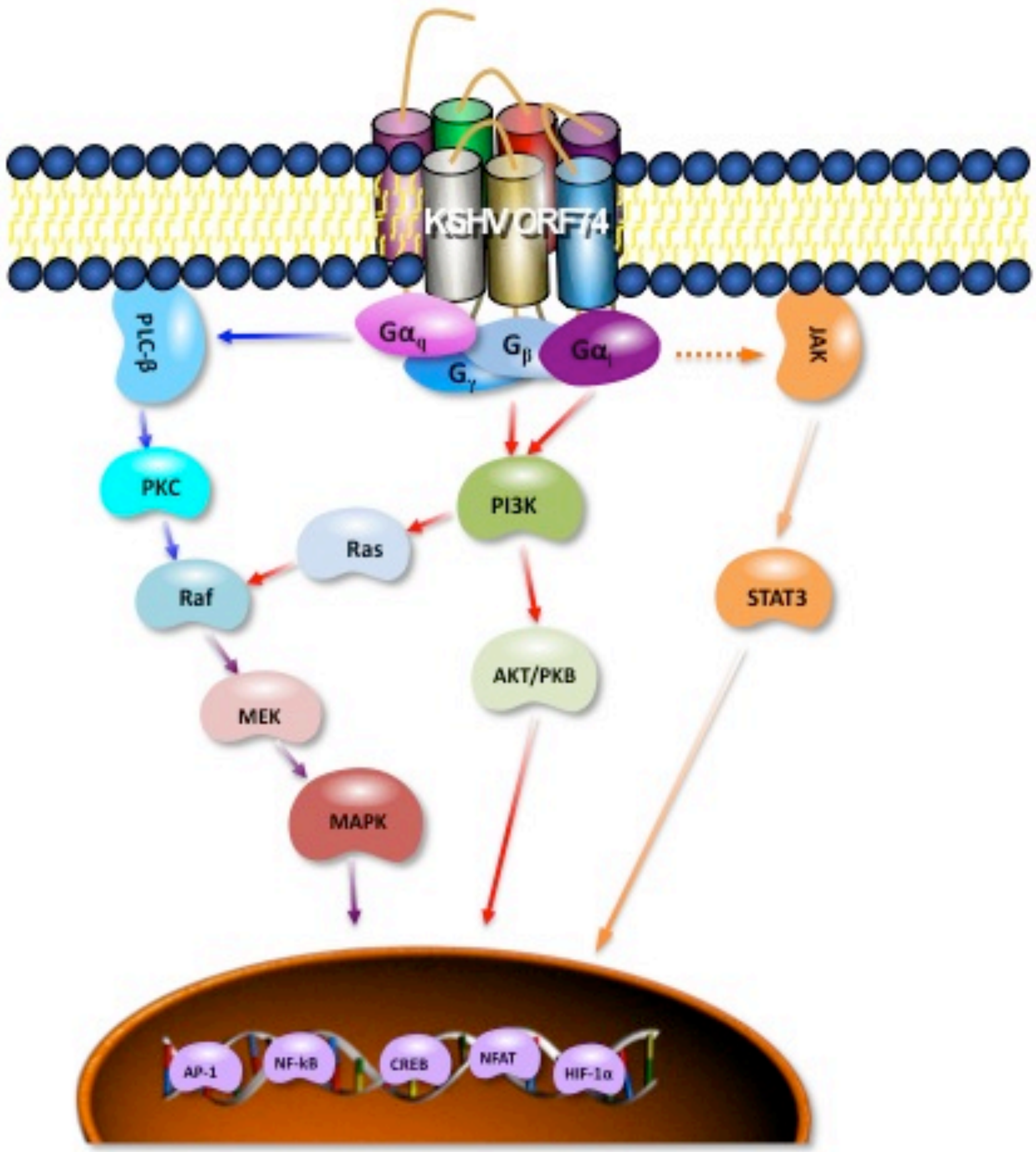
KSHV ORF74
PLC-β
Gαq
Gβ
Gγ
Gαi
JAK
PKC
PI3K
Ras
Raf
STAT3
AKT/PKB
MEK
MAPK
AP-1
NF-kB
CREB
NFAT
HIF-1α

GPCRs in Cancer

Experimental and clinical evidence indicates that GPCRs have a critical role in cancer progression and metastasis. However these mechanisms cannot completely explain all origins of cancer. Recently it has been suggested that malignant cells hijack the normal physiological function of GPCRs leading to autonomous proliferation, immune evasion, increased nutrient and oxygen supplies, invasion of the surrounding tissues, and dissemination to other organs [19]. Cancer cells will often overexpress GPCRs and their subsequent stimulation via autocrine or paracrine agonists released by tumor or stromal cells stimulate GPCRs and their signal transduction pathways. In fact, many GPCRs are overexpressed in different cancers (Table 4) and contribute to tumor cell proliferation mediated through autocrine and paracrine activation. For instance, the activation of chemokine receptors such as CXCR2 after stimulation with interleukin-8 (IL-8, also known as CXCL8) and GRO-α (also known as CXCL1 and melanoma growth stimulatory activity α) from tumor cells contributes

Table 4. GPCRs in cancers.

GPCRs and their cognate ligand interaction contribute to tumor growth, survival, metastasis, invasion and/or angiogenesis.

Abbrevivation: AT (angiotensin receptor), β1AR and β2AR (β1- and β2-adrenergic receptors), CCK (cholecystokinin), ET_A (endothelin receptor type A), ET_B (endothelin receptor type B), GPR30 (G protein- coupled receptor 30), GRPR (gastrin-releasing peptide receptor), IL8 (interleukin 8) LPA (lysophosphatidic acid), MC1R (melanocortin 1 receptor), MSH (melanocortin 1), NMBR (neuromedin B receptor), PAR-1(ptotease-activated receptor-1), PGE2 (prostaglandin E2), SDF1 (stromal cellderived factor 1).

Modified from Dorsam and Gutkind [19].

Cancer	Receptor	GPCR Class	Ligand	Function
Breast cancer	PAR1	A	Thrombin	**Growth;metastasis;angiogenesis**
	EP2;EP4	A	PGE2	**Growth;metastasis;angiogenesis**
	CXCR4	A	SDF1	**Metastasis;angiogenesis**
	GPR30	A	Oestogen	**Growth?Hormone-therapy resistance?**
Colon cancer	EP2;EP4	A	PGE2	**Growth;metastasis;angiogenesis**
	LPA_1	A	LPA	**Growth**
	ET receptors	A	Endothelin-1	**Survival**
	PAR1	A	Thrombin	**Growth;migration**
	Frizzleds	C	Wnts	**Growth**
Head and neck cancer	CXCR2	A	IL8;Groα	**Growth;metastasis;angiogenesis**
	CXCR4	A	SDF1	**metastasis**
	EP receptors	A	PGE2	**Growth;angiogenesi;metastasiss**
	GRPR	A	GRP	**Growth;survival**
	PAR1	A	Thrombin	**Metastasis;angiogenesis**
Small-cell lung cancer	GRPR	A	IL8;Groα	**Growth**
	NMBR	A	Neuromedin B	**Growth**
	CCK_1;CCK_2	A	CCK	**Growth;survival**
	CXCR4	A	SDF1	**Growth; metastasis**

Continued on the next page

Cancer	Receptor	GPCR Class	Ligand	Function
Non-small-cell lung cancer	EP receptors	A	PGE2	**Growth;metastasis;angiogenesis**
	CXCR2	A	IL8;Groα	**Growth;metastasis;angiogenesis**
	CXCR4	A	SDF1	**Migration;metastasis**
	β1AR; β2AR	A	NNK	**Growth?**
Ovarian cancer	LPA1-LPA3	A	LPA	**Growth;metastasis;angiogenesis**
	CXCR2	A	Groα	**Growth;angiogenesis**
Pancreatic cancer	GRPG	A	GRP	**Growth**
	CCK_1;CCK_2	A	Groα	**Growth;angiogenesis**
Prostate cancer	PAR1	A	Thrombin	**Growth;invasion**
	ET_A	A	Endothelin-1	**Growth;survival;metastasis**
	AT_1	A	Angiotensin1	**Growth**
	EP2,EP4	A	PGE2	**Growth;metastasis;angiogenesis**
	LPA_1	A	LPA	**Growth;invasion**
	B1,B2	A	Bradykinin	**Growth;survival;invasion**
	GRPR	A	GRP	**Growth;migration**
Melanoma	MC1R	A	MSH	**Sensitivity to UV-induced DNA damage**
	CXCR2	A	IL8;Groα	**Growth;metastasis;angiogenesis**
	ET_B	A	Endothelin-1/3	**Growth**

to the progression of some tumors, such as squamous carcinomas of the head and neck (HNSCC) and melanoma [115, 116]. GPCRs are also considered key mediators of inflammation, thus providing a possible connection between chronic inflammation and cancer. Inflammation is considered an important component in tumorigenesis and offers novel therapeutic targets [117-119]. Furthermore GPCRs, especially chemokine receptors, play a central role in tumor-induced angiogenesis and could induce GPCR-guided migration of cancer cells to other organs. Cancer cells manipulate GPCR signaling to attract endothelial cells and lead them to invade the tumor mass, thereby forming new vessels to provide nutrients and oxygen. Therefore, distracting or inhibiting GPCRs and their downstream targets might provide an opportunity for the development of novel mechanism-based strategies for cancer diagnosis, prevention, and treatment [19].

CHAPTER 2. CHEMOKINES AND CHEMOKINE RECEPTORS

An Overview

Initially chemokines were defined in 1989 as novel cytokines activating neutrophils [120]. They consist of a superfamily of proinflammatory mediators that promote the recruitment of leukocytes, and other cell types through GPCRs [121-123]. Chemokines contain a heparin-binding domain in the C-terminus that is responsible for binding to proteoglycans in the extracellular matrix [124]. Chemokines have been classified into 4 subfamilies, based on the spacing of the cysteines in the amino terminus: CXC, CC, CX3C and C [125]. Among chemokine subfamilies, CXC chemokines are further classified into Glu-Leu-Arg $(ELR)^+$ and ELR^- CXC chemokines, based on the presence or absence of the ELR motif in the N-terminus. IL-8, epithelial neutrophil activating protein (ENA also known as CXCL5), granulocyte chemotactic peptide-2 (GCP-2 also known as CXCL6), neutrophilic activating protein (NAP also known as CXCL7), melanoma growth stimulatory activities (MGSA (or GRO) α, β and γ also known as CXCL1, CXCL2 and CXCL3) belong to the ELR^+ CXC subfamily [125].

The ELR motif in the N-terminus of CXC chemokines modulates their specificity for binding to their cognate receptors. For example, ELR+ CXC

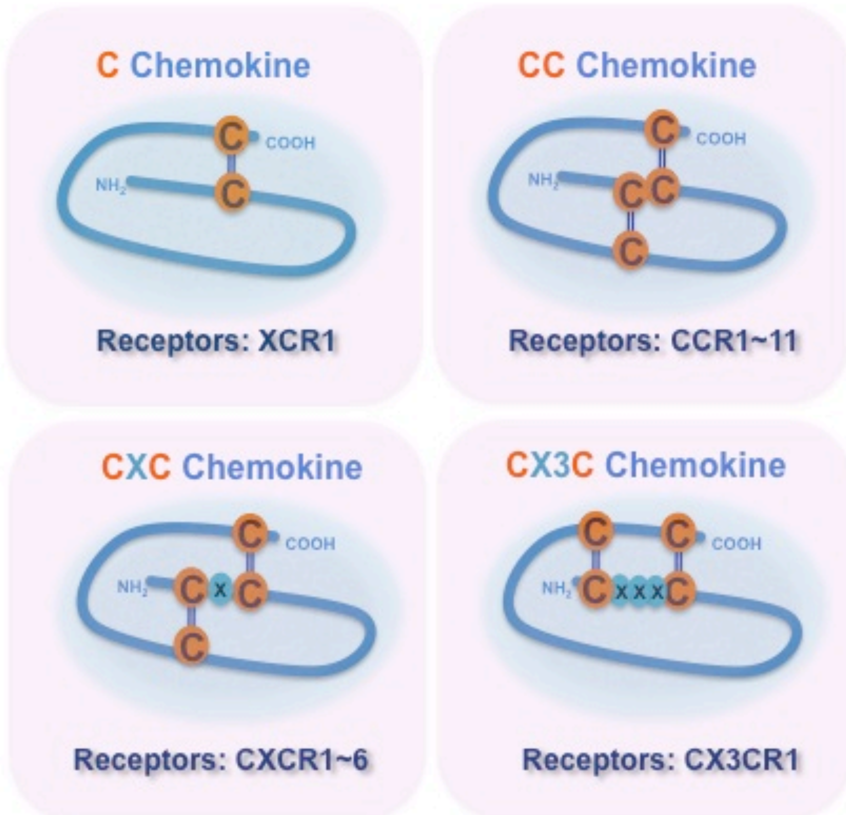

Figure 4. **Chemokine superfamily and their cognate chemokine receptors.** Chemokines are classified based on the location of the highly conserved cysteine residues (orange round) in the N-terminus. There are four families, such as C, CC, CXC and CX3C chemokines. “x (blue round)” represents any amino acid between cysteine residues. Each chemokine interacts with their chemokine receptors expressed on a variety of cell types including leukocytes, epithelial and endothelial.

Adapted from Sodhi et al [102].

chemokines in the N-terminus of the molecule that immediately precedes the first cysteine are potent promoters of angiogenesis [126, 127]. By contrast, ELR-CXC chemokines, such as platelet factor-4 (PF-4) and interferon gamma-inducible protein-10 (IP-10), are potent inhibitors of angiogenesis [128]. The structural dissimilarity in the N-terminus of these CXC chemokines plays an important role in receptor specificity. Based on the unique functional differences of the CXC chemokines, there has been increasing interest in their ability to regulate angiogenesis in cancer [124].

The function of the chemokine is initiated upon binding to their chemokine receptors, a member of the GPCR family [122]. Initially two specific chemokine receptors for IL-8, CXCR1 and CXCR2, were identified on the cell surface [129, 130]. Since then, 18 functional chemokine receptors have been identified [131]. In addition there are two ‘decoy’ or ‘scavenger’ receptors, DARC and D6, which are known to bind several chemokines but do not induce signaling. It has been speculated that their function may be to modulate inflammatory responses through their ability to remove chemokine ligands from inflammatory sites [131].

There are a number of common characteristics of chemokine receptors. All chemokine receptors identified so far are membrane-bound proteins composed of an N-terminus, 7-transmembrane domains, 3-extracellular and intracellular loops and a C-terminus, and can couple to G-proteins. The chemokine receptor is comprised of approximately 350 amino acids. The N-terminus of the receptor is relatively shorter than other GPCRs and contains many acidic residues and N-linked glycosylation sites. An intracellular C-terminus contains serine and threonine residues that act as phosphorylation sites for receptor regulation. Also, a disulfide bond links highly conserved cysteines in extracellular loops 1 and 2 [132].

Chemokine receptor 4, CXCR4, has drawn a lot of attention recently because it is a co-receptor for human immunodeficiency virus (HIV) [133] and its involvement in tumor progression and metastasis [134, 135]. CXCR4 was originally cloned as an orphan chemokine receptor, which is expressed on neutrophils, myeloid cells, and T lymphocytes [136]. Two years later CXCR4 was identified as a cofactor for T-tropic HIV-1 and HIV-2 envelope-mediated fusion and entry into CD4+ T cells [133]. The ELR^- CXC chemokine, stromal cell-derived factor (SDF-1α (also known as CXCL12)) is the only host ligand for CXCR4 and is a highly effective lymphocyte chemoattractant. It interferes with HIV-1 infection of permissive CD4+ cells in accordance with CXCR4 expression patterns [137, 138]. Stimulation with IL-4 induces an increase in cell-surface expression of CXCR4 on resting peripheral and cord blood T cells, whereas stimulation with CD28 or CD3 and CD2 lead to down-regulation of CXCR4 expression [139]. CXCR4 knockout mice exhibit impaired B lymphopoiesis, myelopoiesis, hematopoiesis, derailed cerebellar neuron migration, and defective vascularization of the gastrointestinal tract [140-142] illustrating its role in a variety of developmental processes. CXCR4 is abnormally expressed on a variety of tumor cells, such as breast, head and neck, small-cell lung cancer (SCLC) and non-small-cell lung cancer (NSCLC). CXCR4 stimulation is believed to play an important role in tumor cell proliferation, survival, angiogenesis and migration [19]. Interestingly metastatic tumor cells express higher levels of CXCR4 than primary tumors in SCLC, NSCLC, neuroblastoma, melanoma, HNSCC, colorectal, thyroid, prostate, ovarian and renal-cell cancers, as well as in multiple haematopoietic malignancies, including chronic lymphocytic leukaemia, multiple myeloma and acute leukaemia. This circumstantial evidence implicates a central role for CXCR4 and SDF-1α in tumor progression and metastasis [19, 143, 144]. CXCR4 is the best example of the role that chemokine receptors play in tumor development and progression.

CXCR2 Activation and Signaling

Most chemokines stimulate more than one chemokine receptor and many chemokine receptors are functionally activated by a number of chemokines [125]. IL-8 activates CXCR1 and CXCR2. Both receptors are highly homologous (77%) [129, 130], with most of the divergence in the N-terminus (29%) and ECL2 (55%) regions [145]. CXCR1 selectively bind either IL-8 or GCP-2, whereas CXCR2 can interact with CXCL-1, 2, 3, 5, 6, 7 and 8 [123]. Activation of both receptors upon ligand binding induces phosphatidylinositol (PI) hydrolysis, intracellular Ca^{2+} mobilization, and chemotaxis. All can be inhibited with PTX, indicating that the both receptors couple to $G\alpha_i$ in neutrophils where $G\alpha_{i2}$ is very abundant [120, 146]. A major difference between CXCR1 and CXCR2 is phospholipase D activation, which is mediated via CXCR1 activation, implicating that the two receptors have different cellular functions [147]. In addition to phospholipase D activation, receptor trafficking is a distinguishing characteristic between CXCR1 and CXCR2, which induces leukocyte activation and regulation in response to IL-8 [148, 149]. Over 95% CXCR2 internalizes within 5 min of activation with IL-8 compared with about 10% for CXCR1 [150, 151]. This implies that receptors are regulated differently upon stimulation and that they induce differential signaling.

Initially CXCR2 was cloned in 1991 from human promyelocytic leukemia cells, HL60s [129]. CXCR2 is expressed on various cell types and tissues including neutrophils, monocytes, eosinophils, mast cells, basophils, lymphocytes, epithelial cells, endothelial cells, smooth muscle and cells of the central nervous system [152]. Treatment of CXCR2 expressing cell lines with PTX completely disrupted IL-8 mediated inhibition of forskolin-stimulated cyclic AMP accumulation indicating that CXCR2 activation induces $G\alpha_i$ dependent signal transduction pathways [153]. This $G\alpha_i$ dependent signaling stimulates the accumulation of intracellular inositol phosphate and increases intracellular calcium. CXCR2 activation, followed by the initiation of G proteins including βγ subunit mediated signals, induces important downstream regulators of intracellular signaling such as cAMP/protein kinase A (PKA), protein kinase C (PKC), phospholipase C (PLC), phosphoinositide 3-kinase (PI3Kinase)/AKT/mTOR, Ras/Raf/MEK/JNK/p38/ERK1/ERK2, and activates NF-kB pathways. These pathways subsequently induce proliferation, migration, and inhibition of apoptosis [154-157].

Initially, Burger et al [93] demonstrated a constitutively activate mutant CXCR2 could be generated with a single point mutation in the highly conserved DRY motif (D138V). This residue was chosen based on KSHV ORF74. KSHV

ORF74 is constitutively active and induces tumorigenesis. This receptor encodes a VRY motif instead of a DRY motif at the junction of the TM3 and ICL2. The CXCR2 mutant (D138V) induced cellular transformation in NIH3T3 cells that is comparable to KSHV ORF74. To evaluate G protein-coupled signaling through the PLC pathway, accumulation of inositol phosphate in NIH3T3 cells expressing D138V mutant was measured. KSHV ORF74 and the CXCR2 (D138V) mutant increased the amount of inositol phosphate 3.5 and 3.0 fold higher than untransfected NIH3T3 cells.. PTX treatment did not completely inhibit the accumulation of inositol phosphate for both the KSHV ORF74 and the D138V mutant, which suggests that the D138V mutant induces an agonist-independent signal transduction pathway similar to the KSHV ORF74. In addition, both receptors showed only a small Ca^{2+} response upon IL-8 stimulation suggesting constitutive activity is independent of ligands. Constitutively active mutant CXCR2 (D138V) mediated cellular transformation was dependent on constitutive STAT3 phosphorylaton on Tyr705 as part of JAK2 activation [114]. This laid the foundation for our current studies of CAM CXCR2 and their role in cellular transformation.

CXCR2 IN TUMORIGENESIS

The role of CXCR2 mediated, ELR+ CXC chemokine-induced angiogenesis *in vivo* has been investigated using the corneal micropocket assay for angiogenesis. Interestingly $CXCR2^{-/-}$ mice or $CXCR2^{+/+}$ mice treated with neutralizing antibodies (Abs) to CXCR2 interfered with ELR+ CXC chemokine-mediated angiogenesis [158]. This evidence demonstrated that CXCR2 is both essential and sufficient to mediate the angiogenic effects of ELR+ CXC chemokines. Because of its role in angiogensis and the role that angiogensis plays in tumor formation, there has been an increasing focus on CXCR2 and its relationship to cancer. Another *in vivo* model described a correlation between the expression of endogenous ELR^+ CXC chemokines that induce tumor growth and the metastatic potential of Lewis lung cancer (LLC) tumors in $CXCR2^{+/+}$ mice. The LLC primary tumors and spontaneous metastasis to the lungs were significantly reduced in $CXCR2^{-/-}$ mice. Morphometric analysis of the primary tumors in $CXCR2^{-/-}$ mice described areas with greater tumor-associated necrosis and reduced tumor-associated angiogenesis when compared with tumors grown in $CXCR2^{+/+}$ mice. These findings were further confirmed in $CXCR2^{+/+}$ mice treated with neutralizing Abs to CXCR2 [159]. This evidence supports the view that CXCR2 mediates the angiogenic activity of ELR+ CXC chemokines in a preclinical model of lung cancer.

IL-8, activation of CXCR1 and CXCR2 induces mitogenic and angiogenic factors that contribute to human cancer progression [160]. Higher-grade human melanoma specimens and metastases express higher levels of CXCR2 suggesting an association between the expression of IL-8 and CXCR2 [161]. Singh et al [162] demonstrated that CXCR1 or CXCR2 overexpressed in non-tumorigenic and low-tumorigenic melanoma cells enhanced cellular proliferation, chemotaxis and invasiveness *in vitro*. Interestingly, CXCR1 or CXCR2 overexpression in non-tumorigenic melanoma cells induces tumorigenicity as examined *in vivo* [162]. In addition IL-8-induced and CXCR1- or CXCR2-dependent melanoma cell proliferation and migration was mediated through the ERK1/2 MAP kinase pathway. However, the functional significance of these receptors, CXCR1 and CXCR2, in melanoma progression remains unclear [162].

In human ovarian cancer cells, SK-OV-3, CXCR1 and CXCR2 are strongly expressed. IL-8 stimulation through p44/42 MAP (Erk1/2) kinase transformed ovarian cancer cells to have increased membrane ruffling and the formation/retraction of thin actin-like projections. All of these phenotypes are indicators cancer cell metastasis [163].

Overexpression of CXCL-1 and 2 (also known as GRO-α and β) and CXCR2 in esophageal squamous cell carcinoma tissues, WHCO1, 5 and 6, demonstrated an important role for CXCR2 activation in cellular proliferation. This proliferative autocrine loop between GRO α/β and CXCR2 indicated a critical role for CXCR2 in the development and maintenance of squamous esophageal cancer [164].

Heterotropic and orthotopic models of murine renal cell carcinoma using $CXCR2^{-/-}$ and $CXCR2^{+/+}$ BALB/c mice demonstrated that CXCR2 induces tumor-associated angiogenesis and tumor growth. In this murine model, CXCR2 ligand (CXCL-1, 3, 5 and 8) expression directly correlated with tumor growth in $CXCR2^{+/+}$ mice. In contrast, a significant reduction in tumor growth in $CXCR2^{-/-}$ mice was observed and correlated with decreased angiogenesis and increased tumor necrosis [165].

Human prostate cancer biopsy tissue analysis showed a progressive increase in IL-8 expression in the early stages (Gleason 3 or 4) compared with normal prostate epithelium [166]. Elevated IL-8 expression was also detected in the serum of prostate cancer patients. There was a 2-5 fold higher elevation of IL-8 in patients with prostate cancer compared with normal or benign prostatic hypertrophy patients [167]. In addition, the localization of IL-8 and CXCR1 and 2 expression to the cytoplasm and the basal membrane of prostate cancer cells was even more distinct in the transurethral resection of the prostate biopsy samples of advanced and androgen-independent disease (Gleason pattern 5) [166]. The androgen-independent prostate cancer cell line, PC3, exhibited high IL-8 expression and activation of its receptors, CXCR1 and CXCR2, which promoted tumorigenicity of the cells [166].

The human pancreatic cancer cell line, Capan-1, had increased IL-8 and CXCL-1 expression, and these chemokines induced mitogenic effects through CXCR1 and CXCR2 *in vitro* [168]. Additionally CXCR2 inhibition completely abolished neovascularization in the human pancreatic cancer cell line, BxPC-3 [169].

The highly metastatic colon cancer cell line, KM12L4, expressed higher levels of IL-8 and cognate receptors, CXCR1 and CXCR2, than the low metastatic cell line, KM12C, and non-metastatic cell line, Caco2. Also IL-8 stimulation induced higher cellular proliferation for Caco2 than KM12C and KM12L4 cell lines respectively. Inhibition of IL-8, CXCR1, or CXCR2 reduced cellular proliferation in both KM12C and KM12L4 cells. Moreover, the expression level of IL-8 was directly involved in the migratory potential of colon cancer cell [170]. These data suggest that IL-8 and its receptors potentially modulate human colon cancer tumorigenesis.

Taken together, CXCR2 activation induced by its ligands is a contributing factor to tumor-associated angiogenesis, tumorigenesis and metastasis. Development of novel agents targeting multiple angiogenic mediators is currently in progress [171, 172]. Among those targets, CXCR2 is one of the best candidates for anti-angiogenic therapies in that it is the universal receptor for all angiogenic CXC chemokines. Therefore targeting CXCR2 along with other angiogenic factors is a promising strategy to overcome tumorigenesis and metastases in a variety of cancers [159, 165].

Summary and Statement of Research Aims

The metastatic potential of primary tumors correlates with tumor proliferation and the level of tumor-related angiogenesis [165, 173]. In fact, solid tumors lacking a vascular conduit cannot grow more than several cubic millimeters, because nutrients and gas exchange cannot occur [165, 173]. Evidence suggests that the function of CXCR2 in tumor formation, proliferation and metastasis is associated with its expression and activation in endothelial cells. CXCR2-induced neovascularization promotes tumor cell proliferation providing tumor cell access to the vasculature [159, 165]. Based on this information, CXCR2 is an attractive target for inhibiting tumor-related angiogenesis. CXCR2 binds to all angiogenic ELR+ CXC chemokines and the inhibition of CXCR2 results in the lack of angiogenic activity *in vivo.* Many studies show that CXCR2 inhibition promotes a significant decrease in tumor size and an increase in tumor necrosis *in vitro* and *in vivo* [159, 165].

The main focus of this dissertation is not only the role of constitutive activation of CXCR2 followed in cellular transformation, but also the mapping of intracellular signal transduction pathways mediated by constitutive activation. The hypothesis of this dissertation is that the CAM CXCR2 induced by an N-terminal single point mutation promotes tumor development. To investigate this hypothesis, the following research objectives were performed:

1. Screening and identification of CXCR2 CAMs using the yeast model system

2. Verification of tumorigenicity mediated by CXCR2 CAMs *in vitro* and *in vivo*.

3. Identification of an intracellular signal transduction cascades induced by CXCR2 CAMs.

PART II. SCREENING FOR NOVEL CONSTITUTIVELY ACTIVE CXCR2 MUTANTS AND THEIR CELLULAR EFFECTS

In Press as "**Screening for Novel Constitutively Active CXCR2 Mutants and their Cellular Effects**" ***Methods in Enzymology****: Constitutive Activity and Inverse Agonism*, **Giljun Park,** Tom Masi, Chang K. Choi, Heejung Kim, Jeffrey M. Becker, and **Tim E. Sparer**

CHAPTER 1. ABSTRACT

Chemokines play an important role in inflammatory, developmental, and homeostatic processes. Deregulation of this system results in various diseases including tumorigenesis and cancer metastasis. Deregulation can occur when constitutively active mutant (CAM) chemokine receptors, which are locked in the "on" position. This can lead to cellular transformation/tumorigenesis.

The CXC chemokine receptor 2 (CXCR2) that has homology with CAM receptor, ORF74 is a G-protein-coupled receptor (GPCR) expressed on neutrophils, some monocytes, endothelial cells, and some epithelial cells. CXCR2 activation with ELR+ CXC chemokines induces leukocyte migration, trafficking, leukocyte degranulation, cell differentiation, and chemokine mediated angiogenesis. Activation of CXCR2 can lead to cellular transformation. We hypothesized that CAM CXCR2s may play a role in cancer development. In order to identify CXCR2 CAMs, mutant CXCR2s were screened using a modified *Saccharomyces cerevisiae* high-throughput system. *Saccharomyces cerevisiae* has been successfully used to identify GPCR and G-proteins interactions and autocrine selection for peptide agonists. The CXCR2 CAMs identified from this screen were characterized in the mammalian system. Their ability to transform cells *in vitro* was shown using foci formation, soft-agar growth, impedence measurement assays and *in vivo* tumor growth following hind flank inoculation. Signaling pathways contributing to cellular transformation were identified using luciferase reporter assays. Studying constitutively active GPCRs is an approach

for “capturing” a pluridimensional GPCRs in a “locked” activation state. In order to address the residues necessary for CXCR2 activation, we used *Saccharomyces cerevisiae* for screening novel CAMs and characterized them in mammalian reporter assays.

CHAPTER 2. INTRODUCTION

Although there are many contributing factors to tumorigenesis, chemokines and their receptors can contribute to tumorigenesis and metastasis [134]. Chemokines function normally as small chemoattractant cytokines that are involved in inflammatory, developmental, and homeostatic processes [174]. Deregulation of this system is associated with the development of cancers and metastasis. One example of disruption of the chemokine pathway is the constitutively active mutant (CAM) receptors [134, 175]. These CAMs cause an alteration of the structural constraints, locking it into an active conformation. This conformational change induces ligand independent activation called constitutive activity [176]. CAM GPCRs are associated with the development of a variety of human diseases [177]. The best example of a constitutively active chemokine receptor causing cancers is the Kaposi sarcoma herpesvirus chemokine receptor, ORF74, which is a homolog for human CXCR2 [108]. This receptor has a 'VRY' motif instead of a 'DRY' motif between third transmembrane domain and second intracellular loop and has been shown to be constitutively active. Stable lines of NIH3T3 fibroblasts expressing ORF74 lead to cellular transformation [93, 106, 178]. These transfectants are tumorigenic in nude mouse and a transgenic mouse expressing ORF74 developed tumors resembling Kaposi's sarcoma (KS) lesions [111].

CXC chemokine receptor 2 (CXCR2) is a G-protein-coupled receptor (GPCR) [179] and expressed on neutrophils, some monocytes, endothelial cells, and some epithelial cells [180]. Activation of CXCR2 with ELR+ CXC chemokines leads to leukocyte migration, trafficking, leukocyte degranulation, cell differentiation, and ELR+ CXC chemokine mediated angiogenesis [123] [181].

Utilizing the induction of the natural pheromone response pathway, *Saccharomyces cerevisiae* has been successfully used to identify GPCR/G-proteins interactions and selection of peptide agonists [182-185]. Recently allosteric peptide agonists for CXCR4 were identified using this system. The pheromone responsive pathway was modified to include a hybrid G-protein to interact with CXCR4, elimination of growth arrest genes, and an auxotrophic marker under the control of the pheromone responsive element. With these modifications a library of CXCR4 ligands was screened to identify novel agonists [186].

To identify CXCR2 CAMs, the open reading frame (ORF) of CXCR2 was randomly mutated and expressed in this genetically engineered yeast. Using a simple selection for growth on media lacking histidine we identified novel CXCR2 CAMs. Constitutive activation was confirmed with induction of beta-galactosidase, which was under the control of the pheromone responsive element. In order to characterize the CXCR2 CAMs in the mammalian system and to link them to cellular transformation, the first step in tumorigenesis, we generated stable transfectants using CXCR2 CAMs and measured foci formation, anchorage-independent growth in soft agar, impedance, and tumor formation *in vivo*. To address the downstream constitutively active signal transduction pathways immunoblotting and flowcytometry were used to identify specific phosporylated signaling pathways. Luciferase reporter constructs with CREB, STAT3, and NF-kB responsive elements can be used to identify important signaling pathways that could contribute to cellular transformation. Here we describe detailed approaches for successful identification and cellular characterization of CXCR2 CAMs.

CHAPTER 3. MATERIALS AND MATHODS

Strains, media, and plasmids

Yeast strain CY1141 (*MATα FUS1p-HIS3 can1 far1*1442 gpa1 (41)-G@ai2 his3 leu2 lys2 ste14::trp1::LYS2 ste3*1156 tbt1-1 trp1 ura3*) contains an integrated copy of a hybrid Gα subunit ($GPA1_{(41)}G\alpha_{i2}$) in which the N-terminal 33 residues of human $G\alpha_{i2}$ are substituted with the 41 N-terminal residues of GPA1 [185]. For strain CY12946 (*MAT2 FUS1p-HIS3 GPA1G@ai2(5) can1 far1*1442 his3 leu2 lys2 sst2*2 ste14::trp1::LYS2 ste3*1156 tbt1-1 trp1 ura3*) also contains a chimeric G protein $GPA1G\alpha_{i2(5)}$ in which the 5 residues of C-terminal GPA1 were replaced with the C-terminal 5 residues of human $G\alpha_{i2}$ [187]. In addition *S. cerevisiae* strain, BJS21 (*MAT**a**, prc1-407 prb1-1122 pep4-3 leu2 trp1 ura3-52 ste2::Kan^R*) was used as a control to see the receptor expression on the plasma membrane.

Yeast expression vector, p426GPD (ATCC, #87361), was used to clone wild type and mutated human CXCR2. To estimated basal activity of receptor pMD1325 (a gift from Dr. Dumont, University of Rochester, School of Medicine and Dentistry) were transformed into yeast.

YPD is a basic enriched media to culture BJS21, CY1141 and CY12946, which contains 1% of BactoYeast extract (Difco), 2% of BactoPeptone (Difco), and 2% dextrose. For selective medium MLU (medium lacking uracil) contains 1x Yeast Nitrogen Base (YNB) without amino acids plus ammonium sulfate (Difco), 2% glucose, 1% casamino acids (Difco). When also selecting for histidine and/or leucine in combination with uracil the casamino acids is not added due to it containing both histidine and leucine.

Cell lines, growth medium, mouse strain and plasmids

NIH3T3 (ATCC) and HEK293 (ATCC) were maintained in the medium containing DMEM with 10% bovine calf serum (Hyclone). 6 to 8 week old athymic *nu/nu* mice (Jackson Laboratory) were used for *in vivo* tumogigenesis assay. pcDNA3.1 (Invitrgen) and pcDNA3.1+GFP plasmids were used to clone wild type and mutants CXCR2 into mammalian cell line. Lipofectamine 2000™ (Invitrogen) was used for transfection. Neomycin (G418 Sulfate, Cellgro) was applied to select single clonal population.

Reagents for Yeast transformation

1.0 M lithium acetate (LiAc) and 50% (w/v) polyethylene glycol (PEG) 3350 are sterilized with 0.2 and 0.45 μm pore size filtration respectively and stored at room temperature. Single strand DNA (ssDNA, salmon sperm DNA, Sigma-Aldrich) is boiled for 10 min, cooled down on ice, and frozen at -20 degrees Celsius.

Reagents for Yeast Immunofluorescence

Potassium phosphate (KPi, 0.1 M, pH 6.5), SHA (1 M Sorbitol, 0.1 M NaHepes (pH 7.5), 5 mM NaN_3), 4% formaldehyde, β-mercaptoethanol, and yeast cell wall lytic enzyme (Fisher, *Cat.No. BP2683-25*). WT buffer: 1% fat free dry milk, 0.5 mg/ml BSA, 150 mM NaCl, 50 mM HEPES (pH 7.5), 0.1% Tween 20, and 1 mM NaN_3. For anti-CXCR2 immunoblotting an antibody specific for human CXCR2 (sc-7304, *SantaCruz Biotechnology*) is used. HRP-conjugated secondary Ab was applied, and then detected with enhanced chemiluminescence system (ECL, Amersham). Hoechst dye (1 µg/ml, Molecular Probe) for nuclear staining is used to identify individual cells.

Reagents for Subcellular fractionation

Sorbitol buffer (10 mM Tris (pH 7.6), 0.8 M sorbitol, 10 mM NaN_3, 10 mM KF, 1 mM EDTA, pH 8.0), and sucrose buffer (10 mM Tris (pH 7.6), 1 mM EDTA, 10% [w/v] sucrose) were used.

Reagents for Immunoblotting

NuPAGE 12% Bis-Tris SDS-polyacrylamide gel (Invitrogen) and PVDF membrane (Invitrogen) were used. Primary antibodies: anti-FLAG M2 antibody (Eastman Kodak Co.) and anti-human CXCR2 (sc-7304-*SantaCruz Biotechnology)*, and secondary antibody: anti-mouse HRP-conjugated secondary Ab (eBioscience) were applied. Blocking media (1% dried milk in PBS/0.1% Tween 20) and wash media (PBS/0.1% Tween 20) were prepared. ECL development kit (Amersham) and 2x SDS Sample Buffer (Invitrogen) were applied. PE-conjugated human CXCR2 specific antibody (R&D Systems, FAB331P) for FACs anaysis was applied.

Reagents for error-prone PCR

Primers forward and reverse for the CXCR2 ORF were synthesized to include unique restriction sites (Forward with *HindIII* 5'-CCC*AAGCTT*ATGGAAGATTTTAACATGGAGAGTG-3' and Reverse with *XbaI* 5'-GC*TCTAGATTA*GAGAGTAGTGGAAGTGTGC-3'). Low fidelity Taq polyerase (Fisher BioReagents) is preferred for error-prone PCR than high fidelity Taq polymerase. In addition dATP, dGTP, dTTP, dCTP, and manganese chloride were added separately to the reaction because they were modified in order to increase the error rate of the PCR reaction.

Reagents for β-galactosidase assay

Basal activity of β-galactosidase was measured using a yeast β-galactosidase assay kit (Pierce) according to the manufacturer's instruction. The amount of β-galactosidase is expressed as Miller units.

Yeast transformation

Maintain and culture yeast strains on YPD medium. Inoculate a fresh colony into 5 ml YPD and incubate with movement overnight at 30°C. Using the overnight culture inoculate 50 mls of YPD in a sterile flask to a final density of

$5x10^6$ cells/ml. Incubate the culture as above until a cell concentration of $2x10^7$ (usually 3-5 hours) is achieved. Centrifuge the cells at 4,000 rpm for 5 minutes and discard the supernatant. Wash the cells one time in 25 ml sterile water, centrifuge and then resuspend in 1 ml of 100 mM LiAc and transfer to a 1.5 ml microcentrifuge tube. Centrifuged the cells at top speed in a microcentrifuge for 15 seconds and remove the LiAc. Resuspend the cells in 400 μl of 100 mM LiAc. For each plasmid to be transformed, aliquot 50ul of cells to a clean microfuge tube. Boil the ssDNA for 5 min, and keep on ice until needed. Centrifuge each aliquot of cells and the discard the supernatant. In the following order, carefully add each of the following reagents: 240 μl of 50% PEG, 36 μl of 1.0 M LiAc, 25 μl of ssDNA, 5 μl (0.1-10 μg) of cloned DNA (e.g. wild type CXCR2 cloned into p426 GPD) and 45 μl of sterile water. Vortex the mixture until cell pellet is completely resuspended (about 1-2 min). Include a negative control reaction without cloned DNA. Incubate the mixture at 30°C for 30 min and heat shock at 42°C for 25 min. Centrfuge the heat shocked cells at top speed in a microcentrifuge for 2 min, and then remove the supernatant. Resuspend the cells in 1 ml of sterile water and plate 200 μl on selective media lacking uracil and incubate at 30°C. Transformed yeast colonies will be seen in 2-3 days.

Yeast Immunofluorescence analysis

Fix 1×10^8 cultured yeast cells in 0.1 M KPi (pH 6.5) and 4% formaldehyde for at least 1 hr then centrifuge and resuspend again in fix (as above) for at least 12 hrs but less than 24 hrs. After fixation, resuspend the cells in 5 ml of SHA (1

M Sorbitol, 0.1 M NaHepes, pH 7.5, 5 mM NaN_3) and store at 4°C for up to 2 weeks. To remove the cell wall, incubate 500 μl of the resuspended cells in 1 ml of SHA, 0.2% of β-mercaptoethanol, and 10 mg/ml of yeast cell wall lytic enzyme (Fisher, *BP2683-25*) at 30°C for 1.5 hrs. After incubation, centrifuge the cells and resuspended in 1% SDS, wash with 1ml of SHA and resuspend with SHA (~100 μl). After spinning down the cells, incubate the cells with a primary specific human CXCR2 antibody (sc-7304, *SantaCruze Biotechnology*) (1:100 dilution in WT buffer (1% fat free dry milk, 0.5 mg/ml of BSA, 150 mM of NaCl, 50 mM HEPES (pH 7.5), 0.1% Tween 20, and 1 mM NaN_3)) overnight at 4ºC. Wash the cells 5 times with WT buffer, and then add a FITC labeled anti-mouse secondary antibody (sc-2099, *SantaCruz Biotechnology*) (1:1,000 dilution in WT buffer). After incubation at room temperature for 30 min, wash the cells 5 times with WT buffer and stain with 100 μl of Hoechst dye (1 μg/ml, Molecular Probes). Wash the cells 3 times in sterile water and store at 4ºC in the dark. Take photomicrographs using an Olympus BX 50 microscope and photograph with *Pictureframe* version 2.3 (Olympus).

Subcellular fractionation

Harvest 1×10^7 cells grown in selective medium lacking uracil, wash once with 1 ml sorbitol buffer (10 mM Tris, pH7.6, 0.8 M sorbitol, 10 mM NaN_3, 10 mM KF, 1 mM EDTA, pH 8.0), centrifuge and remove supernatant. Wash again with 1 ml sucrose buffer (10 mM Tris pH7.6, 1 mM EDTA, 10% [wt/vol] sucrose), and then resuspend the cells in 1 ml sucrose buffer containing protease inhibitors (10 μg/ml phenylmethylsulfonyl fluoride, 2 μg/ml leupeptin, and 2 μg/ml pepstatin A). Mechanically disrupt the cells with glass beads and centrifuge at 300xg for 5 min to remove any unlysed cells. Mix 0.5 ml of supernatant with 0.5 ml of 50 % (wt/vol) sucrose in 10 mM Tris (pH 7.6), 1 mM EDTA, and layer on top of a 4 ml of 30-60% linear sucrose gradient prepared in 10 mM Tris (pH 7.6) and 1 mM EDTA. For the gradient separation, overlay the cells on the sucrose cushion and centrifuge at 150,000×g for 20 hours. Collect fractions (≈250 μl) from bottom of the gradient by inserting a long blunt-end needle into the bottom of the tube. Make sure that the needle rests on the bottom of the ultracentrifuge tube. Dilute 10 μl of each fraction 1:1 in 2x sample buffer. Warm samples for 10 min at 37ºC and then load on a NuPAGE 12 % Bis-Tris SDS-polyacrylamide gel (Invitrogen). Other gels can be substituted but this manufactured gel gave the best-looking gel for publication. Transfer the proteins via wet transfer onto a PVDF membrane (Invitrogen). After transfer, block the membrane in 1% non-fat dried milk in PBS/0.1% Tween 20. The yeast pheromone receptor, Ste2p-FLAG, which is expressed by the BJS21 strain, was used as a positive control for plasma membrane expression of the receptor. After blocking, probe the membrane for Ste2p-FLAG expression with an anti-FLAG M2 antibody (1:25,000 dilution, Eastman Kodak Co.) and human CXCR2 antibody (1:10,000 dilution, sc-7304, *SantaCruz Biotechnology*) together, which were incubated at 4ºC overnight. Make all dilutions in wash buffer. Wash twice with PBS/0.1% Tween 20, then add the anti-mouse HRP-conjugated secondary Ab (1:10,000 dilution, eBioscience) for 30min. Wash blots 4x with PBS/0.1% Tween 20 and then detect with ECL (Amersham).

Identification of CXCR2 CAMs in the yeast strains

CXCR2 CAMs were identified in the *FUS1-HIS3* yeast strains when they grew on medium lacking uracil, histidine and in the presence of 3-amino-1,2,4-triazole (3-AT), which is used to suppress endogenous *HIS* expression. The CAMs activate the chimeric G proteins resulting in activation of the pheromone response pathway and subsequent activation of the *fus1* promoter upregulating the *HIS* auxotrophy gene. In order to confirm and quantify the degree of constitutive activation, a plasmid containing β-galactosidase (*lacZ*) under the control of the *FUS1* promoter was transformed into these strains. The plasmid *FUS1-lacZ* (pMD1325) allows expression of *lacZ* after induction of the pheromone pathway. This plasmid also contains a *LEU2* selectable marker for selecting transformants [188]. Once the transformants were created, the amount of β-galactosidase produced was quantified using a standard kit.

Random mutagenesis

Perform random mutagenesis by using error-prone PCR [189]. Synthesize primers up and downstream of the CXCR2 ORF to include unique restriction sites for cloning into the expression vector (*HindIII* and *XbaI*). Alter three parameters in order to increase the mutagenic potential of the PCR reaction. First, use low fidelity Taq polymerase (Fisher BioReagents). Second, adjust the final concentration of dTTP/dCTP to 0.8 mM while keeping the remaining nucleotides at 0.25 mM [190]. Alteration of the ratio of nucleotides increases the likelihood of misincorportions during the amplicon synthesis. Finally, add manganese chloride to a final concentration of 500nM. Manganese chloride concentrations lower than 500 nM are less mutagenic. Digest the PCR products from random mutagenesis with *HindIII* and *XbaI*, and ligate into the p426GPD yeast expression vector by standard cloning procedures. Select yeast colonies (about 200) on media lacking uracil. Extract plasmid encoding the CXCR2 CAMs by using a yeast plasmid miniprep kit (Zymoprep^{TM}, ZYMO RESEARCH). Then transform the extracted yeast plasmid *E.coli* (MAX Efficiency® DH5α™ Competent Cells, Invitrogen) in order to acquire enough DNA for sequencing. Purify the CXCR2 CAMs/p426GPD plasmid using a miniprep kit (Promega) and sequence using primers flanking the multiple cloning regions.

β-galactosidase assay

Plasmid pMD1325 (gifted from Dr. Dumont) contains a *FUS1-lacZ* that is inducible by receptor activation [188]. β-galactosidase assay was performed as previously described [191]. Briefly, grow transformed yeast strains CY1141 and/or CY12946 (with the p426GPD expressing CXCR2 CAMs and pMD1325) overnight in selective growth media at 30ºC until they reach 5×10^6 cells/ml. Wash with sterile water, and grow at 30ºC in selective media for one doubling based on a hemocytometer count, Measure basal activity of β-galactosidase using a yeast β-galactosidase assay kit (Pierce) according to the manufacturer's instructions.

This allowed the comparison of β-galactosidase production from yeast expressing the wild-type CXCR2 containing strains normalized to the activity of each mutant.

Transfection of NIH3T3 cells to establish stable cell lines expressing CXCR2 CAMs

In a 6-well dish transfect 2 μg of DNA and 4 μl of lipofectamine 2000 (Invitrogen) into $5x10^6$ NIH3T3 cells. The transfection efficiency was optimized by varying DNA and lipofectamine concentrations with an indicator plasmid such as pcDNA3.1 expressing GFP. About 24-48 post transfection, change the growth medium with medium supplemented with 0.8 g/L of G418 sulfate. Replace the medium with fresh selection media and wash with ice-cold PBS every 3 days for 14-21 days. This is the period required for the selection of stably transfected NIH3T3 cells. Untransfected NIH3T3 cells will detach and will be washed away during the medium exchanges. Once all of the cells have died in the untransfected control, keep the growing cells in selective medium until colonies develop. Once colonies have formed, remove media from the plate and circle colonies with a colored pen on the bottom of the plate. Choose 5-10 colonies per construct to check for expression. Place a cloning disc (Scienceware) that has been soaked in trypsin-EDTA solution (Hyclone), over the top of the colony for 2-3 minutes. Place the disc containing the stable clone into a well of a 24-well plate containing selection media. Change the media everyday until the cells have achieved 80-90% confluency. Trypsinize the confluent well of cells and transfer to a 6-well dish and maintain in selection media until 80-90 % confluency. Expand the cells into a T-25 cell culture flask and analyze for CXCR2 expression. Verify the surface expression of the receptor for each of the clonal population by immunostaining followed by flow cytometery analysis using a FACs machine (Calibur, BD biosciences). Trypsinize 1×10^6 stably transfected cells, wash with ice-cold PBS and then block with 1% goat serum in PBS. Incubate cells with a PE-conjugated human CXCR2 specific antibody (R&D Systems, FAB331P) for 30 min at room temperature. Wash cells once with PBS and fix with 4% paraformaldehyde and analyze by flowcytometry. After verifying expression, expand cells and store in 10% DMSO in media in the freezer (-140 ºC) (liquid nitrogen is adequate) until further analysis. This is step is important as NIH3T3 cells will spontaneously transform upon passages above 10-15.

Characterization of CXCR2 CAMs in mammalian cells

To characterize the constitutive activity of the different CXCR2 CAMs, NIH3T3 stable cell lines were assessed for anchorage independent growth and the loss of contact inhibition [192]. Additionally, impedance measurements allowed quantitative measurements of cellular proliferation and morphological changes associated with cellular transformation. This electrochemical technique has been applied to biological studies that include cellular barrier function, attachment, spreading, and adhesion [193] [194] [195] [196]. To characterize the specific genes that may be involved these morphological changes, luciferase reporter assay were utilized. For example, Cannon and Cesarman [197] demonstrated that KSHV ORF74 constitutively activates transcription of AP-1, NF-kB, CREB, and NFAT-responsive promoters using luciferase assays. The ultimate test of whether these CXCR2 CAMs lead to tumorgenicity, was the implantation of cells into the hind flank of nude mice and measuring tumor formation in *vivo*.

Foci formation assay

Seed 100 stably transfected NIH3T3 cells on top of 2×10^5 untransfected NIH3T3 cells in normal growth medium with a CXCR2 antagonist, SB225002 (Calbiochem) added to a final concentration of 1μM. This is added in order to prevent growth of the WT CXCR2 transfectants, which may respond to CXC chemokines present in the serum. Change the growth media every 2 or 3 days. After 5-7 days the cells should start to form colonies. 10-14 days after initial the seeding, fix the cells in 70% ethanol and stain with crystal violet solution. If the cells grow too fast and begin to detach from the plate, stop the culture earlier and fix and stain. To enumerate the number of colonies, photograph the well and analyze the images using *ImageJ* version 1.43 (Rasband, W.S., ImageJ, U. S. National Institutes of Health, Bethesda, Maryland, USA, http://rsb.info.nih.gov/ij/, 1997-2009).

Soft-agar growth assay

Blend a total of 1×10^3 stably transfected NIH3T3 cells in pre-warmed (37°C) 0.4 % soft-agar containing regular medium, and then pour the mixture on top of 0.8 % agar in a 6-well plate. Feed cells every 3 days with 5 drops of media per well. After incubation for 3 weeks, add 500 μl of 0.5 mg/ml p-iodonitrotetrazolium violet and incubate for overnight at 37°C. Photograph wells and visualize colonies under an image analyzer (LAS 4000, Fujifilm Co.). Count and measure the number and size of colonies using *ImageJ*.

Electrical impedance measurements for cellular proliferation

Figure 5 shows schematic diagrams, three key factors, and exemplified images in regard to cellular micro-impedance measurement. Impedance is the frequency-dependent opposition of a conductor to the flow of an alternating electrical current. An alternating current is used for bioelectrical impedance measurement because it penetrates the cells at low levels of voltage and amperage. The corresponding experimental setup consists of lock-in amplifier, data acquisition board, computer, and electrodes. Dynamic biophysical analysis is followed by cellular micro-impedance data obtained by using LabVIEW (National Instruments Corp.). An ac 1 Vrms reference signal via a series 1 MΩ resistor is provided as a reference voltage. A National Instruments SCXI-1127 switch is successfully employed to connect the various working electrodes with the counter electrode of each array. The source voltage generator resistance (Rs) was 50 and the input impedance equivalent to a parallel resistor (Rv) and capacitor (Cv) combination of 10 MΩ and 10pF, respectively.

During the cellular micro-impedance scans, data is acquired at a rate of 32 Hz for 2 seconds using a 30 ms filter time constant and 12 dB/decade roll off.

Averages and standard deviation estimates are obtained from the 64 sampled data points over the 2 second time intervals. During the experiments, cultures are maintained at 37 °C and 5% CO2. Naked scans are always preceded to optimize the sensitivity, to check for any electrodes debris or defects and, most importantly to be used as reference levels for normalization. After repeated careful examination to select pertinent a cell density, a total of 3×10^4 transfectants and untransfected NIH3T3 cells are inoculated in 400 µl normal growth medium onto the electrode. One well remained untreated to provide a control.

Electrical impedance measurements for the foci formation assay

The impedance apparatus, as described above, is also employed to dynamically examine colony-like foci formation of mutated cell lines. 400 µl of normal growth medium containing 6×10^4 untransfected NIH3T3 cells is filled in each well to produce a cellular base layer providing growth factors. A total of 3×10^4 transfectants, or untransfectant controls, are seeded on top of the untransfected NIH3T3 layer. Seeding is performed at the saturated growth time point (approximately 27 hours) with another 100 µl normal growth medium. Impedance measurements continue without any interruption during the seeding process for another 61 hours to produce a second set of scans. Time-dependent changes in the normalized resistance and reactacne can be obtained in real time.

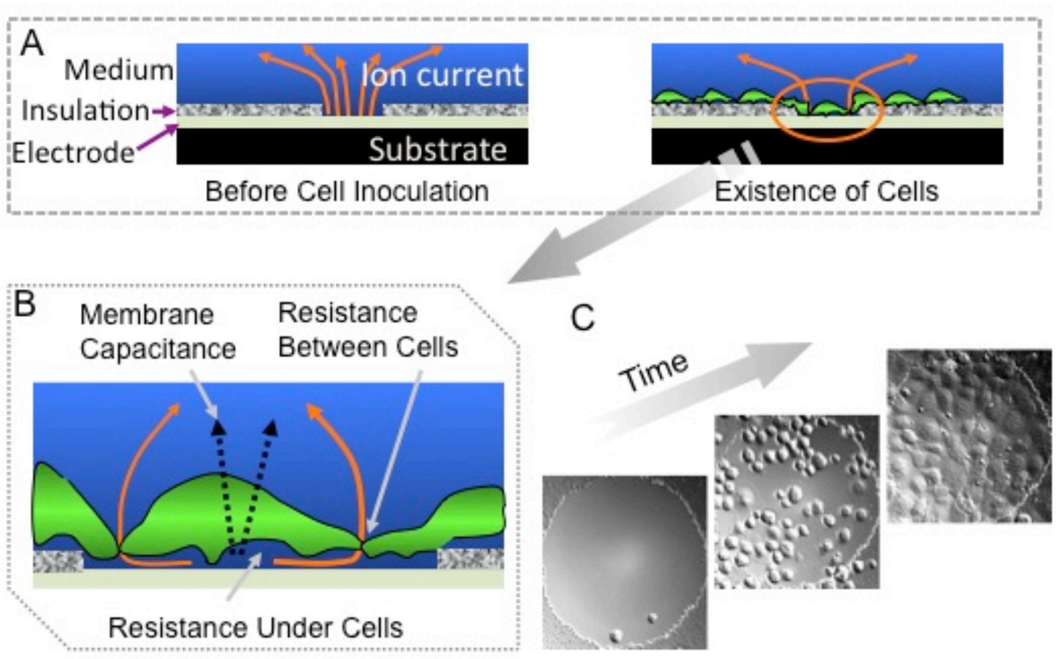

Figure 5. Overview of cellular micro-impedance measurement.

Impedance measurements reflect the electrical resistance and reactance across a cellular membrane and through a cell monolayer. (A) Schematic drawings show current flows before and after cell inoculation. Each chamber contains a substrate with an electrode, a layer of conductive material, an insulation layer and a small chamber containing the cellular growth medium. As cells attach, there is a modification of the current flow. (B) This drawing shows the three important parameters in impedance measurements, which characterize the cellular barrier (1) the current flow under the cells (2) the current flow between the cells and (3) the capacitively coupled current through the cellular membranes. (c) Cellular growth images on 250-micron diameter electrodes. These photomicrographs show cellular changes in their morphology, their adherence to each other, and to the substrate over time.

The bioelectrical impedance measurement can provide an invasive, sensitive, and quick ways of dynamically examine cellular physiological changes.

Luciferase reporter assays

To measure the basal level of NF-κB, transiently co-transfect HEK293 cells (4.0×10^5), in a 6-well plate, with 2.0 μg of 3X MHC-Luc [198], 0.5 μg of pRL-CMV as an internal control, and 0.5 μg of CXCR2 constructs with LipofectamineTM 2000 (Invitrogen). At 24 h posttransfection, synchronize transfected cells by serum starvation and then harvest. Assay cells with Dual-Glo^{TM} Luciferase Assay System following manufacturer's instructions (Promega).

Tumor Formation in vivo

Subcutaneously inject stably expressed NIH3T3 (2×10^5/mice) into the flanks of 6 to 8 week old athymic *nu/nu* mice (Jackson Laboratory). The protocol for this animal experiment was reviewed and approved by the Institutional Animal Care and Concerns Committee of the University of Tennessee. Once tumors are beginning to appear to be seen (from 3-4 wks), measure daily. If one member in the group achieved a tumor size of 1.5 cm, all members of the group were euthanized. Resect, measure and place tumors into 10% buffered formalin. Cut thin sections and stain with hematoxilin and eosin to characterize the types of cells that have infiltrated and the morphology of the tumors themselves.

CHAPTER 4. RESULTS

Receptor expression in the S. cerevisiae strains CY1141 and CY12946

To identify the expression of CXCR2 CAMs in the yeast, Immunofluorescence and subcellular fractionation were used to demonstrate proper expression and cellular localization before beginning CXCR2 CAM selection. Yeast strains, CY12946, expressing CXCR2 stained with an anti-CXCR2 antibody (E-2, SantaCruz Biotechnology), and a nuclear was stained with Hoechst (Molecular Probe) (Figure 6). Since the localization of the CXCR2 is not precisely distinguishable, subcellular fractionation was accomplished (Figure 7). Yeast strain, BJS21, is known to express yeast pheromone (α-factor) receptor, Ste2p, on the plasma membrane, which is a positive control (Figure 7A). CXCR2 stained with antibody specific CXCR2 show a same fraction with Ste2p in BJS2i, which indicate CXCR2 localized to the plasma membrane like as Ste2p in BJS21 (Figure 7B).

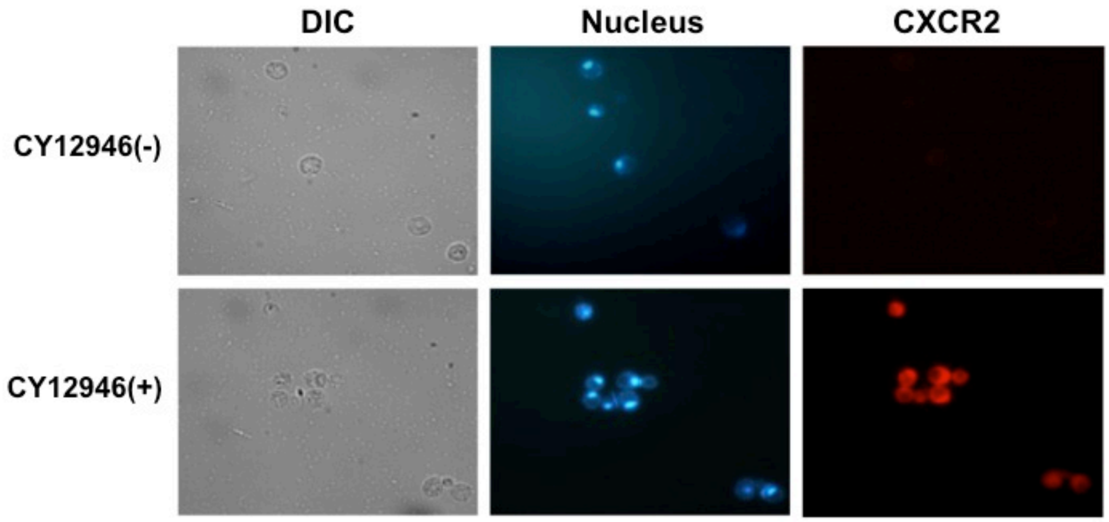

Figure 6. Human CXCR2 expression in transformed yeast strains.

Spheroplasts were generated from CXCR2 untransformed (-) and transformed (+) yeast strain, CY12946. Cells were fixed and stained with an anti-CXCR2 antibody (E-2, SantaCruz Biotechnology) and a nuclear stain (Hoechst, Molecular Probe). Cells were observed and photographed using an Olympus BX50 fluorescence microscope (100x magnification) equipped with a CCD camera and analyzed using pictureframe version 2.3 (Olympus).

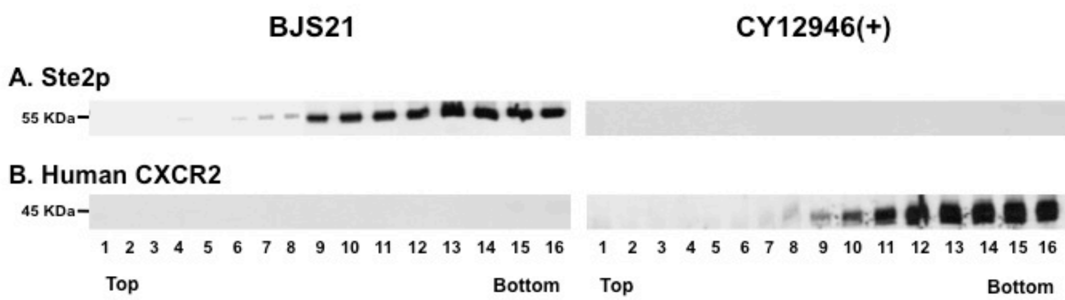

Figure 7. CXCR2 is expressed in the CY12946 strain and localizes to the plasma membrane.

Total membrane preparations from control strain, BJS21 that expresses Ste2p [199], and CXCR2 transformed strain CY12946 (+) were run over a 4 ml sucrose gradient (30-60%) and 250 ul fractions were collected from the bottom to the top of the tube. 10 ul of each fraction was run on the SDS PAGE gel and immunoblotted with either (A) anti-FLAG antibody or (B) CXCR2 (E-2, Santa Cruz Biotechnology) followed by anti-mouse HRP antibody. Blots were developed with ECL (Amersham).

PART III. Electrical impedance measurements predict cellular transformation

Published as "**Electrical impedance measurements predict cellular transformation**" **Giljun Park**, Chang K. Choi, Anthony E. English, **Tim E. Sparer** in ***Cell Biol. Int. 2009*** Mar;33(3):429-33. Epub 2009 Jan 27.

CHAPTER 1. ABSTRACT

Cellular transformation is the first step in cancer development. Two features of cellular transformation are proliferation in reduced serum and anchorage independent growth. Impedance measurements have been used to measure proliferation and attachment in normal cells. This study describes the use of impedance measurements to distinguish normal cells from transformed cells. NIH3T3 cells were transformed with a constitutively active chemokine receptor (D143V_CXCR2) and growth in reduced serum and anchorage independent growth were measured using established biological assays and compared to impedance measurements. The results of this study show that impedance measurements provide a quick and reliable way of measuring cellular transformation.

CHAPTER 2. INTRODUCTION

In Europe, there were approximately 1.7 million deaths due to cancer in 2006 [200]. Understanding the cellular processes involved in the transformation of a normal cell into a cancerous cell will lead to more effective cancer treatments. There are five characteristics of transformed cells: immortalization, growth in reduced serum, anchorage independent growth, loss of contact inhibition, and tumor formation in nude mice. Mutations in cell cycle control genes [201], growth factors [202], transcription factors [203] and degradation pathways [204] can lead to cellular transformation. One of these triggers is the over expression of a constitutively active chemokine receptor, CXCR2 [93]. The receptor normally functions to induce cellular activation, but when it is constitutively active, it induces cellular transformation. A single point mutation, Aspartic acid (D) → Valine (V) at position 143, on this receptor causes the continuous activation of signaling pathways leading to transformation [114]. Using this receptor for the transfection of mouse fibroblasts as model for cellular transformation, the ability of impedance measurements to discern transformed cells from normal cells was assessed.

Giaever and Keese [205, 206] pioneered the use of small micro-electrodes with a large counter electrode to measure cellular impedances. Impedance measurements are based on the electrical resistance and reactance across a cellular membrane and through a cell layer. This electrochemical technique has been applied to biological studies that include cellular barrier function, attachment, spreading, and adhesion [193, 195, 196, 207]. In addition, frequency dependent electrical impedance measurements have been used to evaluate the model parameters associated with cell-cell and cell-matrix junction formation [208-210]. In this study, micro-impedance measurements are used to quantitatively examine the proliferation and the morphological changes associated with cellular transformation.

CHAPTER 3. MATERIALS AND METHODS

Cell lines and expression vector

NIH3T3 mouse fibroblasts (ATCC, Manassas, VA), cultured in DMEM (Dulbecco's modified Eagle's medium) containing 10% Fetal Calf Serum (FCS) (Hyclone, Logan, UT), were transfected with pRc/CMV (Invitrogen) expressing either WT_CXCR2 or D143V_CXCR2 with the Lipofectamin ™ 2000 (Invitrogen, Carlsbad, CA) according to the manufacturer's instructions. Stable transfectants were selected with 800 µg/ml of G418.

Mutagenesis

To generate D143V_CXCR2, the WT_CXCR2 pRc/CMV expression plasmid was mutagenized using the complementary primers (D143V_Forward: 5'-GCA TCA GTG TGG TTC GTT ACC TGG CCA TTG TCC ATG C-3'; D143V_ Reverse: 5'-GCC AGG TAA CGA ACC ACA CTG ATG CAG GCC AGT AGC -3') and a modified QuickChange® method (Stratagene). Briefly, Takara LA taq™ polymerase (Takara Bio, Madison, WI) was used for the mutagenesis. Dpn I treatment was followed by PCR amplification (98 °C for 3 min, 35 cycles of 98 °C for 30 sec, 55 °C for 30 sec, and 1 cycle of 72 °C for 10 min and 72 °C for 20 min). The PCR reaction, initially cleaned with a QIAquick PCR purification kit (QIAGEN, Valencia, CA), transformed the plasmid DNA into MAX Efficiency®

DH5α™ Competent Cells (Invitrogen, Carlsbad, CA). Mutants, set up without polymerase and/or without a primer, provided negative controls.

Focus formation assay

The focus formation assay was performed based on Burger *et al.* [93]. One hundred stably transfected NIH3T3 cells were seeded on top of $2x10^5$ untransfected NIH3T3 cells in normal growth medium with 1 μM of CXCR2 inhibitor (SB 225002, Calbiochem, San Diego, CA). Foci were photographed and counted after 2 weeks incubation at 37 °C and 5% CO_2.

Cellular Proliferation Assay

Stable transfectants expressing either WT_CXCR2, D143V_CXCR2, or untransfected NIH3T3 cells were plated at $1×10^5$ cells and grown in reduced (2%) serum at 37 °C and 5% CO2. At the time points indicated, cells were trypsinized, stained with trypan blue (Freshney, 1987), and counted using a hemocytometer (Bonifacino, 2001). Each time point was measured in triplicate.

Electrical impedance measurements for the cellular proliferation assay

Figure 8 shows a schematic diagram of the micro-impedance measurement apparatus. A data acquisition and analysis system was

A.

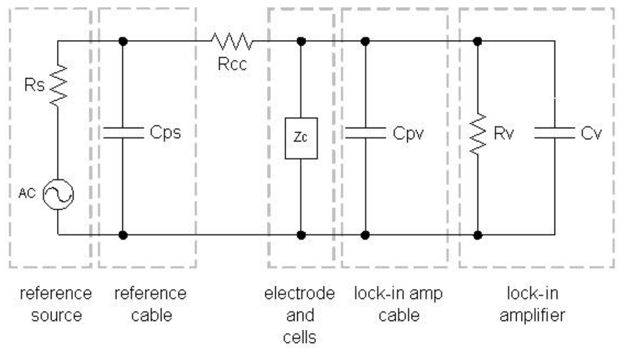

B.

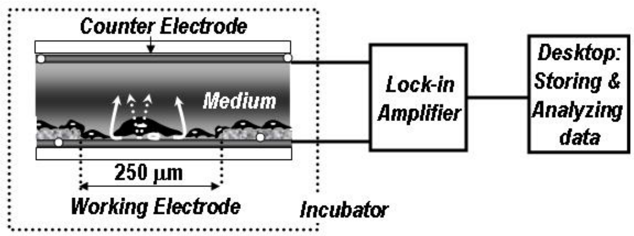

Figure 8. Electrical impedance measurement system schematics.

(a) A 1Vrms signal is applied to an electrode via a 1MΩ resistor, Rcc. The source resistance, Rs, is 50Ω and the input impedance to the lock-in amplifier is equivalent to a parallel combination of a 10MΩ resistor and 25pF capacitor, Rv and Cv, respectively. The reference cable coaxial leads and lock-in amplifier coaxial leads introduce parallel capacitances Cps and Cpv, into the circuit. The electrode impedance, Zc, is estimated by voltage measurements and a voltage-to-impedance conversion based on this circuit. (b) An environmental chamber maintains a humidified, 37°C and 5% CO_2 atmosphere for dynamic long time-lapse measurements. The measured impedance is a function of the current flow under the cells, between the cells, and the capacitively coupled current through the cell membranes.

implemented using LabVIEW (National Instruments Corp.). A reference voltage source provided an ac 1 Vrms reference signal via a series 1 MW resistor, Rcc, to a gold electrode array (Applied Biophysics). A National Instruments SCXI-1127 switch made successive connections between the various working electrodes and the counter electrode of each array. The source voltage generator resistance, Rs, was 50W. An SR830 lock-in amplifier (Stanford Research Instruments) with an input impedance equivalent to a parallel resistor, Rv, and capacitor, Cv, combination of 10 MW and 10 pF, respectively, measured the electrode voltage. Direct measurements of the cable parasitic capacitances were made using an LCR meter and incorporated into a circuit model to estimate the impedance based on the lock-in amplifier voltage measurements.

Preliminary naked scans were performed to optimize the sensitivity and to check for any electrodes debris or defects. A total of $3x10^4$ transfectants and untransfected NIH3T3 cells were inoculated in 400 µl normal growth medium with 1 µM of CXCR2 inhibitor, SB225002, onto the electrode. One well remained untreated to provide a control.

Electrical impedance measurements for foci formation

Using the impedance apparatus, as described above, electrodes were inoculated with 400 µl of normal growth medium containing $6x10^4$ untransfected NIH3T3 cells to produce a cellular base layer providing growth factors. A total of $3x10^4$ transfectants, or untransfectant controls, were seeded on top of the NIH3T3 layer. Seeding was performed at the saturated growth time point (approximately 26 hours) using 100 µl of normal growth medium in the presences of a CXCR2 inhibitor to give a 1 µM final concentration. Impedance measurements were acquired for another 61 hours to produce a second set of scans. During the cellular micro-impedance scans, data was acquired at a rate of 32 Hz for 2 seconds using a 30 ms filter time constant and 12 dB/decade roll off. Averages and standard deviation estimates were obtained from the 64 sampled data points over the 2 second time intervals. During the experiments, cultures were maintained at 37 °C and 5% CO_2.

CHAPTER 4. RESULTS

Impedance measurement for measuring cellular proliferation

One of the hallmarks of cellular transformation is growth in reduced serum. In order compare micro-impedance measurements with traditional measurements of cellular growth, the growth of stable transfectants were measured in reduced serum media. Figure 9A shows the results of harvesting and counting the cells at different time points. The D143V transfectant proliferation rate is significantly greater ($p<0.00001$) than the WT_CXCR2 or untransfected controls. Figures 9B and 9C summarize the resistance and reactance micro-impedance measurements that were carried out in parallel with the growth measurements shown in Fig. 9A. Although resistance measurements initially did not show a marked difference between WT_CXCR2 and D143V_CXCR2, at 58hrs (35000 min.) the WT_CXCR2 growth plateaued while D143V_CXCR2 continued growing for the remainder of the experiment (Figure 9B). Micro-impedance fluctuations, a measurement of cellular motility/attachment, were also consistently higher in transformed cells. The reactance measurements, however, more closely mimicked the growth curves generated with more traditional hemacytometer measurements. These data show that impedance measurements can be used to distinguish growth patterns of transformed cells compared to non-transformed cells.

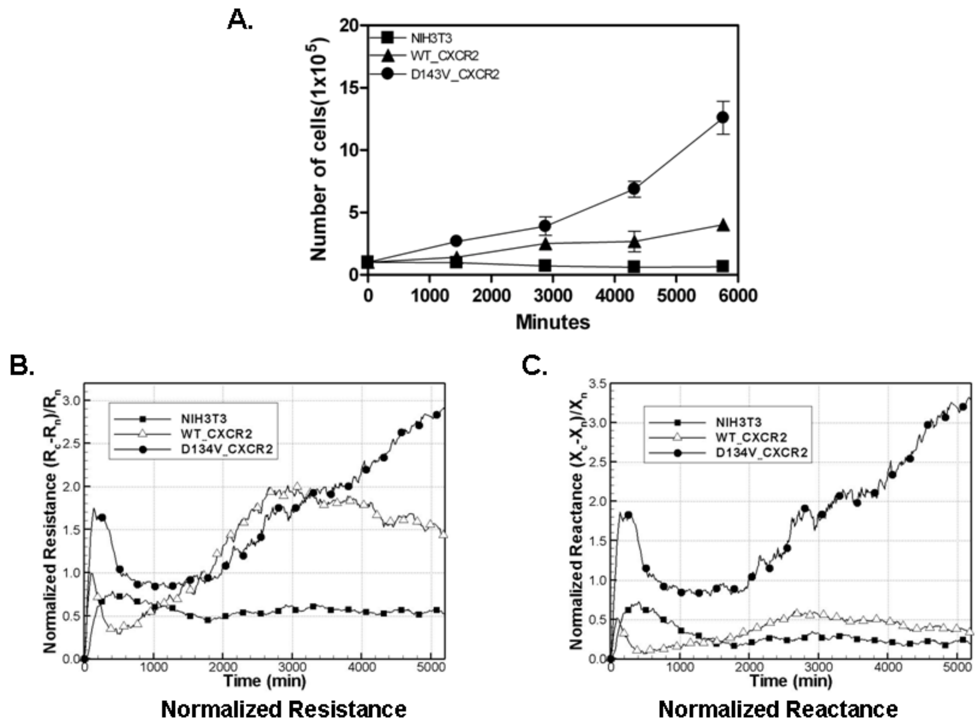

Figure 9. Impedance measurements distinguish the growth rates of transformed verses untransformed cells.

Stable transfectants expressing either WT_CXCR2, D143V_CXCR2, or untransfected NIH3T3 cells were grown in reduced (2%) serum and counted at different time points (A). Each data point represents the mean (± s.e.m.) of three independent experiments; (B) Normalized resistance $(R_c-R_n)/R_n$, recorded at 5.62 kHz, and (C) normalized reactance $(X_c-X_n)/X_n$, recorded at 56.2 kHz, for the direct inoculation of untransfected and transfected NIH3T3 cells. The terms R and X represent the resistance and reactance, respectively and the subscripts c and n indicate cell covered and naked scans, respectively.

Foci formation can be detected with impedance measurements

The loss of contact inhibition during cellular transformation allows these cells to grow on top of one another forming foci. Historically, foci were counted visually after staining with a dye such as crystal violet. Using this technique, the number of foci formed with either WT_CXCR2 or D143V_CXCR2 transfectants (Figure 10A, 10B) was quantified. These data show that the transformed cells (D143V_CXCR2) form significantly more foci than WT_CXCR2 ($p<0.00001$).

To compare these findings with the micro-impedance measurements, impedance measurements using an experimental set up similar to the one described above. The main difference is that a monolayer of untransfected NIH3T3 cells is attached to the electrode to provide growth factors for foci development. In spite of this more complex set up, both resistance (Figure 10C) and reactance measurements (Figure 10D) show that D143V_CXCR2 attaches and proliferates much more rapidly than either WT_CXCR2 or untransfected cells. This illustrates that impedance measurements can accurately measure foci formation as an indicator of cellular transformation.

Figure 10. Impedance measurements assess increased attachment and foci formation in transformed cells.

In parallel with impedance measurements, foci were measured after 2 weeks. Stable transfectants expressing either WT_CXCR2, D143V_CXCR2, or untransfected NIH3T3 cells were seeded on top of the untransfected NIH 3T3 cells, and cultured in the presence of CXCR2 inhibitor (SB 225002, Calbiochem). (A) An example of the foci that were counted is representative of three independent experiments. (B) No foci were detected on the untransfected contols. Bars represent the mean (± s.e.m.) of three independent experiments each carried out in triplicate. Impedance measurements were carried out under a similar experimental setup. (C) Normalized resistance (Rc-Rn)/Rn, recorded at 5.62 kHz, and (D) normalized reactance (Xc-Xn)/Xn, recorded at 56.2 kHz, for untransfected and transfected NIH3T3 cells. The terms R and X represent the resistance and reactance, respectively, and the subscripts c and n indicate cell covered and naked scans, respectively. For the sake of clarity, symbols represent 30 data intervals. The arrows indicate the point of addition of either the transfectants or untransfected controls. The increases in resistance and reactance are consistent with increased cellular proliferation and multi-layer focus formation.

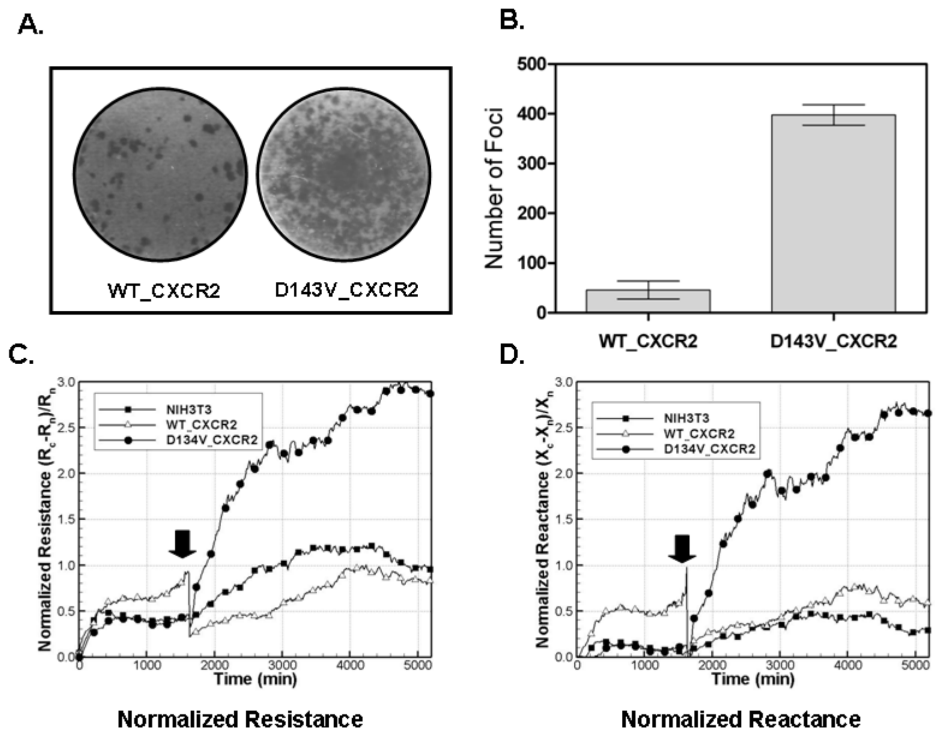
A.
WT_CXCR2
D143V_CXCR2
B.
Number of Foci
500
400
300
200
100
0
WT_CXCR2
D143V_CXCR2
C.
NIH3T3
WT_CXCR2
D134V_CXCR2
Normalized Resistance (R_c-R_n)/R_n
Time (min)
Normalized Resistance
D.
NIH3T3
WT_CXCR2
D134V_CXCR2
Normalized Reactance (X_c-X_n)/X_n
Time (min)
Normalized Reactance

CHAPTER 5. DISCUSSION

Several well-known methods to examine cell proliferation include fluorescence microscopy, flowcytometry, and biochemical assays [211]. While these methods are stationary and need fluorescent or radioactive probes, micro-impedance measurements are a bio-analytical technique capable of non-invasively and dynamically monitoring proliferation in real time without the use of chemical probes. Another benefit is its high sensitivity to distinguish between transformed and untransformed cells. Both the resistance and reactance of transformed cells increased faster and to larger values than WT_CXCR2 or untransfected NIH3T3.

The measured impedance is a sensitive and complicated function of the degree of cellular proliferation, cell-matrix attachment, and cell-cell attachment. As the cells proliferate and attach to the surface and each other, a systematic increase in the measured impedance occurs. Uncontrolled proliferation characteristic of transformed cells is, therefore, consistent with the systematic impedance increase observed in this study. Although, the actual impedance values vary between different experiment runs, this pattern was consistently observed with transformed cells compared to untransformed cells. The increase in the microimpedance fluctuations is also consistent with increased micromotility associated with transformed cells.

PART IV. Novel constitutively active point mutations in the NH2 domain of CXCR2 capture the receptor in different activation states

CHAPTER 1. ABSTRACT

The chemokine receptor, CXCR2, is a member of the rhodopsin family of GPCRs. Normal CXCR2 activation leads to cellular migration, wound healing, and angiogenesis. Using a high throughput yeast screen we identified a novel point mutation, D9H, which leads to constitutive activation (CA). Generation of stable transfectants expressing mutant CXCR2s (either D9H or positively charged substitutions, D9K and D9R, or D143V as a positive control) showed that all lead to CA but differential levels of cellular transformation (i.e. foci formation and soft agar growth). To further investigate how D9 mutations lead to differential CA, we used pertusiss toxin (PTX) sensitivity in foci formation assays to show that D9R uses the $G\alpha_i$ like WTCXCR2 and D143V, while D9H and D9K do not. All CA receptors use the JAK pathway based on sensitivity to the inhibitor, AG490. Phosphorylation of PLC β3 and the sensitivity of foci formation to the inhibitor of PLC β3, U73122, demonstrates that all utilize the $G\alpha_q$ subunit. Interestingly, D9R receptors use both $G\alpha_i$ and $G\alpha_q$. The CA receptors induce phosphorylation of the epidermal growth factor receptor (EGFR), which suggests transactivation between CXCR2 and EGFR. These data illustrate two novel and important findings. First, the amino terminus of CXCR2 controls activation and signaling via multiple G protein subunits to elicit downstream signaling. Second, our work supports the "functional selectivity" model for GPCR activation., The different CA CXCR2s, mimicking agonist activation, have multiple conformations that lead to differential activation.

CHAPTER 2. INTRODUCTION

Although there are many contributing factors in tumorigenesis, chemokines and their receptors play a role in tumorigenesis and metastasis [134]. Chemokines function normally as small chemoattractant cytokines that are involved in inflammatory, developmental, and homeostatic processes [174]. Deregulation of this system is associated with the development of cancers and metastasis. One possible deregulation of chemokine activity is the constitutively active mutant (CAM) receptor [134, 175]. CAM receptors cause the alteration of structural constraints leading to an active conformation. This change induces ligand independent activity called constitutive activity [176]. The CAM GPCR is a valuable model for explaining the basic molecular events involved in the development of a variety of human diseases [177]. The best example of chemokine receptor constitutive activity and cancers is the Kaposi sarcoma herpesvirus chemokine receptor, ORF74, which has a ‘VRY’ motif instead of ‘DRY’ motif between third transmembrane domain and second intracellular loop and has been shown to be constitutively active [93, 106, 178].

CXC chemokine receptor 2 (CXCR2) is a G-protein-coupled receptor (GPCR) [179] expressed on neutrophils, some monocytes, endothelial cells, and some epithelial cells [152] (Figure 11). Activation of CXCR2 with ELR+ CXC chemokines is responsible for the leukocyte migration, degranulation, cellular differentiation, and ELR+ CXC chemokine mediated

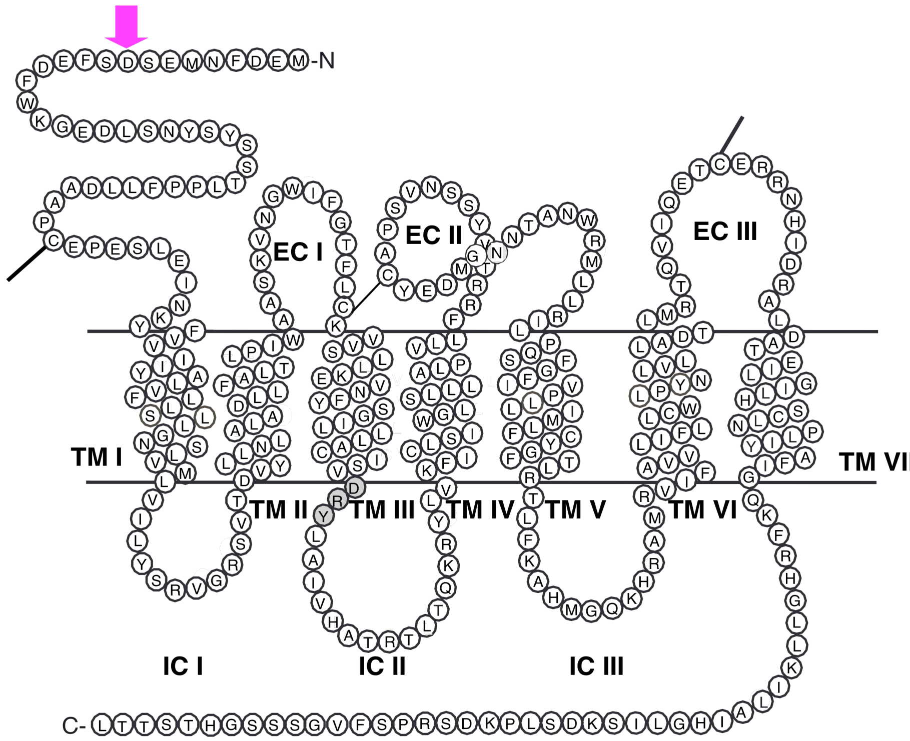

Figure 11. Schematic diagram of the human CXCR2 receptor.

CXCR2 consists of seven transmembrane domains (TM I – TM VII) connected by three extracellular (EC I - EC III) and three intracellular (IC I- IC III) loops. The conserved DRY box is shaded and the D9 residue is indicated with an arrow. The transmembrane domains were predicted using HMMTOP, TMPred, and PHD.

angiogenesis [123]. Binding and activation of CXCR2 with CXCL1 (Groα) was shown to increase melanoma growth [212]. The degree of CXCR2 expression was shown to correlate with metastasis in a nude mouse [213]. Moreover, CXCR2 expression is related to of the metastatic potential in renal carcinomas [165], adult myeloblastic leukemias [214], liver [215] and lung cancers [159]. The most extensive evidence for CXCR2 expression/transformation/metastasis comes from melanomas. CXCR2 is found on highly malignant melanoma cell lines as well as from isolates of human melanomas [161, 216-218].

In GPCRs that have been mutagenized *in vitro* to generate CAMs, most mutations mapped to the transmembrane regions, C-terminal region, and second and third intracellular loops [81, 219]. However, no mutations or deletions in the N-terminal domain have been identified that result in a constitutively active chemokine receptor.

In this study, human CXCR2 is expressed a genetically engineered yeast strain of *Saccharomyces cerevisiae* to screen for potential CXCR2 CAMs. Randomly mutagenized copies of the CXCR2 ORF cloned into a yeast expression plasmid allows for an unbiased selection of CAM receptors. From this yeast screen we described a single amino acid substitution in the N-terminal region of CXCR2 leads to a constitutively active CXCR2. Substitution of the aspartic acid residue (D9) to amino acids with different properties results in constitutive activity in yeast. These CAM receptors expressed in NIH3T3 cells induce cellular transformation as evaluated by foci formation, anchorage-independent growth in soft agar and tumorigenesis in nude mice. In addition, these constitutively active receptors lead to a PLC β3 mediated signal transduction cascade potentially induced by $G\alpha_{q/11}$ as well as NF-κB activation, which plays an important role in transactivation of angiogenic CXC chemokines [220].

Our results suggest that the N-terminal domain of the CXCR2 plays an important role in the regulation of structural constraints that serve as regulators of receptor activation. In addition, differential usage of Gα proteins, such as $G\alpha_i$ and/or $G\alpha_{q/11}$, induced with the different CAM CXCR2 addresses important aspects of functional selectivity.

CHAPTER 3. MATERIALS AND METHODS

Yeast strains and expression vector

Genetically modified *Saccharomyces cerevisiae* strains, CY1141 (*MATα far1Δ1442 FUS1p-HIS3 ste14::trp1::LYS ste3Δ1156 gpa1(41)-G*α_{i2} *lys2 ura3 leu2 trp1 his3*) [185] and CY12946 (*MATα FUS1p-HIS3 GPA1G*$\alpha_{i2(5)}$ *can1 far1Δ1442 his3 leu2 sst2Δ2 ste14::trp1::LYS ste3Δ1156 tbt1-trp1 ura3*) [186], were a generous gifts from Dr. J. Broach (Princeton University). The plasmid p426 (ATCC #87361) contains the wild type or mutated CXCR2 gene under the control of a constitutively active promoter (GPD) and URA3 auxotrophic marker. Yeast cells were transformed each plasmid construct by the lithium acetate transformation method [221].

β-galactosidase assay

Plasmid pMD1325 (a gift from Dr. Dumont M.E., University of Rochester, School of Medicine and Dentistry) contains a FUS1-lacZ gene that is induced by receptor activation [188]. β-galactosidase assays was performed as previously described [191]. Briefly, yeast transformed with either wild type CXCR2 or mutants and pMD1325 were grown overnight in selective growth medium at 30°C to 5×10^6 cells/ml, washed by centrifugation, and grown for one doubling based on hemocytometer count at 30°C. Basal activity of β-galactosidase was measured by using a yeast β-galactosidase assay kit (Pierce) according to the manufacturer's protocols, activation is measured in Miller units. Comparing β-galactosidase activity for the wild-type strain normalized the activity of each mutant.

Random Mutagenesis

Random mutagenesis was performed by error-prone PCR [189]. Primers upstream and downstream of the CXCR2 ORF were synthesized to include unique restriction sites (*HindIII* and *XbaI*). These were used in a mutagenic PCR reaction that had three modifications in order to increase the mutagenic potential of the reaction. First, low fidelity Taq polymerase was used (Takara Biosystems). Secondly, the ratio of nucleotides used was altered to increase mistakes in the polymerase. dTTP/dCTP was adjusted to 0.8 mM (final conc.) while the other nucleotides remained at 0.25 mM [190]. Finally, manganese chloride was added to final concentration of 500nM.

Immunofluorescence Microscopy

2.0×10^5 NIH3T3 and stable transfectant cells grown on Lab-Tek II Chamber Slide (Nalge Nunc) were fixed with 4% paraformaldehyde for 10 min at room temperature, permeabilized with Triton X-100 (0.01% in PBS) for 5 min, and blocked with goat serum (1% BSA and 10% goat serum in PBS). Cells were washed three times with 1ml of PBS. After incubated with mouse monoclonal Na^+/K^+-ATPase (1:100, Santa Cruz Biotech) as a marker for plasma membrane localization for 2 h, cells were washed three times and incubated with rabbit polyclonal anti-CXCR2 antibody (1:500, Abcam) at 4°C overnight. After washing three times, cells were stained with Alexa Flour 488-conjugated goat anti-rabbit IgG (1:500, Molecular Probes) and Alexa Flour 633-conjugated goat anti-mouse IgG (1:200, Molecular Probes) for 30 min. After washing three times, cells were mounted by SuperMount medium (BioGenex) and sealed with cover slip. The cell was photographed with confocal laser scanning microscope (SP2 LSCM, Leica Microincorporation Inc.) and analyze with ImageJ version 1.43 (Rasband, W.S., ImageJ, U. S. National Institutes of Health, Bethesda, Maryland, USA, http://rsb.info.nih.gov/ij/, 1997-2009).

Reagents

Selective CXCR2 inhibitor (SB225002, Cat.No. 559405), JAK inhibitor (AG490, Cat.No. 658411), and $G\alpha_i$ inhibitor (Pertussis Toxin, Cat.No. 516562) were purchased from Calbiochem. Phospholipase C inhibitor (U73122, Cat.No. U6756) was purchased from Sigma-Aldrich.

Plasmids, Cell lines and Transfection

cDNA encoding human CXCR2 was provided by Dr. Philip M. Murphy (National Institutes of Health). The luciferase reporter plasmid 3X MHC-Luc was provided by Dr. Albert S Baldwin, Jr. (University of North Carolina School of Medicine, Chapel Hill), and pRL-CMV (promega) was a gift from Dr. William E.

Miller (University of Cincinnati College of Medicine, Cincinnati). Mouse fibroblasts (NIH3T3) and human embryonic kidney cells (HEK293) were cultured in DMEM (Dulbecco's modified Eagle's medium) containing 10% Fetal Clone (FC) 3. Immortalized mouse melanocyte cell line, parental melan-a (a gift from Dr. Ann W. Richmond, Vanderbilt University School of Medicine) was cultured as previously described [222]. Lipofectamin™ 2000 (Invitrogen) was used for both transient and stable transfections. Stable cell lines (NIH3T3 or parental melan-a) were selected with 800 µg/ml of G418 (Mediatech Inc.).

Site-Directed Mutagenesis

Single point mutations of CXCR2 in pcDNA3 were induced using the QuikChange site-directed mutagenesis kit (Stratagene) according to the manufacturer's protocols. Mutations were confirmed by sequencing.

Single Nucleotide Polymorphism Genotyping

PCR for genotyping was done as followed by Masi et al [223]. The CXCR2 coding region from either genomic DNA of lung cancer cell lines were amplified with the following primers: CXCR2 Forward with *HindIII:* 5'-CCC*AAGCTT*ATGGAAGATTTTAACATGGAGAGTG-3' and CXCR2 Reverse with *XbaI:* 5'-GC*TCTAGATTA*GAGAGTAGTGGAAGTGTGC-3'.

Cellular transformation assays

The cellular transformation assay was performed as previously described [93]. For foci formation assay, 100 stably transfected NIH3T3 cells were seeded on top of 2.0×10^5 untransfected NIH3T3 cells in normal growth medium with 1 μM of CXCR2 inhibitor (SB 225002, Calbiochem). Foci were photographed and counted after 2 weeks. For the anchorage-independent growth assay, a total of 1.0×10^4 stably transfected NIH3T3 cells were cultured in 0.3 % agar containing regular medium with SB 225002, on top of 0.6 % agar. Cells were fed every 3 days with 5 drops of growth media, and photographed after 3 wk. Photographed images were analyzed using *ImageJ* version 1.43 (Rasband, W.S., ImageJ, U. S. National Institutes of Health, Bethesda, Maryland, USA, http://rsb.info.nih.gov/ij/, 1997-2009).

Luciferase assays

NF-κB reporter assay was performed based on Sherril *et al*. [198]. To measure basal level of NF-κB, HEK293 cells (4.0×10^5) were transiently co-transfected in a 6-well plate with 2.0 μg of 3X MHC-Luc, 0.5 μg of pRL-CMV as an internal control, and 0.5 μg of CXCR2 constructs with Lipofectamine™ 2000 (Invitrogen). At 24 hours post-transfection, transfected cells were synchronized during 24 hours, and then assayed with Dual-Glo™ Luciferase Assay System following manufacturer's protocol (Promega).

Immunostaining for CXCR2 and phosphorylated signaling molecules

For the staining of stable CXCR2 transfectants, PE-conjugated CXCR2 specific antibody (R&D Systems, Cat.No. FAB331P) was utilized. Analysis of phosphorylated signaling molecules was performed as previously described [224]. Briefly, stably transfected NIH3T3 cells were serum starved during 24 hrs and fixed with 70% ethanol at -20°C for at least 1 hr, and then permeablized with 0.25% Triton X-100 in PBS on ice for 15 min. Permeablized cells were blocked with 1% goat serum at room temperature for 30 min, and then cells were stained with antibody specific phosphorylated PLC β3 (Santacruz Biotech. Cat.No. sc-34392) and PKC α/β2 (Cell Signaling, Cat.No. 9375). Alexa Fluor® 488 (Invitrogen) was used as a secondary antibody.

Tumor Formation in vivo

Stably expressed NIH3T3 (2×10^5/mice) were injected subcutaneously into the flanks of 6 to 8 wk old athymic *nu/nu* mice (Jackson Laboratory). The protocol for animal experiment was reviewed and approved by the Institutional Animal Care and Concerns Committee of the University of Tennessee.

CHAPTER 4. RESULTS

Screening for CXCR2 CAMs using a genetically modified Saccharomyces cerevisiae high-throughput system

Genetically modified yeast strains, CY1141 and CY12946, were used to identify CXCR2 CAMs. CY1141 expresses a hybrid G alpha subunit, which encodes the first 33 N-terminal residues of human $G\alpha_{i2}$ replaced with the first 41 N-terminal residues of the endogenous yeast GPA1 protein. CY12946 contains a modified Gα subunit with the last 5 C-terminal residues of yeast GPA1 replaced with human $G\alpha_{i2}$. These genetically modified G proteins allow coupling to the mammalian receptor, which induces the yeast pheromone responsive signaling pathway (Figure 12). To identify CXCR2 CAMs, wild type CXCR2 (WT_CXCR2) was randomly mutated using error prone PCR and cloned into the yeast expression vector, p426GPD. This plasmid contains an origin of replication, a glyceraldehyde-3-phosphate dehydrogenase (GPD) promoter driving expression of the inserted open reading frame, and a uracil (URA) auxotrophic marker. Transformation into the above mentioned yeast strains allowed for the selection of CXCR2 CAMs that activated the signaling pathway, which leads to activation of the pheromone responsive element and the gene for histidine auxotrophy. in the presence of 3-AT.

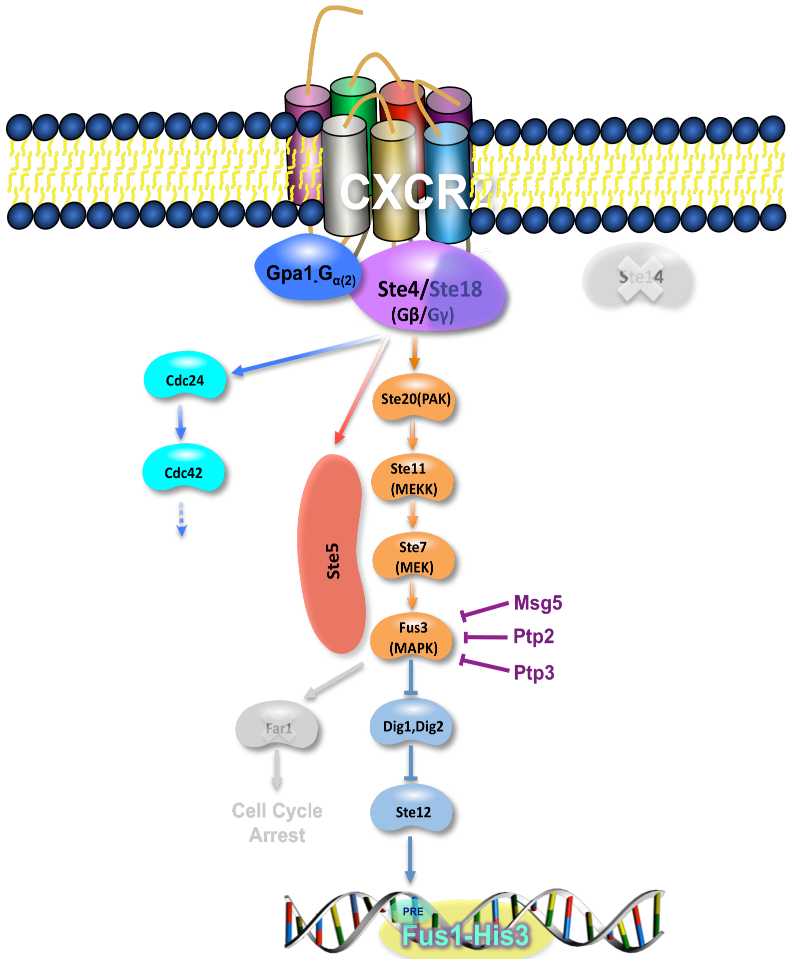

Figure 12. Schematic of yeast signaling used to identify CXCR2 CAMs.

Knock-out genes are showed in grey and an “X”. Expression of *HIS3* is under the control of the *Fus1* promoter with a pheromone-response element (*PRE*). The plasmid p426 contains the human CXCR2 gene under the control of a constitutively active promoter (GPD) and URA3 auxotrophic marker. CXCR2 CAMs are selected on media lacking histidine and uracil in the presence of 3-amino-1,2,4-triazole (3-AT) to suppress endogenous levels of histidine biosynthesis.

Approximately 300 yeast colonies grew on the His minus plates and 30 clones (approx. 30) were sequenced after retransforming the plasmids into bacterium. Among them, a single point mutation in the N-terminus of CXCR2 was identified as a CAM. The 9^{th} residue (aspartic acid (D)) was mutated to a histidine (H). The D9H mutant demonstrated constitutive activity (CA) in a β-galactosidase assay in yeast (Figure 13). These factors led us to further investigate the role of the 9^{th} residue of CXCR2. To verify the cellular and structural function of the 9^{th} residue of CXCR2 in the N-terminus, different single point mutations were generated in the 9^{th} residue. Since WT_CXCR2 encodes the negatively charged aspartic acid (D) at the 9^{th} residue, we generated mutants encoding positively charged amino acids, such as lysine (K), and arginine (R). An asparagine (N) substituted CXCR2 was generated because we had identified this mutation from a small cell lung cancer (SCLC) line, H69. As mentioned above (Part I in this dissertation) mutation of the DRY motif in CXCR2 induces CA. Therefore CXCR2 DRY mutant, D143V, was also generated and used as a positive control in all experiments.

After generating the CXCR2 mutants, the constitutive activity of each receptor was measured. A β-galactosidase assay was used to measure the degree of receptor activation in yeast using *FUS1-lacZ* reporter construct.

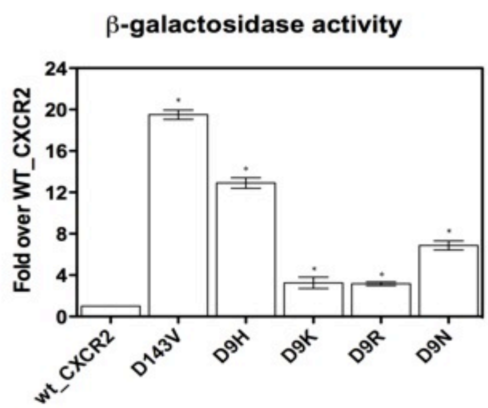

Figure 13. Constitutive activity of CA CXCR2 measured via β-galactosidase activity.

Yeast strain, CY1141, contains a plasmid, pMD1325, with the *lacZ* gene under the control of the pheromone responsive element, *FUS1*. Yeast β-galactosidase assay kit (Pierce) was used to measure β-galactosidase activity and is represented in Miller units. Bars represent the average of three independent experiments plus/minus standard deviation. Student's *t*-test (*PRISM(ver. 5.0b)* was used to determine statistical significance versus WT_CXCR2 (*; $p < 0.05$).

CXCR2_D143V shows the highest degree (approx. 20 folds over WT_CXCR2) of receptor activation in the yeast. CXCR2_D9H and D9N mutants are also higher than background (approx. 12 and 7 fold over WTCXCR2 respectively). Also, the activity of CXCR2_D9K and _D9R demonstrate significantly higher levels than WT_CXCR2 ($p<0.05$) albeit less than CXCR2_D9H and _D9N (Figure 13).

Establishment of NIH3T3 cell lines stably expressing CXCR2 CAMs

NIH3T3 cells, established from NIH Swiss mouse embryo culture, [225], have been used historically for identifying transforming events. To identify fully transformed cells due to CXCR2 CAMs, we generated clonal, stable NIH3T3 cell lines. These lines were then used in various assays for assessing the degree of transformation.

To verify the expression and localization, confocal microscopy was used (Figure 14). As a positive control to verify plasma membrane localization, an antibody specific Na^+/K^+ ATPase (Santa Cruz Biotech) was used. As shown in figure 14, WT_CXCR2 and mutants co-localized with Na^+/K^+ ATPase indicating WT_CXCR2 and CXCR2 CAMs are expressed on the plasma membrane. In addition to localization, the expression level of each receptor was analyzed using flowcytometry (Figure 15).

Figure 114. Cell surface co-localization of CXCR2 CAMs with Na^+/K^+ ATPase in NIH3T3.

Stably transfected WT_CXCR2 and CXCR2 CAMs in NIH3T3 were fixed, permeablized, and stained with a specific human CXCR2 antibody (Abcam, Cat.No. ab14935) and Na^+/K^+ ATPase (Santa Cruz Biotech. Cat.No. sc-48345). Alexa Flour 488 and 633 -conjugated secondary antibodies (Invitrogen) were visualized and photographed at a magnification x100 by confocal laser scanning microscope. Scale bar indicates 30.0 μm.

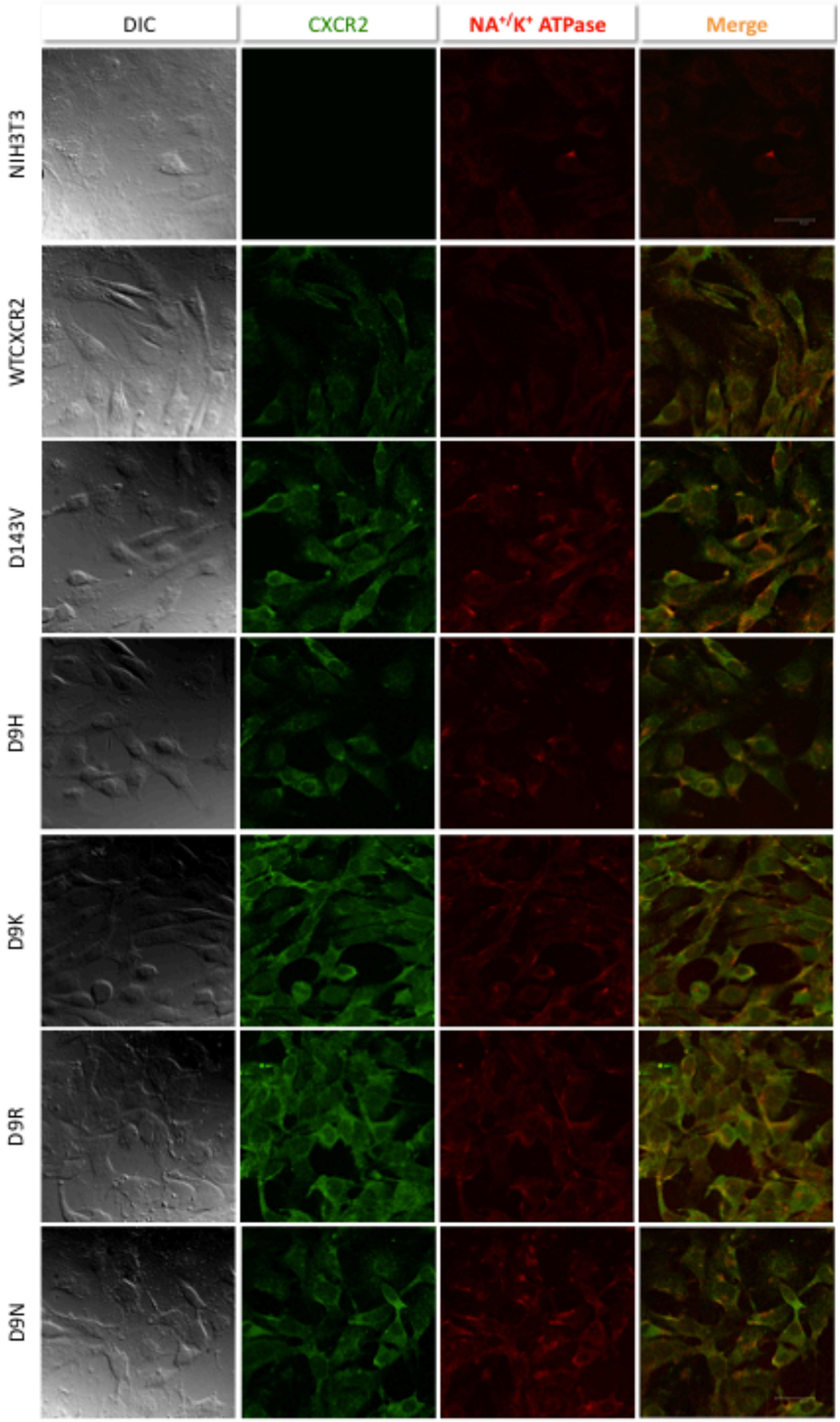
DIC
CXCR2
NA+/K+ ATPase
Merge
NIH3T3
WTCXCR2
D143V
D9H
D9K
D9R
D9N

The surface localization and relative expression level of the receptors for cell line were verified with immunostaining followed by flow cytometery analysis (Calibur, BD biosciences) (Figure 15). As shown in figure 15, all transfectants had similar cell surface expression levels. Therefore, NIH3T3 cell lines stably expressing WT_CXCR2 and CXCR2 CAMs had similar expression levels and were then used in assays for assessing the degree of transformation.

CXCR2 CAMs induction of cellular transformation

Foci formation assays, which indicate the loss of contact inhibition between adjacent cells, and growth in soft agar, which mimics anchorage independent growth were used as measurements for the degree of cellular transformation in our stable cell lines. Foci formation assay was performed by seeding 100 stably transfected NIH3T3 cells on top of the untransfected NIH3T3 cells. NIH3T3 cells expressing CXCR2_D143V, which served as the positive control, led to high numbers of foci as was previously report [93] (Figure 16). Interestingly, cells expressing the CXCR2 CAMS (D9H, D9K and D9R) also induced a high number of foci (average 50 number of foci). However cells expressing WT_CXCR2 and CXCR2_D9N induced only a few foci. These data show that CXCR2_D9H, D9K, and D9R are capable of transforming NIH3T3 cells while CXCR2_D9N does not.

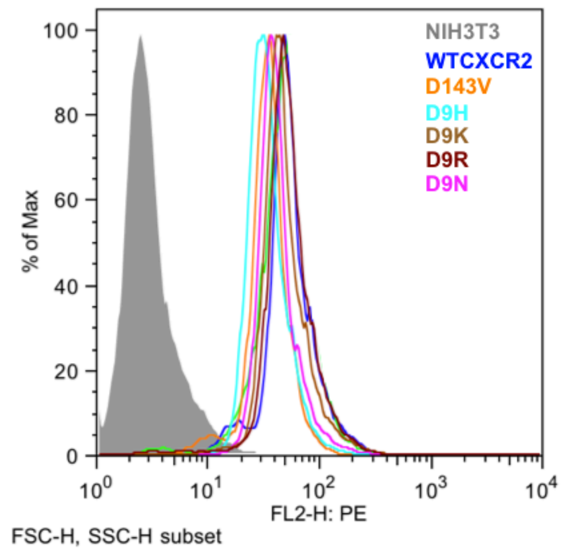

Figure 15. CXCR2 surface expression of stable transfectants.

Stable NIH3T3 transfectants were stained with PE conjugated CXCR2 specific antibody and analyzed with flowcytometry (R&D Systems, Cat.No. FAB331P).

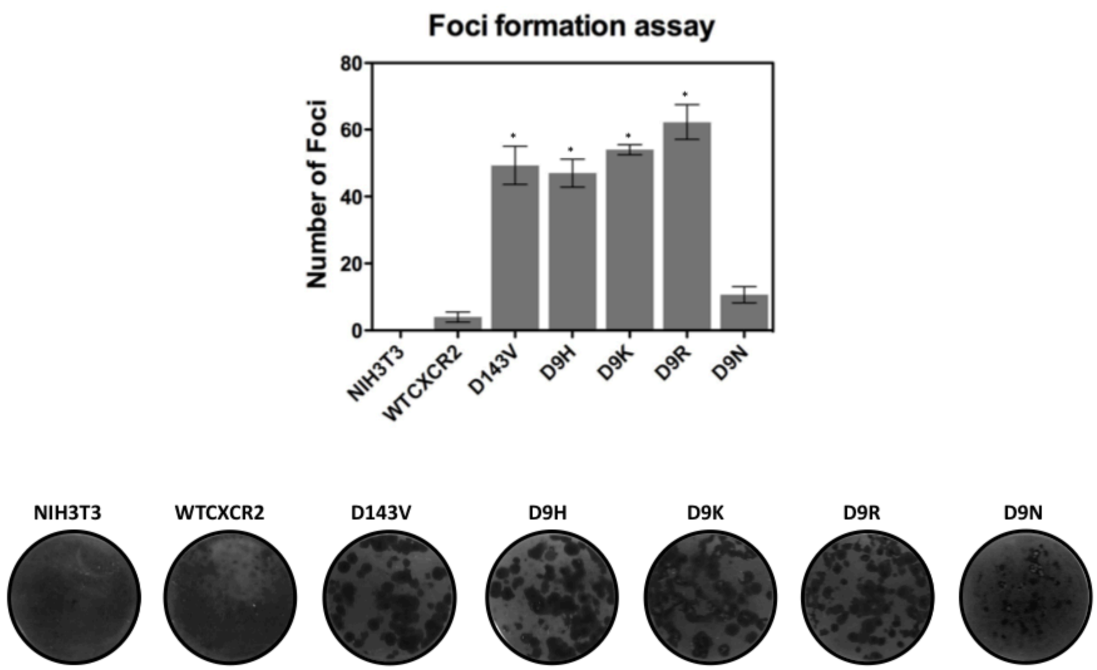

Figure 16. **CXCR2 CAMs differentially induce foci formation.**

As a measure of their transformation ability, foci formation of stably transfected WT_CXCR2 and mutants in the presence of CXCR2 antagonist (SB225002, 1 μM) were measured. Foci were photographed after 2 weeks, except D9K and D9R mutants, which were photographed after 10 days. Bars represent the average of three independent experiments +/- standard deviation. Student's *t*-test (*PRISM (version 5.0b)* was used to determined statistical significance verus CXCR2_WT (*; $p<0.05$).

Since anchorage-independent growth strongly correlates with tumorigenicity [226] and tumor metastasis [227], a soft-agar growth assay was performed to assess anchorage-independent growth. Compared to WT_CXCR2, _D9H,_D9R and_D9K showed significantly a higher number of colonies (Figure 17). In contrast, CXCR2_D9N was similar to WT_CXCR2. Interestingly, CXCR2_D9K and D9R formed a higher number of colonies than CXCR2_D143V (approx. 200 and 190 respectively), which is the positive control. Taken together the oncogenic potential of CXCR2 CAMs, such as CXCR2_D143V, D9H, D9K and D9R, was verified by their ability to form foci and colonies under soft agar under the different conditions. Mutants D9K and D9R demonstrated the most oncogenic activity because they had the most colonies and their foci developed the fastest. Although CXCR2_D143V and D9H had a lower number of colonies in soft-agar, these mutants showed a significant increase (*; $p<0.05$) compared to WT_CXCR2 and D9N. D9N was similar to background and does not have transforming abilities.

CXCR2 CAMs induction of tumor formation in vivo

Since CXCR2 mutants induced cellular transformation *in vitro*, we assessed the tumorigenic potential *in vivo* using hind flank injection of cells in nude mice. Stable transfectants were injected subcutaneously into the flanks of 6 to 8 wk old athymic *nu/nu* mice (Jackson Laboratory). After inoculation, mice were monitored and terminated once tumors reached 1.5 cm in any direction.

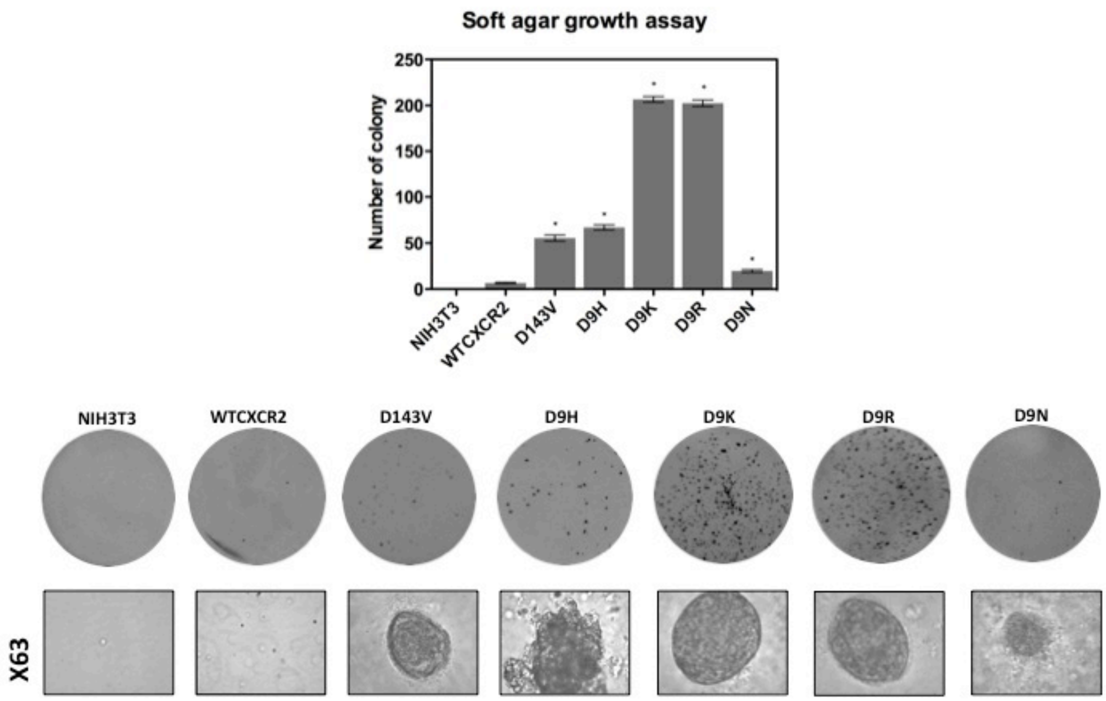

Figure 17. CXCR2s CAMs lead to differential anchorage independent growth.

Anchorage independent growth (i.e. growth in soft agar) was used as a measure of cellular transformation. Each field is representative of the overall colony formation in a six well dish (63x). Number of colonies were counted and measured using ImageJ. Bars represent the average of three independent experiments +/- standard deviation. Student's *t*-test (*PRISM (version 5.0b)* was used to determine statistical significance versus WT_CXCR2 (*; $p < 0.05$).

As shown in Table 5, untransfected NIH3T3 cells injected into the flank of nude mice did not show any tumor formation, but other mutants, including WT_CXCR2, showed tumor formation at the injection site. However CXCR2_D9K, D143V and D9H showed aggressive and fast tumor progression compared to WT_CXCR2, which required a longer incubation period to form tumors. Only 50% of the mice inoculated with cells expressing CXCR2_D9N developed tumors and showed slow formation and were terminated at 73 days after inoculation. These data indicate that constitutive activity induced by single point mutation in the N-terminus of CXCR2 plays an important role in tumor formation *in vivo*.

CXCR2 CAMs Induce differential signal transduction pathways during foci formation

Based on phenotypic transformation *in vitro and vivo*, these data strongly suggest that CXCR2 CAMs are oncogenic. These CXCR2 CAMs appear to induce differential signaling pathways based on the degree of foci formation, soft agar growth, and growth *in vivo*. In order to investigate the signal transduction pathways that contribute to cellular transformation, a number of specific signal transduction inhibitors were utilized. U73122 specifically inhibits PLC-β, which prevents IP_3 accumulation [228, 229].

Table 5. Differential tumor growth in mice.

Transfectants	Number of mice with tumors	Time until termination (Days)
NIH3T3	0/10	.
WT_CXCR2	9/10	39
CXCR2_D143V	10/10	21
CXCR2_D9H	8/10	21
CXCR2_D9K	10/10	17
CXCR2_D9N	5/10	73

2×10^5 of NIH3T3 transfectants were injected into the flanks of 6 to 8 wk old athymic *nu/nu* mice. Total mouse inoculated one cell line were termination once the tumor develops approx. 1.5 cm from one mouse in each group.

The PLC β pathway is downstream of $G\alpha_{q/11}$ activation [67, 229]. AG490 was used as an inhibitor of Janus Kinases (JAKs) which activate the transcription factors (STATs) [230]. As mentioned above PTX prevents $G\alpha_i$ mediated signal transduction cascade. Using these inhibits we mapped the downstream signaling pathways that are induced in our stable transfectants.

As shown in Figure 18, WT_CXCR2 showed transforming potential in the presence of IL-8, but in the presence of PTX formation of foci was inhibited (Figure 18-A, $P<0.05$ compared with unstimulated WT_CXCR2). Therefore, WT_CXCR2 activation with IL-8 induces $G\alpha_i$ mediated signaling pathways. PTX also prevent approximately 50% of foci formation in the case of CXCR2_D143V and D9R. However, statistical analysis using student *t*-test indicated that CXCR2_D143V ($P<0.05$) is different compared with WT_CXCR2. Otherwise CXCR2_D9R showed no difference compared with WT_CXCR2 ($P>0.05$). This indicates that G protein usage can be different between WT_CXCR2 and CXCR2_D143V. Previously Burger et al [93] also demonstrated that PTX only partially (approx. 50%) prevents IP_3 accumulation mediated by CXCR2_D143V so our data match this previous publication. Surprisingly, CXCR2_D9H and D9K show PTX independent foci formation implying that they not inducing the same pathways as WT_CXCR2 or CXCR2_D143V. CXCR2_D9R showed no statistical difference with both WT_CXCR2 and CXCR2_D143V showing that this is mutant is using a different pathway in spite of showing similar foci formation with D9H and D9K. U73122 differentially inhibits foci formation mediated by CXCR2 CAMs as well as WT_CXCR2 activation (Figure 18-B).

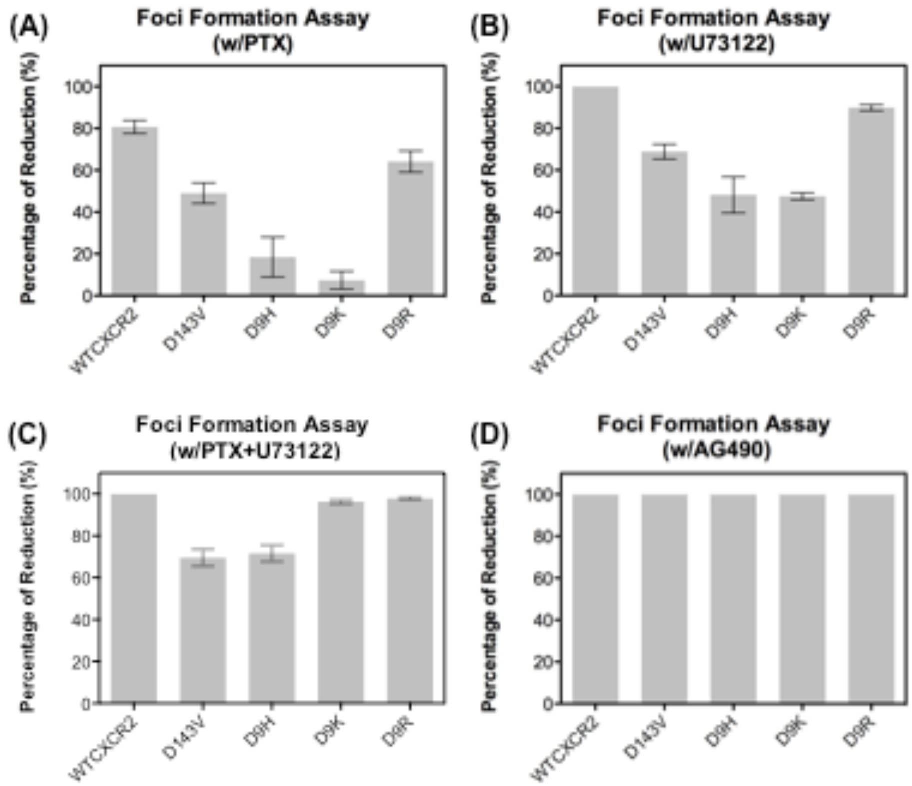

Figure 118. Inhibitors define differential signal transduction pathways for CXCR2 CAMs during foci formation.

Foci formation assay was performed in the presence of specific signal transduction inhibitors: (A) PTX (100nM) for $G\alpha_i$, (B) U73122 (2μM) for PLC-β, and (D) AG490 (50μM) for JAK. Foci formation of WT_CXCR2 was induced with IL-8 (100nM) stimulation as a positive control. Percentage reduction was expressed as (the number of foci in the untreated samples- the number of foci in the inhibitor treated samples / the number of foci in the untreated samples)x 100 **is this right? Statistical analysis using Student's *t*-test (*PRISM (version 5.0b)* was explained in the text.

There is a statistically significant difference for CXCR2_D143V, D9H, and D9K except D9R ($p>0.05$) compared with WT_CXCR2. Comparing with CXCR2_D143V and others indicated that CXCR2_D9H, D9K and D9R are not statistically significant implying that they are using PLC β as part of their signaling repertoire.

A number of CXCR2 CAMs, such as CXCR2_D9H, D9K and D9R, showed a different combinational effect with both PTX and U73122 (Figure 18-C). However, CXCR2_D143V only showed either PTX or U73122 dependent foci formation not a combinational effect. Statistically CXCR2_D143V ($p<0.05$) and D9H ($p<0.05$) showed a significant difference compared with WT_CXCR2. Only CXCR2_D9H ($p>0.05$) presented is statistically significant compared with CXCR2_D143V showing that this is using yet another more complex pattern of signaling.

Interestingly, AG490 completely inhibited foci formation for WT_CXCR2 (Figure 18-D) and others indicating that the JAK-STAT signaling pathway is directly involved in cellular transformation. This is a parallel result with a previous study that showed AG490 completely prevented foci formation for WT_CXCR2 and CXCR2_D143V [114]. Taken together these data suggest that WT_CXCR2 and CXCR2 CAMs potentially activate $G\alpha_i$ and $G\alpha_q$ mediated signaling pathways. In addition to Gα protein mediated signaling, the JAK-STAT signaling pathway probably contributes to foci formation in a G protein independent manner.

CXCR2 CAMs induction of constitutive PLC-β3 activation

Since CXCR2 CAMs demonstrated U73122 dependent foci formation, activation of PLC β was tested to determine if the CXCR2 CAMs induce this signaling pathway. Phosphatidylinositol phospholipase C (PLC) plays an important role in the induction of receptor mediated signal transduction through the origination of the two kinds of secondary messengers that are inositol 1,4,5-triphosphate (IP_3) and diacylglycerol (DAG) from phosphatidylinositol 4,5 biphosphate (PI2P) [231, 232]. There are a number of PLC isoforms that have been described, such as PLC β1, PLC β2, PLC β3, PLC β4, PLC γ1, PLC γ2, PLC δ1 and PLC δ2 [233]. Among these isoforms, the $G\alpha_{q/11}$ family and certain Gβγ subunits activate PLC β1, PLC β2 and PLC β3, and PLC β3 is phosphorylated on Ser537 in the basal state [234-236]. Also IP_3 and DAG accumulation leads to intracellular Ca^{2+} release, which causes phosphorylation of the protein kinase C (PKC) family [237, 238]. Therefore, modulation of PLC β3 and PKC mediated by CXCR2 CAMs was investigated by FACs analysis with phospho-specific PLC β3 (Ser537) and PKC (α/β_2) antibodies. Figure 19A shows dephosphorylation of PLC β3 for WT_CXCR2 stimulated by IL-8 (100 nM) after the cells were synchronized (serum starved). As mentioned above PLC β3 is phophorylated on Ser537 in the basal state in cells. Therefore interaction between WT_CXCR2 and IL-8 possibly induce PLC β3 activation ($p<0.05$). In addition to WT_CXCR2, CXCR2 CAMs induced differential PLC β3 activation. Interestingly, CXCR2_D9K ($p<0.05$) and D9H ($p<0.05$) activated PLC β3 more than WT_CXCR2 stimulated by IL-8.

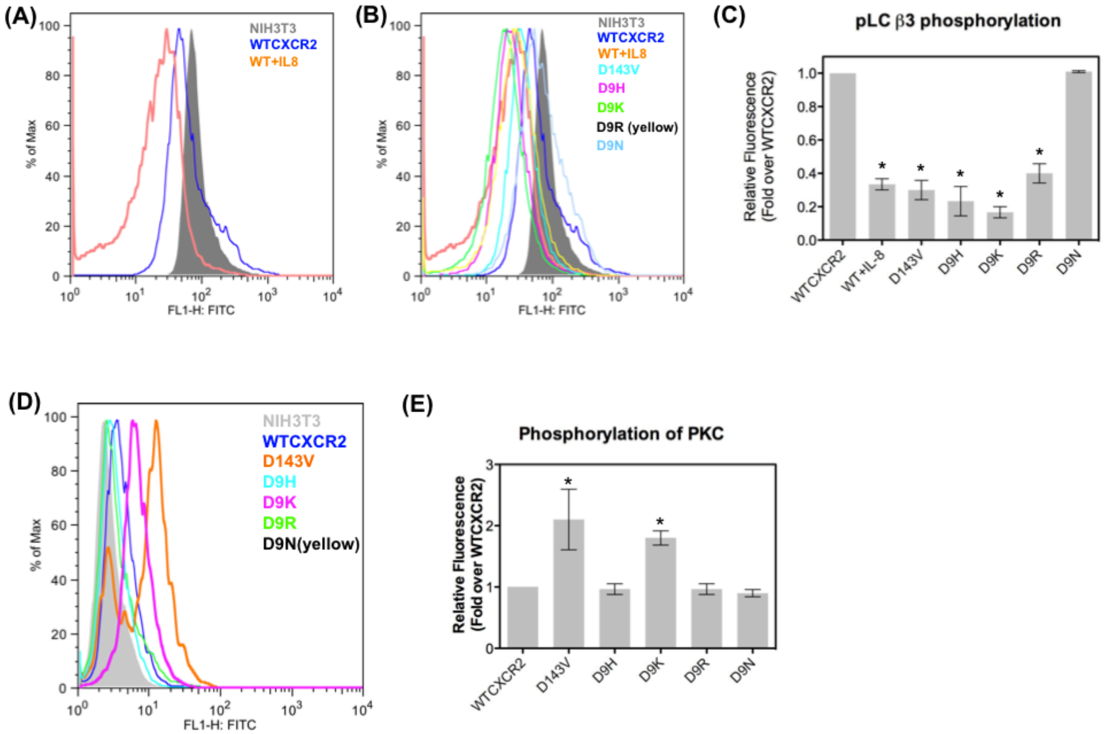

Figure 119. CXCR2_CAMs induce differential signal transduction pathways through PLC β and PKC.

Stably transfected NIH 3T3 cells were serum starved, permeablized, and stained with phospho-PLC β3 specific antibody (A and B) (Santacruz Biotech) and phospho-PKC specific antibody (D) (Cell Signaling). Induction of wild type CXCR2 was performed with IL-8 (100nM) after serum starvation. Stained cells were analyzed by FACs analysis (BD FACSCalibur). Data is representative of three independent experiments. Student's *t*-test (*PRISM (version 5.0b)* was used to determine statistical significance (*; $p < 0.05$) (C and E).

However CXCR2_D9N still remained at a basal level of PLC β3 phosphorylation ($p>0.05$, Figure 19B and C).

As mentioned above, PLC β3 activation induces PKC phosphorylation. Figure 19D and E indicated CXCR2_D143V ($p<0.05$) and D9K ($p<0.05$) lead to phosphorylation of PKC, which means PKC is a potential downstream signaling pathway for both CXCR2 CAMs. Taken together CXCR2 CAMs potentially utilize the $G\alpha_{q/11}$ family and one of downstream target pathway is PKC.

CXCR2 CAMs Transactivation of Epidermal Growth Factor Receptor (EGFR)

The epidermal growth factor receptor (EGFR) activates several signaling cascades in response to epidermal growth factor stimulation. One of these signaling events involves JAK activation [239]. Since CXCR2 CAMs use JAK dependent foci formation, the potential transactivation of EGFR was investigated.

To identify the IL-8 or CXCR2 CAMs mediated transactivation pathway, the phosphorylation state of the EGFR was assessed in stably transfected NIH3T3 cells using a phospho-EGFR specific antibody (pY1173, BD Biosciences). Figure 20 shows that CXCR2 CAMs differentially phosphorylate EGFR. There is a also the possibility of autocrine EGFR phosphorylation mediated by secreted EGF. To test this possibility, a mouse specific ELISA assay was used to measure the concentration of mouse EGF. The concentration of EGF was below the detection limit of 3 pg/ml indicating EGF independent EGFR transactivation.

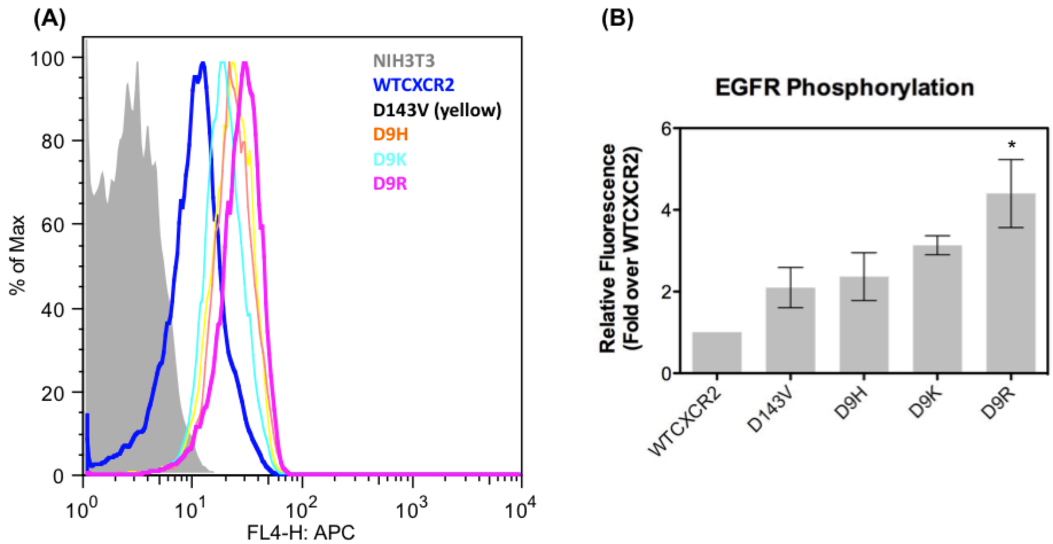

Figure 20. CXCR2 CAMs induce EGF independent EGFR phosphorylation.

(A) Stable transfectants were serum starved, permeablized, and stained with phospho-EGFR specific antibody (pY1173, BD Biosciences). Stained cells were analyzed by FACs analysis (BD FACSCalibur). Data is representative of three independent experiments. (B) Student's *t*-test (*PRISM (version 5.0b)* was used to determine statistical significance *(**; $p< 0.05$).

EGFR transactivation mediated by heterotrimeric G protein, Gα_i

CXCR2 activation mediated by IL-8 stimulation led to EGFR transactivation through heparin binding EGF (HB-EGF) [240]. Also, IL-8 stimulation of cathepsin B expression involved HB-EGF activation [240]. Since the EGF concentration was undetectable, it is possible that there is a transactivator that signals from the CXCR2 CAMs to EGFR. To investigate the possible connection between CXCR2 CAMs and EGFR phosphorylation, the CXCR2_D9R, which highly transactivated EGFR, and CXCR2_D9K, a more modest transactivator of EGFR were treated with PTX and EGFR phosphorylation assessed. In Figure 21, PTX inhibited CXCR2_D9R/EGFR transactivation suggesting that Gα_i subunit is involved in EGFR transactivation.

CXCR2 CAMs Stimulation of NF-κB transcriptional activity

A number of studies have shown that GPCR CAMs stimulate NF-κB transcriptional activity, which induces cellular transformation *in vitro*

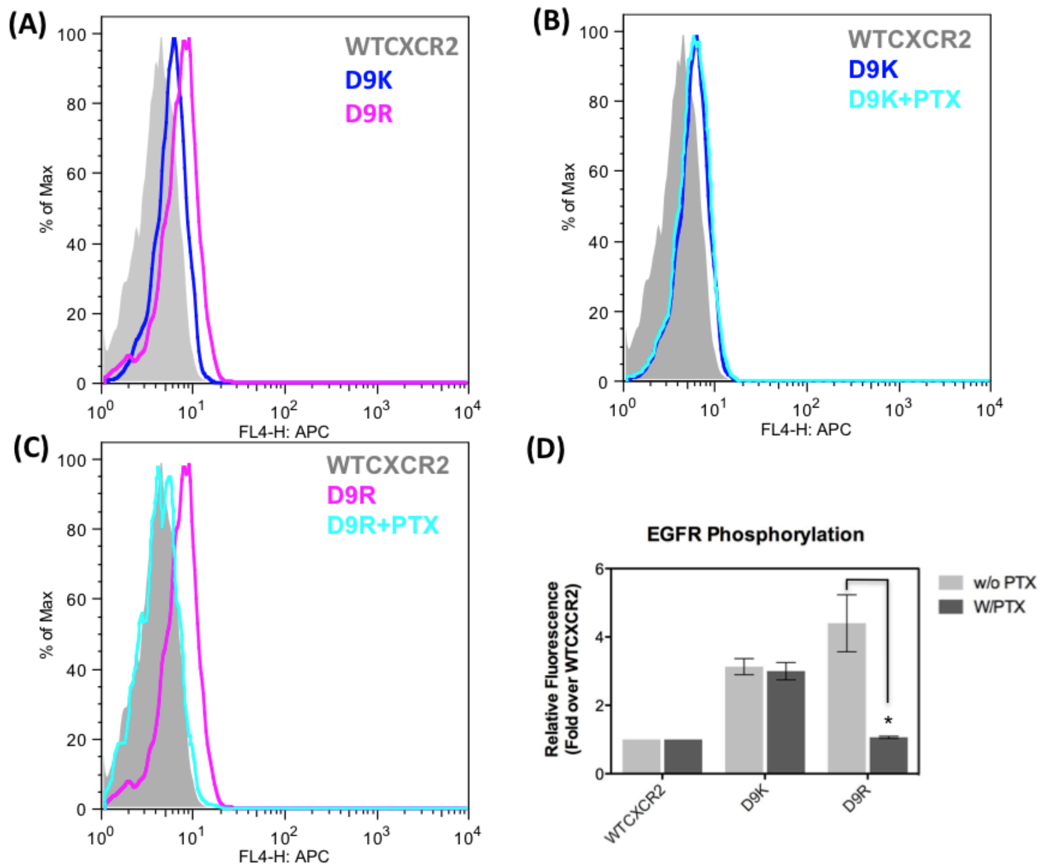

Figure 21. CXCR2_D9R induce Gα_i mediating EGFR transactivation.

NIH3T3 cell stably expressing WT_CXCR2, D9K and D9R were serum starved in the presence of PTX (100ng/ml) for Gα_i mediated signal transduction. Cells were permeablized, and stained with phospho-EGFR specific antibody (pY1173, BD Biosciences). Stained cells were analyzed by FACs analysis (BD FACSCalibur). Data is representative of three independent experiments. (D) Student's *t*-test (*PRISM (version 5.0b)* was used to determine statistical significance *(**; $p < 0.05$).

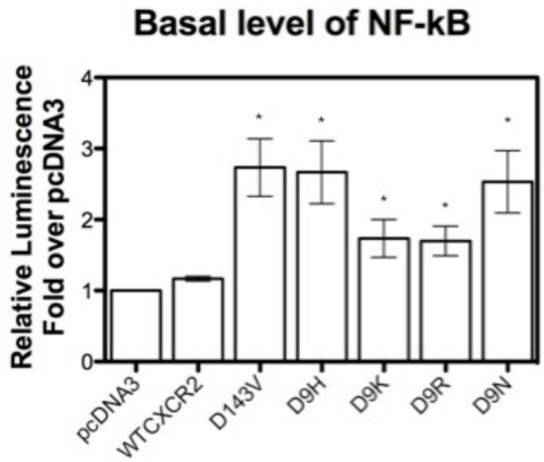

Figure 22. CXCR2 CAMs induce differential basal levels of NF-κB

HEK 293 cells were co-transfected with luciferase reporter constructs for NF-κB. For each transfection, luciferase activity was normalized for transfection efficiency and measured with Dual-Glo^{TM} luciferase assay system (Promega). Bars represent the average of three independent experiments +/-standard deviation (* p≤ 0.05).

and *vivo* [229, 241, 242]. In Figure 22, the basal level of NF-κB transcriptional activity was assessed for WT_CXCR2 and CXCR2 CAMs using a luciferase reporter assay. All CXCR2 CAMs induced NF-κB transcriptional activity except mock control and WT_CXCR2. Although CXCR2_D9N did not induce any phenotypic cellular transformation, the basal level of NF-κB transcriptional activity indicated CXCR2_D9N induces constitutive NF-κB transcriptional activity. Thus, there was no correlation between level of cellular transformation and NF-κB activity.

CHAPTER 5. DISCUSSION

The results from this study suggest that CXCR2 CAMs initiate the activation of intracellular signal transduction cascades through multiple G proteins usage, which are $G\alpha_i$ and $G\alpha_{q/11}$ families (Figure 18). Surprisingly a single point mutation in N-terminal 9^{th} residue of CXCR2 caused this event.

Classically, CXC chemokine receptors were suggested to mediate intracellular signaling through $G\alpha_i$ [93, 243]. Treatment of CXCR2 expressing cells line with PTX completely disrupted IL-8 mediated inhibition of forskolin-stimulated cyclic AMP accumulation, which indicates CXCR2 activation induces a $G\alpha_i$ family dependent signal transduction pathway [153]. This $G\alpha_i$ dependent signaling stimulates the accumulation of intracellular inositol phosphate and increases intracellular calcium [150]. This induces a cascade of downstream intracellular signaling pathways for cellular proliferation, migration, and inhibition of apoptosis, and activation of NF-kB pathways [154-157]. Interestingly, our results suggest a different view of Gα protein family usage for chemokine receptors. WT_CXCR2 stimulated with IL-8 and CAMs probably induces a $G\alpha_{q/11}$ mediating signaling as well as $G\alpha_i$. CXCR2 activation mediated by IL-8 stimulation or CAMsexcept CXCR2_D9N, triggered differential PLC β3 and PKC activation (Figure 19), and activates NF-κB transcription activation (Figure 22). These G protein-dependent signal pathways, $G\alpha_{q/11}$ – PLC β – PKC, and NF-κB activation are also shown in virally encoded GPCR CAMs. Other virally encoded CAMs such as human cytomegalovirus (HCMV)-encoded chemokine receptor, US28 [241, 244] and murine cytomegalovirus-encoded GPCR homologue, M33 [229] use $G\alpha_{q/11}$ followed by PLC β and PKC activation [241, 245].

Interestingly, CXCR2_D9R potentially uses both $G\alpha_i$ and $G\alpha_{q/11}$ proteins cooperatively (Figure 18). Recently, promiscuous G protein usage was reported by Kaposi's sarcoma herpes virus (KSHV)-encoded GPCR, ORF74, which is a homologue of human CXCR2 [197]. In primary effusion lymphoma (PEL)-derived cell lines, KSHV ORF74 activates ERK and p38, and AP-1, NF-κB, CREB (cyclic-AMP-response-element-binding protein) and NFAT (nuclear factor activator of T cells) transcriptional factors concommitantly with $G\alpha_{q/11}$ and $G\alpha_i$. KSHV ORF74 utilized $G\alpha_i$ that induced AP-1 and CREB transcriptional activation via PI3K/Akt-Src intracellular pathways. $G\alpha_{q/11}$ usage of KSHV ORF74 led to transcriptional activation of AP-1, CREB, and NFAT via ERK-1/2. However, NF-κB transcriptional activation is probably mediated by not $G\alpha_i$ but Rac 1 [197]. Additionally US28 potentially uses promiscuous G-protein in a similar fashion with KSHV ORF74 [102, 246]. US28 showed that $G\alpha_{q/11}$ and $G_{\beta\gamma}$ activate NF-κB indicting a modulation of transcriptional factors through differential G protein usage. Taken together, CXCR2_D9R seems to modulate multiple signal transduction cascades through $G\alpha_{q/11}$ and $G\alpha_i$ usage not like other CXCR2 CAMs but like viral GPCR CAMs, which induces a potent of cellular transformation.

The mutation of the DRY motif from aspartic acid (D) to valine (V) at the junction of third TM domain and intracellular loop was the first identified CXCR2 CAM [93]. The CXCR2 mutation in the DRY motif resulted in anchorage independent growth and loss of contact inhibition. However, this result is quite reasonable due to the importance of D/ERY motif for G protein activation. In addition to D/ERY motif, mutation or deletion of a non-TM region, such as a large ectodomain [81, 97] and C-terminal intracellular domain [98], induces constitutive activity. Our study is the first to describe an N-terminal single point mutation causing chemokine receptor constitutive activity. One possible explanation is a gain-of function phenotype induced by the loss of an intramolecular interaction suggested by Kjelsberge et al [87]. In their study, mutation of Ala293 to one of the 19 other amino acids in the α_{1B}-adrenergic receptor resulted in constitutive activation. Based on this report, they established propose a structural constraint that maintains the receptor in the inactive state. Another possible explanation of an N-terminal point mutation inducing CAM is the gain of intramolecular interaction that induces differential activation. To confirm the mechanism for constitutive activation mediated by N-terminal point mutations, additional biochemical and biophysical studies will be necessary.

ACKNOWLEDGMENTS

We would like to thank Dr. Ann Richmond (Vanderbilt University), Dr. William P. Schiemann (Case Western Reserve University), Dr. Seung Joon Baek (University of Tennessee at Knoxville) and Dr. William E. Miller (University of Cincinnati) for valuable discussion and supplying reagents. This work is supported by NIH grant #R01AI07104-02.

CHAPTER 6. SUMMARY AND CONCLUSIONS

Much evidence suggests that CXCR2 activation is involved various types of cancer development and metastasis. To elucidate CXCR2 activation and its relationship with tumorigenesis, CXCR2 constitutively active mutants were screened using a genetically modified *Saccharomyces cerevisiae* high-throughput system. Surprisingly, a single point mutation in N-terminal 9th residue of CXCR2 led to constitutive activity, which motivated generating positive charged substitutions, D9K and D9R, and D143V as a positive control for a known CXCR2 CAM. Stably transfected NIH3T3 cells expressing CXCR2 CAMs demonstrate the loss of contact inhibition and anchorage independent growth, which are two characteristics of cell that have undergone cellular transformation. Since the PLC β inhibitor U73122 and the $G\alpha_i$ inhibitor PTX were able to prevent cellular transformation, PLC β and $G\alpha_i$ mediated signal transduction pathways were investigated further. Interestingly, both IL-8 stimulation of WTCXCR2 and the CXCR2 CAMs induced constitutive PLC β activation indicating that the $G\alpha_{q/11}$ subunit family are involved. Additionally, CXCR2 CAMs induced differential basal levels of NF-κB. Although CXCR2_D9N showed weak ability for cellular transformation, NF-κB transcriptional activity showed higher levels than D9K and D9R suggesting a high degree of cellular transformation. Using the inhibitor AG490, the JAK pathway was shown to be directly involved cellular contact inhibition. Also, CXCR2 CAMs were demonstrated to transactivate EGFR in a PTX sensitive fashion suggesting $G\alpha_i$ associated transactivation of EGFR.

Taken together, CXCR2 CAMs mediate constitutively activated intracellular signaling pathways, which are proposed in Figure 23. Our model, based on our data, shows a complex relationship between CXCR2 activation, downstream signaling and phenotypic readouts. Treatment of cells with the inhibitor for PLC β, U73122, showed that IL-8 stimulated WT_CXCR2 and CXCR2 CAMs, such as D143V, D9H, D9K and D9R, induce $G\alpha_{q/11}$ stimulation of the PLC β pathway. All CAMs including CXCR2_D9N activate NF-κB transcription. In the case of CXCR2_D9N, heterotrimeric G protein usage was not investigated due to weak growth and low numbers of foci. However, low activity in loss of contact inhibition and anchorage independent growth assays potentially indicate that NF-κB activation may be involved in cell survival. Because foci are still induced after using both U73122 and PTX inhibitors it is possible that D143V and D9H possibly utilize another Gα family or the Gβγ proteins, which are also capable of mediating downstream signal transduction pathways. Interestingly, a specific inhibitor of JAK signaling, AG490, inhibited all foci formation in all mutants tested. This strongly suggests that JAK-mediated signaling is a pathway involved in cellular transformation. In order to investigate where this signaling is initiated, we treated CXCR2_D9R with the EGFR specific inhibitor, butain. In this case all foci formation was abolished. This demonstrated that this specific EGFR-mediated signal transduction pathway is involved in cellular transformation. This provides yet another pathway that contributes to foci formation. In summary, our data shows that CXCR2 can use multiple Gα proteins and that the CXCR2 CAMs can capture the differential activation states and signaling pathways. Lastly, activation of CXCR2 leads to activation of the EGFR receptor though an internal transactivation cascade. This internal activation differentially transactivates EGFR in a PTX sensitive manner implying the $G\alpha_i$ protein is the mediator of this activation. Additionally, a number of studies suggest that EGFR activation potentially induces either JAK-independent or JAK-dependent signalling through STAT1 or 3.

Figure 22. Model for CXCR2 CAM induction of ligand-independent signal transduction cascades.

Based on our data, CXCR2 CAMs, such as D143V, D9H, D9K and D9R, including WT_CXCR2 stimulated with IL-8, possibly utilize $G\alpha_{q/11}$ followed by activation of PLC β. Interestingly, WT_CXCR2 stimulated with IL-8, D9R and D143V potentially use both $G\alpha_i$ and $G\alpha_{q/11}$. Combinational treatment with U73122 and PTX suggests D143V and D9H potentially induced constitutive signalling through another Gα famiy or Gβγ protein. Moreover it has been shown that PLC β can possibly be activated by Gβγ (blue dash line) [236]. Also all CXCR2 CAMs induced JAK-mediated signaling. D9R induced transactivatation of EGFR through $G\alpha_i$. In addition it has been suggested that EGFR activation potentially induces either JAK-independent or JAK-dependent signalling through STAT1 or 3 (orange dash line) [239, 247, 248].

Morphological cellular transformation was validated by loss of contact inhibition and anchorage-independent proliferation assays. All of the CXCR2 CAMs except CXCR2_D9N showed both characteristics. CXCR2_D9N demonstrated only anchorage-independent growth.

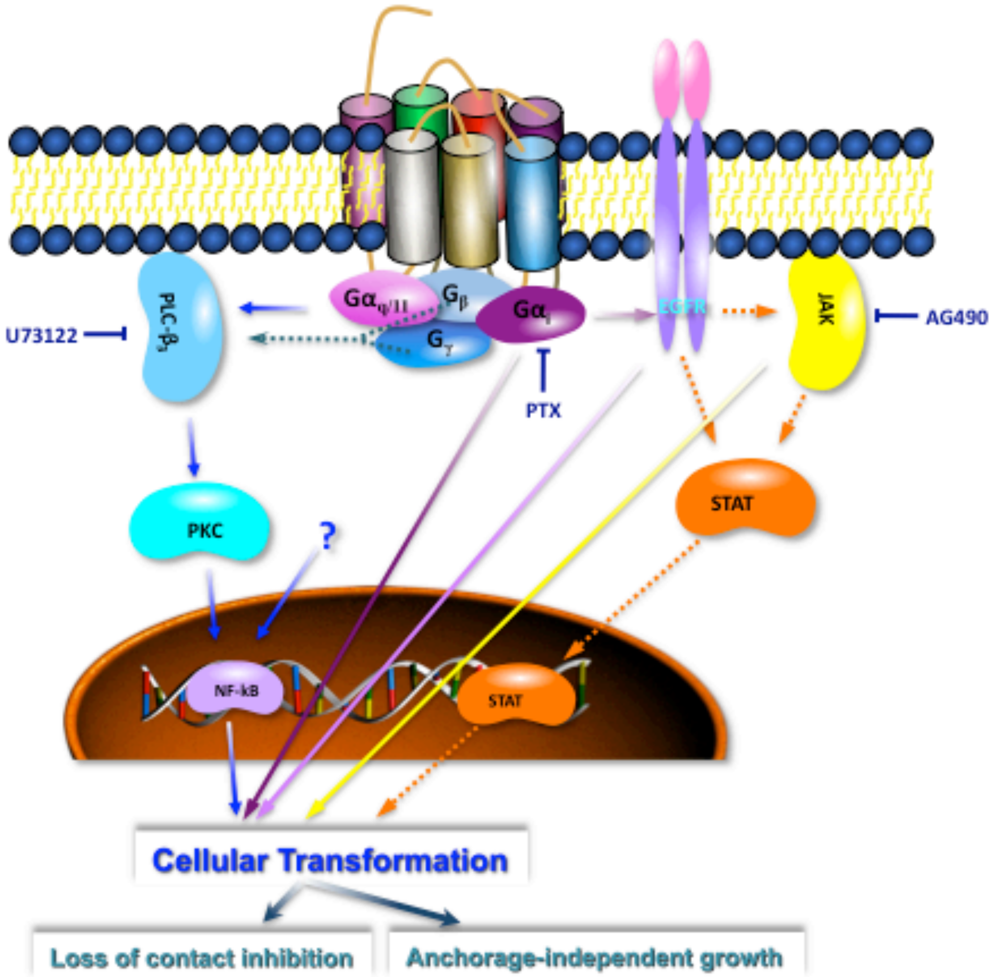
Gα$_{q/11}$
G$_\beta$
G$_\gamma$
Gα$_i$
EGFR
JAK
AG490
U73122
PLC-β$_3$
PTX
PKC
?
STAT
NF-kB
STAT
Cellular Transformation
Loss of contact inhibition
Anchorage-independent growth

LITERATURE CITED

1 Nathans, J. and Hogness, D.S. (1983) Isolation, sequence analysis, and intron-exon arrangement of the gene encoding bovine rhodopsin. *Cell* 34, 807-814

2 Palczewski, K.*, et al.* (2000) Crystal structure of rhodopsin: A G protein-coupled receptor. *Science* 289, 739-745

3 Gloriam, D.E.*, et al.* (2007) The G protein-coupled receptor subset of the rat genome. *BMC Genomics* 8, 338

4 Oldham, W.M. and Hamm, H.E. (2008) Heterotrimeric G protein activation by G-protein-coupled receptors. *Nat Rev Mol Cell Biol* 9, 60-71

5 Malbon, C.C. (2005) G proteins in development. *Nat Rev Mol Cell Biol* 6, 689-701

6 Hoon, M.A.*, et al.* (1999) Putative mammalian taste receptors: a class of taste-specific GPCRs with distinct topographic selectivity. *Cell* 96, 541-551

7 Kolakowski, L.F., Jr. (1994) GCRDb: a G-protein-coupled receptor database. *Receptors Channels* 2, 1-7

8 Bjarnadottir, T.K.*, et al.* (2006) Comprehensive repertoire and phylogenetic analysis of the G protein-coupled receptors in human and mouse. *Genomics* 88, 263-273

9 Lagerstrom, M.C. and Schioth, H.B. (2008) Structural diversity of G protein-coupled receptors and significance for drug discovery. *Nat Rev Drug Discov* 7, 339-357

10 Hepler, J.R. and Gilman, A.G. (1992) G proteins. *Trends Biochem Sci* 17, 383-387

11 Hamm, H.E. and Gilchrist, A. (1996) Heterotrimeric G proteins. *Curr Opin Cell Biol* 8, 189-196

12 Flower, D.R. (1999) Modelling G-protein-coupled receptors for drug design. *Biochim Biophys Acta* 1422, 207-234

13 Jacoby, E.*, et al.* (2006) The 7 TM G-protein-coupled receptor target family. *ChemMedChem* 1, 761-782

14 Jeong, S.W. and Ikeda, S.R. (2000) Effect of G protein heterotrimer composition on coupling of neurotransmitter receptors to N-type Ca(2+) channel modulation in sympathetic neurons. *Proc Natl Acad Sci U S A* 97, 907-912

15 Morris, A.J. and Malbon, C.C. (1999) Physiological regulation of G protein-linked signaling. *Physiol Rev* 79, 1373-1430

16 Bourne, H.R.*, et al.* (1991) The GTPase superfamily: conserved structure and molecular mechanism. *Nature* 349, 117-127

17 Chapter, M.C.*, et al.* (2010) Chemical modification of class II G protein-coupled receptor ligands: frontiers in the development of peptide analogs as neuroendocrine pharmacological therapies. *Pharmacol Ther* 125, 39-54

18 Karnik, S.S.*, et al.* (2003) Activation of G-protein-coupled receptors: a common molecular mechanism. *Trends Endocrinol Metab* 14, 431-437

19 Dorsam, R.T. and Gutkind, J.S. (2007) G-protein-coupled receptors and cancer. *Nat Rev Cancer* 7, 79-94
20 Chalmers, D.T. and Behan, D.P. (2002) The use of constitutively active GPCRs in drug discovery and functional genomics. *Nat Rev Drug Discov* 1, 599-608
21 Hopkins, A.L. and Groom, C.R. (2002) The druggable genome. *Nat Rev Drug Discov* 1, 727-730
22 George, S.R., *et al.* (2002) G-protein-coupled receptor oligomerization and its potential for drug discovery. *Nat Rev Drug Discov* 1, 808-820
23 Civelli, O., *et al.* (2001) Novel neurotransmitters as natural ligands of orphan G-protein-coupled receptors. *Trends Neurosci* 24, 230-237
24 Wise, A., *et al.* (2002) Target validation of G-protein coupled receptors. *Drug Discov Today* 7, 235-246
25 Strader, C.D., *et al.* (1994) Structure and function of G protein-coupled receptors. *Annu Rev Biochem* 63, 101-132
26 Kobilka, B. (1992) Adrenergic receptors as models for G protein-coupled receptors. *Annu Rev Neurosci* 15, 87-114
27 Strader, C.D., *et al.* (1995) The family of G-protein-coupled receptors. *Faseb J* 9, 745-754
28 Ji, T.H., *et al.* (1998) G protein-coupled receptors. I. Diversity of receptor-ligand interactions. *J Biol Chem* 273, 17299-17302
29 Bondensgaard, K., *et al.* (2004) Recognition of privileged structures by G-protein coupled receptors. *J Med Chem* 47, 888-899
30 Hunyady, L., *et al.* (2003) Agonist induction and conformational selection during activation of a G-protein-coupled receptor. *Trends Pharmacol Sci* 24, 81-86
31 Rihakova, L., *et al.* (2002) Methionine proximity assay, a novel method for exploring peptide ligand-receptor interaction. *J Recept Signal Transduct Res* 22, 297-313
32 Chorev, M. (2002) Parathyroid hormone 1 receptor: insights into structure and function. *Receptors Channels* 8, 219-242
33 Tsomaia, N., *et al.* (2004) Cooperative interaction of arginine-19 and the N-terminal signaling domain in the affinity and potency of parathyroid hormone. *Biochemistry* 43, 3459-3470
34 Dong, M., *et al.* (2004) Spatial approximation between the amino terminus of a peptide agonist and the top of the sixth transmembrane segment of the secretin receptor. *J Biol Chem* 279, 2894-2903
35 Bellucci, F., *et al.* (2003) A different molecular interaction of bradykinin and the synthetic agonist FR190997 with the human B2 receptor: evidence from mutational analysis. *Br J Pharmacol* 140, 500-506
36 Schroeder, C., *et al.* (2003) Changes in amino-terminal portion of human B2 receptor selectively increase efficacy of synthetic ligand HOE 140 but not of cognate ligand bradykinin. *Am J Physiol Heart Circ Physiol* 284, H1924-1932
37 Millar, R.P., *et al.* (2004) Gonadotropin-releasing hormone receptors. *Endocr Rev* 25, 235-275

38 Janecka, A., *et al.* (2004) Opioid receptors and their ligands. *Curr Top Med Chem* 4, 1-17
39 Judd, A.K., *et al.* (2003) N-terminal modifications leading to peptide ORL1 partial agonists and antagonists. *J Pept Res* 62, 191-198
40 Sachon, E., *et al.* (2003) Met174 side chain is the site of photoinsertion of a substance P competitive peptide antagonist photoreactive in position 8. *FEBS Lett* 544, 45-49
41 Ulfers, A.L., *et al.* (2002) Extracellular domains of the neurokinin-1 receptor: structural characterization and interactions with substance P. *Biopolymers* 66, 339-349
42 Breton, C., *et al.* (2001) Direct identification of human oxytocin receptor-binding domains using a photoactivatable cyclic peptide antagonist: comparison with the human V1a vasopressin receptor. *J Biol Chem* 276, 26931-26941
43 Wesley, V.J., *et al.* (2002) Agonist-specific, high-affinity binding epitopes are contributed by an arginine in the N-terminus of the human oxytocin receptor. *Biochemistry* 41, 5086-5092
44 Politowska, E., *et al.* (2002) Docking ligands to vasopressin and oxytocin receptors via genetic algorithm. *J Recept Signal Transduct Res* 22, 393-409
45 Smith, C.J., *et al.* (2003) Radiochemical investigations of [188Re(H2O)(CO)3-diaminopropionic acid-SSS-bombesin(7-14)NH2]: syntheses, radiolabeling and in vitro/in vivo GRP receptor targeting studies. *Anticancer Res* 23, 63-70
46 Silvente-Poirot, S., *et al.* (1998) Role of the extracellular domains of the cholecystokinin receptor in agonist binding. *Mol Pharmacol* 54, 364-371
47 Barroso, S., *et al.* (2000) Identification of residues involved in neurotensin binding and modeling of the agonist binding site in neurotensin receptor 1. *J Biol Chem* 275, 328-336
48 Mills, J.S., *et al.* (1998) Identification of a ligand binding site in the human neutrophil formyl peptide receptor using a site-specific fluorescent photoaffinity label and mass spectrometry. *J Biol Chem* 273, 10428-10435
49 Fathy, D.B., *et al.* (1998) A single position in the third transmembrane domains of the human B1 and B2 bradykinin receptors is adjacent to and discriminates between the C-terminal residues of subtype-selective ligands. *J Biol Chem* 273, 12210-12218
50 Fanelli, F., *et al.* (1999) Activation mechanism of human oxytocin receptor: a combined study of experimental and computer-simulated mutagenesis. *Mol Pharmacol* 56, 214-225
51 Flanagan, C.A., *et al.* (2000) Multiple interactions of the Asp(2.61(98)) side chain of the gonadotropin-releasing hormone receptor contribute differentially to ligand interaction. *Biochemistry* 39, 8133-8141
52 Rasmussen, S.G., *et al.* (2007) Crystal structure of the human beta2 adrenergic G-protein-coupled receptor. *Nature* 450, 383-387
53 Kenakin, T. (2002) Drug efficacy at G protein-coupled receptors. *Annu Rev Pharmacol Toxicol* 42, 349-379
54 Kenakin, T. (2005) New concepts in drug discovery: collateral efficacy and permissive antagonism. *Nat Rev Drug Discov* 4, 919-927

55 Rosenbaum, D.M., *et al.* (2009) The structure and function of G-protein-coupled receptors. *Nature* 459, 356-363
56 Kobilka, B. (2004) Agonist binding: a multistep process. *Mol Pharmacol* 65, 1060-1062
57 Berg, K.A., *et al.* (1998) Effector pathway-dependent relative efficacy at serotonin type 2A and 2C receptors: evidence for agonist-directed trafficking of receptor stimulus. *Mol Pharmacol* 54, 94-104
58 Vilardaga, J.P., *et al.* (2005) Molecular basis of inverse agonism in a G protein-coupled receptor. *Nat Chem Biol* 1, 25-28
59 Wei, H., *et al.* (2003) Independent beta-arrestin 2 and G protein-mediated pathways for angiotensin II activation of extracellular signal-regulated kinases 1 and 2. *Proc Natl Acad Sci U S A* 100, 10782-10787
60 Lu, Z.L., *et al.* (2007) Structural determinants for ligand-receptor conformational selection in a peptide G protein-coupled receptor. *J Biol Chem* 282, 17921-17929
61 Keith, D.E., *et al.* (1998) mu-Opioid receptor internalization: opiate drugs have differential effects on a conserved endocytic mechanism in vitro and in the mammalian brain. *Mol Pharmacol* 53, 377-384
62 Perez, D.M. and Karnik, S.S. (2005) Multiple signaling states of G-protein-coupled receptors. *Pharmacol Rev* 57, 147-161
63 Urban, J.D., *et al.* (2007) Functional selectivity and classical concepts of quantitative pharmacology. *J Pharmacol Exp Ther* 320, 1-13
64 Rodbell, M., *et al.* (1971) The glucagon-sensitive adenyl cyclase system in plasma membranes of rat liver. V. An obligatory role of guanylnucleotides in glucagon action. *J Biol Chem* 246, 1877-1882
65 Gilman, A.G. (1987) G proteins: transducers of receptor-generated signals. *Annu Rev Biochem* 56, 615-649
66 Northup, J.K., *et al.* (1980) Purification of the regulatory component of adenylate cyclase. *Proc Natl Acad Sci U S A* 77, 6516-6520
67 Pierce, K.L., *et al.* (2002) Seven-transmembrane receptors. *Nat Rev Mol Cell Biol* 3, 639-650
68 West, R.E., Jr., *et al.* (1985) Pertussis toxin-catalyzed ADP-ribosylation of transducin. Cysteine 347 is the ADP-ribose acceptor site. *J Biol Chem* 260, 14428-14430
69 Freissmuth, M. and Gilman, A.G. (1989) Mutations of GS alpha designed to alter the reactivity of the protein with bacterial toxins. Substitutions at ARG187 result in loss of GTPase activity. *J Biol Chem* 264, 21907-21914
70 Hoshino, S., *et al.* (1990) Identification of sites for alkylation by N-ethylmaleimide and pertussis toxin-catalyzed ADP-ribosylation on GTP-binding proteins. *FEBS Lett* 276, 227-231
71 Camps, M., *et al.* (1992) Isozyme-selective stimulation of phospholipase C-beta 2 by G protein beta gamma-subunits. *Nature* 360, 684-686
72 Boyer, J.L., *et al.* (1992) Beta gamma-subunit activation of G-protein-regulated phospholipase C. *J Biol Chem* 267, 25451-25456

73 Pitcher, J.A., *et al.* (1992) Role of beta gamma subunits of G proteins in targeting the beta-adrenergic receptor kinase to membrane-bound receptors. *Science* 257, 1264-1267
74 Tang, W.J. and Gilman, A.G. (1991) Type-specific regulation of adenylyl cyclase by G protein beta gamma subunits. *Science* 254, 1500-1503
75 Stephens, L., *et al.* (1994) A novel phosphoinositide 3 kinase activity in myeloid-derived cells is activated by G protein beta gamma subunits. *Cell* 77, 83-93
76 Logothetis, D.E., *et al.* (1987) The beta gamma subunits of GTP-binding proteins activate the muscarinic K+ channel in heart. *Nature* 325, 321-326
77 Schmidt, C.J., *et al.* (1992) Specificity of G protein beta and gamma subunit interactions. *J Biol Chem* 267, 13807-13810
78 Xiao, R.P., *et al.* (1999) Recent advances in cardiac beta(2)-adrenergic signal transduction. *Circ Res* 85, 1092-1100
79 Shenoy, S.K., *et al.* (2006) beta-arrestin-dependent, G protein-independent ERK1/2 activation by the beta2 adrenergic receptor. *J Biol Chem* 281, 1261-1273
80 Azzi, M., *et al.* (2003) Beta-arrestin-mediated activation of MAPK by inverse agonists reveals distinct active conformations for G protein-coupled receptors. *Proc Natl Acad Sci U S A* 100, 11406-11411
81 Parnot, C., *et al.* (2002) Lessons from constitutively active mutants of G protein-coupled receptors. *Trends Endocrinol Metab* 13, 336-343
82 Cotecchia, S., *et al.* (1990) Regions of the alpha 1-adrenergic receptor involved in coupling to phosphatidylinositol hydrolysis and enhanced sensitivity of biological function. *Proc Natl Acad Sci U S A* 87, 2896-2900
83 Costa, T. and Herz, A. (1989) Antagonists with negative intrinsic activity at delta opioid receptors coupled to GTP-binding proteins. *Proc Natl Acad Sci U S A* 86, 7321-7325
84 Pitcher, J.A., *et al.* (1998) G protein-coupled receptor kinases. *Annu Rev Biochem* 67, 653-692
85 Krupnick, J.G. and Benovic, J.L. (1998) The role of receptor kinases and arrestins in G protein-coupled receptor regulation. *Annu Rev Pharmacol Toxicol* 38, 289-319
86 Zhang, J., *et al.* (1997) Molecular mechanisms of G protein-coupled receptor signaling: role of G protein-coupled receptor kinases and arrestins in receptor desensitization and resensitization. *Receptors Channels* 5, 193-199
87 Kjelsberg, M.A., *et al.* (1992) Constitutive activation of the alpha 1B-adrenergic receptor by all amino acid substitutions at a single site. Evidence for a region which constrains receptor activation. *J Biol Chem* 267, 1430-1433
88 Cohen, G.B., *et al.* (1993) Constitutive activation of opsin: influence of charge at position 134 and size at position 296. *Biochemistry* 32, 6111-6115
89 Scheer, A., *et al.* (1996) Constitutively active mutants of the alpha 1B-adrenergic receptor: role of highly conserved polar amino acids in receptor activation. *EMBO J* 15, 3566-3578
90 Rasmussen, S.G., *et al.* (1999) Mutation of a highly conserved aspartic acid in the beta2 adrenergic receptor: constitutive activation, structural instability, and

conformational rearrangement of transmembrane segment 6. *Mol Pharmacol* 56, 175-184
91 Ballesteros, J.*, et al.* (1998) Functional microdomains in G-protein-coupled receptors. The conserved arginine-cage motif in the gonadotropin-releasing hormone receptor. *J Biol Chem* 273, 10445-10453
92 Lu, Z.L.*, et al.* (1997) The role of the aspartate-arginine-tyrosine triad in the m1 muscarinic receptor: mutations of aspartate 122 and tyrosine 124 decrease receptor expression but do not abolish signaling. *Mol Pharmacol* 51, 234-241
93 Burger, M.*, et al.* (1999) Point mutation causing constitutive signaling of CXCR2 leads to transforming activity similar to Kaposi's sarcoma herpesvirus-G protein-coupled receptor. *J Immunol* 163, 2017-2022
94 Kosugi, S.*, et al.* (1996) The role of Asp578 in maintaining the inactive conformation of the human lutropin/choriogonadotropin receptor. *J Biol Chem* 271, 31813-31817
95 Scheer, A.*, et al.* (1997) The activation process of the alpha1B-adrenergic receptor: potential role of protonation and hydrophobicity of a highly conserved aspartate. *Proc Natl Acad Sci U S A* 94, 808-813
96 Ballesteros, J.A.*, et al.* (2001) Activation of the beta 2-adrenergic receptor involves disruption of an ionic lock between the cytoplasmic ends of transmembrane segments 3 and 6. *J Biol Chem* 276, 29171-29177
97 Nishi, S.*, et al.* (2002) The ectodomain of the luteinizing hormone receptor interacts with exoloop 2 to constrain the transmembrane region: studies using chimeric human and fly receptors. *J Biol Chem* 277, 3958-3964
98 Prezeau, L.*, et al.* (1996) Changes in the carboxyl-terminal domain of metabotropic glutamate receptor 1 by alternative splicing generate receptors with differing agonist-independent activity. *Mol Pharmacol* 49, 422-429
99 Zhang, M.*, et al.* (2000) The extracellular domain suppresses constitutive activity of the transmembrane domain of the human TSH receptor: implications for hormone-receptor interaction and antagonist design. *Endocrinology* 141, 3514-3517
100 Vlaeminck-Guillem, V.*, et al.* (2002) Activation of the cAMP pathway by the TSH receptor involves switching of the ectodomain from a tethered inverse agonist to an agonist. *Mol Endocrinol* 16, 736-746
101 Murphy, P.M. (2001) Viral exploitation and subversion of the immune system through chemokine mimicry. *Nat Immunol* 2, 116-122
102 Sodhi, A.*, et al.* (2004) Viral hijacking of G-protein-coupled-receptor signalling networks. *Nat Rev Mol Cell Biol* 5, 998-1012
103 Offermann, M.K. (1996) HHV-8: a new herpesvirus associated with Kaposi's sarcoma. *Trends Microbiol* 4, 383-386
104 Nador, R.G.*, et al.* (1996) Primary effusion lymphoma: a distinct clinicopathologic entity associated with the Kaposi's sarcoma-associated herpes virus. *Blood* 88, 645-656
105 Arvanitakis, L.*, et al.* (1997) Human herpesvirus KSHV encodes a constitutively active G-protein-coupled receptor linked to cell proliferation. *Nature* 385, 347-350

106 Rosenkilde, M.M., *et al.* (1999) Agonists and inverse agonists for the herpesvirus 8-encoded constitutively active seven-transmembrane oncogene product, ORF-74. *J Biol Chem* 274, 956-961
107 Rosenkilde, M.M. and Schwartz, T.W. (2000) Potency of ligands correlates with affinity measured against agonist and inverse agonists but not against neutral ligand in constitutively active chemokine receptor. *Mol Pharmacol* 57, 602-609
108 Gershengorn, M.C., *et al.* (1998) Chemokines activate Kaposi's sarcoma-associated herpesvirus G protein-coupled receptor in mammalian cells in culture. *J Clin Invest* 102, 1469-1472
109 Bais, C., *et al.* (1998) G-protein-coupled receptor of Kaposi's sarcoma-associated herpesvirus is a viral oncogene and angiogenesis activator. *Nature* 391, 86-89
110 Yang, T.Y., *et al.* (2000) Transgenic expression of the chemokine receptor encoded by human herpesvirus 8 induces an angioproliferative disease resembling Kaposi's sarcoma. *J Exp Med* 191, 445-454
111 Guo, H.G., *et al.* (2003) Kaposi's sarcoma-like tumors in a human herpesvirus 8 ORF74 transgenic mouse. *J Virol* 77, 2631-2639
112 Balkwill, F. (1998) The molecular and cellular biology of the chemokines. *J Viral Hepat* 5, 1-14
113 Montaner, S., *et al.* (2001) The Kaposi's sarcoma-associated herpesvirus G protein-coupled receptor promotes endothelial cell survival through the activation of Akt/protein kinase B. *Cancer Res* 61, 2641-2648
114 Burger, M., *et al.* (2005) KSHV-GPCR and CXCR2 transforming capacity and angiogenic responses are mediated through a JAK2-STAT3-dependent pathway. *Oncogene* 24, 2067-2075
115 Ondrey, F.G., *et al.* (1999) Constitutive activation of transcription factors NF-(kappa)B, AP-1, and NF-IL6 in human head and neck squamous cell carcinoma cell lines that express pro-inflammatory and pro-angiogenic cytokines. *Mol Carcinog* 26, 119-129
116 Anisowicz, A., *et al.* (1987) Constitutive overexpression of a growth-regulated gene in transformed Chinese hamster and human cells. *Proc Natl Acad Sci U S A* 84, 7188-7192
117 Balkwill, F. and Mantovani, A. (2001) Inflammation and cancer: back to Virchow? *Lancet* 357, 539-545
118 Balkwill, F., *et al.* (2005) Smoldering and polarized inflammation in the initiation and promotion of malignant disease. *Cancer Cell* 7, 211-217
119 Coussens, L.M. and Werb, Z. (2002) Inflammation and cancer. *Nature* 420, 860-867
120 Baggiolini, M., *et al.* (1989) Neutrophil-activating peptide-1/interleukin 8, a novel cytokine that activates neutrophils. *J Clin Invest* 84, 1045-1049
121 Acker, F.A., *et al.* (1996) Chemokines: structure, receptors and functions. A new target for inflammation and asthma therapy? *Mediators Inflamm* 5, 393-416
122 Fernandez, E.J. and Lolis, E. (2002) Structure, function, and inhibition of chemokines. *Annu Rev Pharmacol Toxicol* 42, 469-499

123 Baggiolini, M., *et al.* (1994) Interleukin-8 and related chemotactic cytokines--CXC and CC chemokines. *Adv Immunol* 55, 97-179
124 Strieter, R.M., *et al.* (2006) Cancer CXC chemokine networks and tumour angiogenesis. *Eur J Cancer* 42, 768-778
125 Murphy, P.M., *et al.* (2000) International union of pharmacology. XXII. Nomenclature for chemokine receptors. *Pharmacol Rev* 52, 145-176
126 Luster, A.D. (1998) Chemokines--chemotactic cytokines that mediate inflammation. *N Engl J Med* 338, 436-445
127 Belperio, J.A., *et al.* (2000) CXC chemokines in angiogenesis. *J Leukoc Biol* 68, 1-8
128 Strieter, R.M., *et al.* (1995) The functional role of the ELR motif in CXC chemokine-mediated angiogenesis. *J Biol Chem* 270, 27348-27357
129 Murphy, P.M. and Tiffany, H.L. (1991) Cloning of complementary DNA encoding a functional human interleukin-8 receptor. *Science* 253, 1280-1283
130 Holmes, W.E., *et al.* (1991) Structure and functional expression of a human interleukin-8 receptor. *Science* 253, 1278-1280
131 Zlotnik, A., *et al.* (2006) The chemokine and chemokine receptor superfamilies and their molecular evolution. *Genome Biol* 7, 243
132 Murdoch, C. and Finn, A. (2000) Chemokine receptors and their role in inflammation and infectious diseases. *Blood* 95, 3032-3043
133 Feng, Y., *et al.* (1996) HIV-1 entry cofactor: functional cDNA cloning of a seven-transmembrane, G protein-coupled receptor. *Science* 272, 872-877
134 Muller, A., *et al.* (2001) Involvement of chemokine receptors in breast cancer metastasis. *Nature* 410, 50-56
135 Richard, C.L. and Blay, J. (2008) CXCR4 in Cancer and Its Regulation by PPARgamma. *PPAR Res* 2008, 769413
136 Loetscher, M., *et al.* (1994) Cloning of a human seven-transmembrane domain receptor, LESTR, that is highly expressed in leukocytes. *J Biol Chem* 269, 232-237
137 Bleul, C.C., *et al.* (1996) The lymphocyte chemoattractant SDF-1 is a ligand for LESTR/fusin and blocks HIV-1 entry. *Nature* 382, 829-833
138 Oberlin, E., *et al.* (1996) The CXC chemokine SDF-1 is the ligand for LESTR/fusin and prevents infection by T-cell-line-adapted HIV-1. *Nature* 382, 833-835
139 Jourdan, P., *et al.* (1998) IL-4 induces functional cell-surface expression of CXCR4 on human T cells. *J Immunol* 160, 4153-4157
140 Tachibana, K., *et al.* (1998) The chemokine receptor CXCR4 is essential for vascularization of the gastrointestinal tract. *Nature* 393, 591-594
141 Nagasawa, T., *et al.* (1996) Defects of B-cell lymphopoiesis and bone-marrow myelopoiesis in mice lacking the CXC chemokine PBSF/SDF-1. *Nature* 382, 635-638
142 Dobner, T., *et al.* (1992) Differentiation-specific expression of a novel G protein-coupled receptor from Burkitt's lymphoma. *Eur J Immunol* 22, 2795-2799
143 Chambers, A.F., *et al.* (2002) Dissemination and growth of cancer cells in metastatic sites. *Nat Rev Cancer* 2, 563-572

144 Balkwill, F. (2004) Cancer and the chemokine network. *Nat Rev Cancer* 4, 540-550
145 Ahuja, S.K.*, et al.* (1996) CXC chemokines bind to unique sets of selectivity determinants that can function independently and are broadly distributed on multiple domains of human interleukin-8 receptor B. Determinants of high affinity binding and receptor activation are distinct. *J Biol Chem* 271, 225-232
146 Nasser, M.W.*, et al.* (2007) CXCR1 and CXCR2 activation and regulation. Role of aspartate 199 of the second extracellular loop of CXCR2 in CXCL8-mediated rapid receptor internalization. *J Biol Chem* 282, 6906-6915
147 Jones, S.A.*, et al.* (1996) Different functions for the interleukin 8 receptors (IL-8R) of human neutrophil leukocytes: NADPH oxidase and phospholipase D are activated through IL-8R1 but not IL-8R2. *Proc Natl Acad Sci U S A* 93, 6682-6686
148 Richardson, R.M.*, et al.* (1995) Regulation of human interleukin-8 receptor A: identification of a phosphorylation site involved in modulating receptor functions. *Biochemistry* 34, 14193-14201
149 Richardson, R.M.*, et al.* (2003) Role of the cytoplasmic tails of CXCR1 and CXCR2 in mediating leukocyte migration, activation, and regulation. *J Immunol* 170, 2904-2911
150 Richardson, R.M.*, et al.* (1998) Differential cross-regulation of the human chemokine receptors CXCR1 and CXCR2. Evidence for time-dependent signal generation. *J Biol Chem* 273, 23830-23836
151 Barlic, J.*, et al.* (2000) Regulation of tyrosine kinase activation and granule release through beta-arrestin by CXCRI. *Nat Immunol* 1, 227-233
152 Chapman, R.W.*, et al.* (2009) CXCR2 antagonists for the treatment of pulmonary disease. *Pharmacol Ther* 121, 55-68
153 Hall, D.A.*, et al.* (1999) Signalling by CXC-chemokine receptors 1 and 2 expressed in CHO cells: a comparison of calcium mobilization, inhibition of adenylyl cyclase and stimulation of GTPgammaS binding induced by IL-8 and GROalpha. *Br J Pharmacol* 126, 810-818
154 Sugden, P.H. and Clerk, A. (1997) Regulation of the ERK subgroup of MAP kinase cascades through G protein-coupled receptors. *Cell Signal* 9, 337-351
155 Pawson, T. and Scott, J.D. (1997) Signaling through scaffold, anchoring, and adaptor proteins. *Science* 278, 2075-2080
156 Shyamala, V. and Khoja, H. (1998) Interleukin-8 receptors R1 and R2 activate mitogen-activated protein kinases and induce c-fos, independent of Ras and Raf-1 in Chinese hamster ovary cells. *Biochemistry* 37, 15918-15924
157 Manna, S.K. and Ramesh, G.T. (2005) Interleukin-8 induces nuclear transcription factor-kappaB through a TRAF6-dependent pathway. *J Biol Chem* 280, 7010-7021
158 Addison, C.L.*, et al.* (2000) The CXC chemokine receptor 2, CXCR2, is the putative receptor for ELR+ CXC chemokine-induced angiogenic activity. *J Immunol* 165, 5269-5277
159 Keane, M.P.*, et al.* (2004) Depletion of CXCR2 inhibits tumor growth and angiogenesis in a murine model of lung cancer. *J Immunol* 172, 2853-2860

160 Singh, S., *et al.* (2007) Chemokines in tumor angiogenesis and metastasis. *Cancer Metastasis Rev* 26, 453-467
161 Varney, M.L., *et al.* (2006) Distinct expression of CXCL8 and its receptors CXCR1 and CXCR2 and their association with vessel density and aggressiveness in malignant melanoma. *Am J Clin Pathol* 125, 209-216
162 Singh, S., *et al.* (2009) CXCR1 and CXCR2 enhances human melanoma tumourigenesis, growth and invasion. *Br J Cancer* 100, 1638-1646
163 Venkatakrishnan, G., *et al.* (2000) Chemokine receptors CXCR-1/2 activate mitogen-activated protein kinase via the epidermal growth factor receptor in ovarian cancer cells. *J Biol Chem* 275, 6868-6875
164 Wang, B., *et al.* (2006) A growth-related oncogene/CXC chemokine receptor 2 autocrine loop contributes to cellular proliferation in esophageal cancer. *Cancer Res* 66, 3071-3077
165 Mestas, J., *et al.* (2005) The role of CXCR2/CXCR2 ligand biological axis in renal cell carcinoma. *J Immunol* 175, 5351-5357
166 Murphy, C., *et al.* (2005) Nonapical and cytoplasmic expression of interleukin-8, CXCR1, and CXCR2 correlates with cell proliferation and microvessel density in prostate cancer. *Clin Cancer Res* 11, 4117-4127
167 McCarron, S.L., *et al.* (2002) Influence of cytokine gene polymorphisms on the development of prostate cancer. *Cancer Res* 62, 3369-3372
168 Takamori, H., *et al.* (2000) Autocrine growth effect of IL-8 and GROalpha on a human pancreatic cancer cell line, Capan-1. *Pancreas* 21, 52-56
169 Wente, M.N., *et al.* (2006) Blockade of the chemokine receptor CXCR2 inhibits pancreatic cancer cell-induced angiogenesis. *Cancer Lett* 241, 221-227
170 Li, A., *et al.* (2001) Expression of interleukin 8 and its receptors in human colon carcinoma cells with different metastatic potentials. *Clin Cancer Res* 7, 3298-3304
171 Amato, R.J. (2005) Renal cell carcinoma: review of novel single-agent therapeutics and combination regimens. *Ann Oncol* 16, 7-15
172 Kerbel, R.S., *et al.* (2001) Possible mechanisms of acquired resistance to anti-angiogenic drugs: implications for the use of combination therapy approaches. *Cancer Metastasis Rev* 20, 79-86
173 Bacac, M. and Stamenkovic, I. (2008) Metastatic cancer cell. *Annu Rev Pathol* 3, 221-247
174 Zlotnik, A. (2006) Chemokines and cancer. *International journal of cancer* 119, 2026-2029
175 Kakinuma, T. and Hwang, S.T. (2006) Chemokines, chemokine receptors, and cancer metastasis. *J Leukoc Biol* 79, 639-651
176 Gether, U. and Kobilka, B.K. (1998) G protein-coupled receptors. II. Mechanism of agonist activation. *The Journal of biological chemistry* 273, 17979-17982
177 Leurs, R., *et al.* (1998) Agonist-independent regulation of constitutively active G-protein-coupled receptors. *Trends Biochem Sci* 23, 418-422
178 Rosenkilde, M.M., *et al.* (2001) Virally encoded 7TM receptors. *Oncogene* 20, 1582-1593

179 Kristiansen, K. (2004) Molecular mechanisms of ligand binding, signaling, and regulation within the superfamily of G-protein-coupled receptors: molecular modeling and mutagenesis approaches to receptor structure and function. *Pharmacol Ther* 103, 21-80
180 Horton, L.W.*, et al.* (2007) Opposing roles of murine duffy antigen receptor for chemokine and murine CXC chemokine receptor-2 receptors in murine melanoma tumor growth. *Cancer Res* 67, 9791-9799
181 Ahuja, S.K. and Murphy, P.M. (1996) The CXC chemokines growth-regulated oncogene (GRO) alpha, GRObeta, GROgamma, neutrophil-activating peptide-2, and epithelial cell-derived neutrophil-activating peptide-78 are potent agonists for the type B, but not the type A, human interleukin-8 receptor. *J Biol Chem* 271, 20545-20550
182 King, K.*, et al.* (1990) Control of yeast mating signal transduction by a mammalian beta 2-adrenergic receptor and Gs alpha subunit. *Science* 250, 121-123
183 Price, L.A.*, et al.* (1995) Functional coupling of a mammalian somatostatin receptor to the yeast pheromone response pathway. *Mol Cell Biol* 15, 6188-6195
184 Erickson, J.R.*, et al.* (1998) Edg-2/Vzg-1 couples to the yeast pheromone response pathway selectively in response to lysophosphatidic acid. *J Biol Chem* 273, 1506-1510
185 Klein, C.*, et al.* (1998) Identification of surrogate agonists for the human FPRL-1 receptor by autocrine selection in yeast. *Nat Biotechnol* 16, 1334-1337
186 Sachpatzidis, A.*, et al.* (2003) Identification of allosteric peptide agonists of CXCR4. *J Biol Chem* 278, 896-907
187 Zhang, W.B.*, et al.* (2002) A point mutation that confers constitutive activity to CXCR4 reveals that T140 is an inverse agonist and that AMD3100 and ALX40-4C are weak partial agonists. *J Biol Chem* 277, 24515-24521
188 Sommers, C.M.*, et al.* (2000) A limited spectrum of mutations causes constitutive activation of the yeast alpha-factor receptor. *Biochemistry* 39, 6898-6909
189 Matsumura, I. and Ellington, A.D. (2002) Mutagenic polymerase chain reaction of protein-coding genes for in vitro evolution. *Methods Mol Biol* 182, 259-267
190 Matsumaura, I. and Ellington, A.D. (2001) Mutagenic PCR of Protein-Coding Genes for In Vitro Evolution. In *Methods in Molecular Biology* (Braman, J., ed), pp. 261-268, Humana Press Inc.
191 Kim, H.*, et al.* (2009) Identification of Specific Transmembrane Residues and Ligand-Induced Interface Changes Involved In Homo-Dimer Formation of a Yeast G Protein-Coupled Receptor. *Biochemistry* 48, 10976-10987
192 McGlennen, R.C.*, et al.* (1992) Cellular transformation by a unique isolate of human papillomavirus type 11. *Cancer Res* 52, 5872-5878
193 Burns, A.R.*, et al.* (2000) Analysis of tight junctions during neutrophil transendothelial migration. *J Cell Sci* 113 (Pt 1), 45-57
194 Gainor, J.P.*, et al.* (2001) Platelet-conditioned medium increases endothelial electrical resistance independently of cAMP/PKA and cGMP/PKG. pp. H1992-2001

195 Kataoka, N., *et al.* (2002) Measurements of endothelial cell-to-cell and cell-to-substrate gaps and micromechanical properties of endothelial cells during monocyte adhesion. *Proceedings of the National Academy of Sciences of the United States of America* 99, 15638-15643
196 Choi, C.K., *et al.* (2007) An endothelial cell compatible biosensor fabricated using optically thin indium tin oxide silicon nitride electrodes. *Biosensors and Bioelectronics* 22, 2585-2590
197 Cannon, M.L. and Cesarman, E. (2004) The KSHV G protein-coupled receptor signals via multiple pathways to induce transcription factor activation in primary effusion lymphoma cells. *Oncogene* 23, 514-523
198 Sherrill, J.D., *et al.* (2009) Activation of Intracellular Signaling Pathways by the Murine Cytomegalovirus G Protein-Coupled Receptor M33 Occurs via PLC-beta/PKC-Dependent and -Independent Mechanisms. *Journal of Virology* 83, 8141-8152
199 Son, C.D., *et al.* (2004) Identification of ligand binding regions of the Saccharomyces cerevisiae alpha-factor pheromone receptor by photoaffinity cross-linking. *Biochemistry* 43, 13193-13203
200 Ferlay, J., *et al.* (2007) Estimates of the cancer incidence and mortality in Europe in 2006. *Ann Oncol* 18, 581-592
201 Cordon-Cardo, C. (1995) Mutations of cell cycle regulators. Biological and clinical implications for human neoplasia. *The American journal of pathology* 147, 545-560
202 Inoue, A. and Nukiwa, T. (2005) Gene mutations in lung cancer: promising predictive factors for the success of molecular therapy. *PLoS medicine* 2, e13
203 Latchman, D.S. (1996) Transcription-factor mutations and disease. *The New England journal of medicine* 334, 28-33
204 Guardavaccaro, D. and Pagano, M. (2004) Oncogenic aberrations of cullin-dependent ubiquitin ligases. *Oncogene* 23, 2037-2049
205 Giaever, I. and Keese, C.R. (1984) Monitoring fibroblast behavior in tissue culture with an applied electric field. *Proceedings of the National Academy of Sciences of the United States of America* 81, 3761-3764
206 Giaever, I. and Keese, C.R. (1986) Use of Electric Fields to Monitor the Dynamical Aspect of Cell Behavior in Tissue Culture. *Biomedical Engineering, IEEE Transactions on* BME-33, 242-247
207 Gainor, J.P., *et al.* (2001) Platelet-conditioned medium increases endothelial electrical resistance independently of cAMP/PKA and cGMP/PKG. pp. H1992-2001
208 Giaever, I. and Keese, C.R. (1991) Micromotion of mammalian cells measured electrically. *Proceedings of the National Academy of Sciences of the United States of America* 88, 7896-7900
209 Giaever, I. and Keese, C.R. (1993) Micromotion of mammalian cells measured electrically (Correction). *Proceedings of the National Academy of Sciences of the United States of America* 90, 1634
210 Choi, C.K., *et al.* (2007) Simultaneous dynamic optical and electrical properties of endothelial cell attachment on indium tin oxide bioelectrodes. *Journal of Biomedical Optics* 12, 64028

211 Bonifacino, J.S. and Dell'Angelica, E.C. (2001) Immunoprecipitation. *Curr Protoc Cell Biol* Chapter 7, Unit 7 2
212 Richmond, A. and Thomas, H.G. (1988) Melanoma growth stimulatory activity: isolation from human melanoma tumors and characterization of tissue distribution. *J Cell Biochem* 36, 185-198
213 Francis, J.L.*, et al.* (1998) Hemostasis and malignancy. *Semin Thromb Hemost* 24, 93-109
214 Tobler, A.*, et al.* (1993) Constitutive expression of interleukin-8 and its receptor in human myeloid and lymphoid leukemia. *Blood* 82, 2517-2525
215 Kollmar, O.*, et al.* (2006) Macrophage inflammatory protein-2 promotes angiogenesis, cell migration, and tumor growth in hepatic metastasis. *Ann Surg Oncol* 13, 263-275
216 Luan, J.*, et al.* (1997) Mechanism and biological significance of constitutive expression of MGSA/GRO chemokines in malignant melanoma tumor progression. *J Leukoc Biol* 62, 588-597
217 Norgauer, J.*, et al.* (1996) Expression and growth-promoting function of the IL-8 receptor beta in human melanoma cells. *J Immunol* 156, 1132-1137
218 Li, S.*, et al.* (2005) Overexpression of G protein-coupled receptors in cancer cells: involvement in tumor progression. *Int J Oncol* 27, 1329-1339
219 Gether, U. (2000) Uncovering molecular mechanisms involved in activation of G protein-coupled receptors. *Endocr Rev* 21, 90-113
220 Ghosh, S.*, et al.* (1998) NF-kappa B and Rel proteins: evolutionarily conserved mediators of immune responses. *Annu Rev Immunol* 16, 225-260
221 Gietz, R.D.*, et al.* (1995) Studies on the transformation of intact yeast cells by the LiAc/SS-DNA/PEG procedure. *Yeast* 11, 355-360
222 Wang, D.*, et al.* (2000) MGSA/GRO-mediated melanocyte transformation involves induction of Ras expression. *Oncogene* 19, 4647-4659
223 Masi, T.*, et al.* (2005) Nitrosamine 4-(methyinitrosamino)-1-(3-pyridyl)-1 butanone-induced pulmonary adenocarcinomas in Syrian golden hamsters contain beta 2-adrenergic receptor single-nucleotide polymorphisms. *Genes Chromosomes & Cancer* 44, 212-217
224 Taylor, W.R. (2004) FACS-based detection of phosphorylated histone H3 for the quantitation of mitotic cells. *Methods Mol Biol* 281, 293-299
225 Jainchill, J.L.*, et al.* (1969) Murine sarcoma and leukemia viruses: assay using clonal lines of contact-inhibited mouse cells. *J Virol* 4, 549-553
226 Colburn, N.H.*, et al.* (1978) Correlation of anchorage-independent growth with tumorigenicity of chemically transformed mouse epidermal cells. *Cancer Res* 38, 624-634
227 Garcia, M.*, et al.* (1990) Overexpression of transfected cathepsin D in transformed cells increases their malignant phenotype and metastatic potency. *Oncogene* 5, 1809-1814
228 Broad, L.M.*, et al.* (2001) Role of the phospholipase C-inositol 1,4,5-trisphosphate pathway in calcium release-activated calcium current and capacitative calcium entry. *J Biol Chem* 276, 15945-15952

229 Sherrill, J.D., *et al.* (2009) Activation of intracellular signaling pathways by the murine cytomegalovirus G protein-coupled receptor M33 occurs via PLC-{beta}/PKC-dependent and -independent mechanisms. *J Virol* 83, 8141-8152
230 Faruqi, T.R., *et al.* (2001) Rac1 mediates STAT3 activation by autocrine IL-6. *Proc Natl Acad Sci U S A* 98, 9014-9019
231 Michell, R.H. (1975) Inositol phospholipids and cell surface receptor function. *Biochim Biophys Acta* 415, 81-47
232 Hokin, L.E. (1985) Receptors and phosphoinositide-generated second messengers. *Annu Rev Biochem* 54, 205-235
233 Meldrum, E., *et al.* (1991) The PtdIns-PLC superfamily and signal transduction. *Biochim Biophys Acta* 1092, 49-71
234 Wu, D., *et al.* (1993) Activation of phospholipase C beta 2 by the alpha and beta gamma subunits of trimeric GTP-binding protein. *Proc Natl Acad Sci U S A* 90, 5297-5301
235 Jhon, D.Y., *et al.* (1993) Cloning, sequencing, purification, and Gq-dependent activation of phospholipase C-beta 3. *J Biol Chem* 268, 6654-6661
236 Park, D., *et al.* (1993) Activation of phospholipase C isozymes by G protein beta gamma subunits. *J Biol Chem* 268, 4573-4576
237 Labarca, R., *et al.* (1984) Phorbol esters inhibit agonist-induced [3H] inositol-1-phosphate accumulation in rat hippocampal slices. *Biochem Biophys Res Commun* 123, 703-709
238 Rhee, S.G., *et al.* (1989) Studies of inositol phospholipid-specific phospholipase C. *Science* 244, 546-550
239 Andl, C.D., *et al.* (2004) EGFR-induced cell migration is mediated predominantly by the JAK-STAT pathway in primary esophageal keratinocytes. *Am J Physiol Gastrointest Liver Physiol* 287, G1227-1237
240 Schraufstatter, I.U., *et al.* (2003) IL-8-mediated cell migration in endothelial cells depends on cathepsin B activity and transactivation of the epidermal growth factor receptor. *J Immunol* 171, 6714-6722
241 Casarosa, P., *et al.* (2001) Constitutive signaling of the human cytomegalovirus-encoded chemokine receptor US28. *J Biol Chem* 276, 1133-1137
242 Waldhoer, M., *et al.* (2002) Murine cytomegalovirus (CMV) M33 and human CMV US28 receptors exhibit similar constitutive signaling activities. *J Virol* 76, 8161-8168
243 Berchiche, Y.A., *et al.* (2007) Direct assessment of CXCR4 mutant conformations reveals complex link between receptor structure and G(alpha)(i) activation. *J Biol Chem* 282, 5111-5115
244 Bakker, R.A., *et al.* (2004) Constitutively active Gq/11-coupled receptors enable signaling by co-expressed G(i/o)-coupled receptors. *J Biol Chem* 279, 5152-5161
245 Sherrill, J.D. and Miller, W.E. (2006) G protein-coupled receptor (GPCR) kinase 2 regulates agonist-independent Gq/11 signaling from the mouse cytomegalovirus GPCR M33. *J Biol Chem* 281, 39796-39805
246 Billstrom, M.A., *et al.* (1998) Intracellular signaling by the chemokine receptor US28 during human cytomegalovirus infection. *J Virol* 72, 5535-5544

247 Wong, L. and Johnson, G.R. (1996) Epidermal growth factor induces coupling of protein-tyrosine phosphatase 1D to GRB2 via the COOH-terminal SH3 domain of GRB2. *J Biol Chem* 271, 20981-20984
248 Leaman, D.W.*, et al.* (1996) Roles of JAKs in activation of STATs and stimulation of c-fos gene expression by epidermal growth factor. *Mol Cell Biol* 16, 369-375
249 Konopka, J.B.*, et al.* (1996) Mutation of Pro-258 in transmembrane domain 6 constitutively activates the G protein-coupled alpha-factor receptor. *Proc Natl Acad Sci U S A* 93, 6764-6769
250 Zetter, B.R. (1993) Adhesion molecules in tumor metastasis. *Semin Cancer Biol* 4, 219-229
251 Takeichi, M. (1988) The cadherins: cell-cell adhesion molecules controlling animal morphogenesis. *Development* 102, 639-655
252 Gumbiner, B.M. (2000) Regulation of cadherin adhesive activity. *J Cell Biol* 148, 399-404
253 Rothlein, R.*, et al.* (1986) A human intercellular adhesion molecule (ICAM-1) distinct from LFA-1. *J Immunol* 137, 1270-1274
254 Yang, L.*, et al.* (2005) ICAM-1 regulates neutrophil adhesion and transcellular migration of TNF-alpha-activated vascular endothelium under flow. *Blood* 106, 584-592
255 Vainio, O.*, et al.* (1996) HEMCAM, an adhesion molecule expressed by c-kit+ hemopoietic progenitors. *J Cell Biol* 135, 1655-1668
256 Bardin, N.*, et al.* (2001) Identification of CD146 as a component of the endothelial junction involved in the control of cell-cell cohesion. *Blood* 98, 3677-3684
257 Okumura, S.*, et al.* (2001) Involvement of gicerin in the extension of microvilli. *Exp Cell Res* 271, 269-276
258 Guezguez, B.*, et al.* (2007) Dual role of melanoma cell adhesion molecule (MCAM)/CD146 in lymphocyte endothelium interaction: MCAM/CD146 promotes rolling via microvilli induction in lymphocyte and is an endothelial adhesion receptor. *J Immunol* 179, 6673-6685

APPENDIX

Constitutive Activity of Other CXCR2 Mutants in the Yeast

Introduction

As shown in part 4, genetically modified yeast encoding a part of mammalian Gα protein sequence was used to screen a CAMs and the b glactosidase activity was used to measure the degree of constitutive activity. This appendix presents data for other CXCR2 mutants that we generated including single point mutations, such as D9E, D9A, D9S and D9Y. Deletion mutants that delete only the single D9 residue (ΔD9) and truncation mutants, such as Tru D9 truncate up to the 8^{th} residue (serine), Tru S10 truncated through the 9^{th} residue (aspartic acid) and Tru C39 truncated to 38^{th} residue (proline), which leaves the cysteine residue intact.

Materials and methods

The experimental procedures are same as described in part 4 of chapter 3.

Results

All mutants show very similar activity when compared with WTCXCR2 (Figure 24) except for D9A and D9Y albeit these mutants were much lower than the positive control, D143V. These data show that not all mutations/truncations within CXCR2 lead to constitutive activity in yeast. The next question that we wanted to address is whether the lack of constitutive activity in these mutants is also found in mammalian cells.

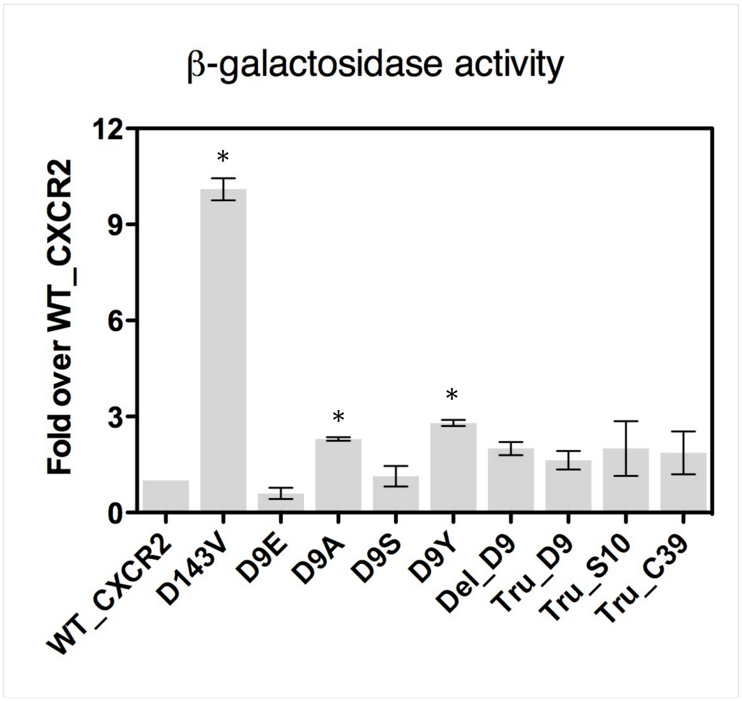

Figure 23. Constitutive activity of CXCR2 mutants measured via β-galactosidase activity in yeast.

Yeast strain, CY1141, contains the plasmid, pMD1325, which has the *lacZ* under the control of the pheromone responsive promoter. β-galactosidase activity was measure using the yeast β-galactosidase assay kit (Pierce) and represented in Miller units. Bars represent the average of three independent experiments plus/minus their standard deviation. Student's t-test (PRISM(ver. 5.0b) was used to determine statistical significance (*; $p \leq 0.05$).

CXCR2 Mutants mediated Cellular Transformation

Introduction

As shown in Chapter 4, CXCR2 CAMs differentially induced foci formation and anchorage-independent growth. This appendix presents the data about foci formation and soft-agar growth assays for other CXCR2 mutants. In addition to the mutations described early in this appendix, proline mutants, P266L and P266L/Y267L, were generated based on evidence from Konopka et al that showed mutations of residues Pro-258 and the adjacent Ser-259 to Leu leads to constitutive activity [1].

Materials and Methods

The experimental procedures are the same as in part 4 of chapter 3.

Results

Foci formation and growth in soft agar were used as indicators of cellular transformation (Figure 24). As shown in Figure 24-A, only proline mutant, P266L, formed statistically significant ($p<0.05$) number of foci (approx. 55 foci) compared with WT_CXCR2, which indicates that the proline residue in TM6 plays an important role in maintaining CXCR2 in an inactive status. However, double mutant, P266L/Y267L, was not significantly different from WT_CXCR2. This differs with previous data from Ste2p_P258L/S256L, which increased CA over 90% based on a β-galatosidase assay [1]. This could be due to the differences in these receptors, the different readouts (β-galatosidase assay vs foci formation) or the different cell types (yeast vs mammalian).

The soft-agar growth assay (Figure 24-B) demonstrated that deletion mutant, ΔD9, was much greater than background ($p<0.05$) number of colony (20 colonies) albeit much lower than our previously described CXCR2 CAM. All other mutants were not greater than WT_CXCR2 indicating they do not lead to constitutive activity.

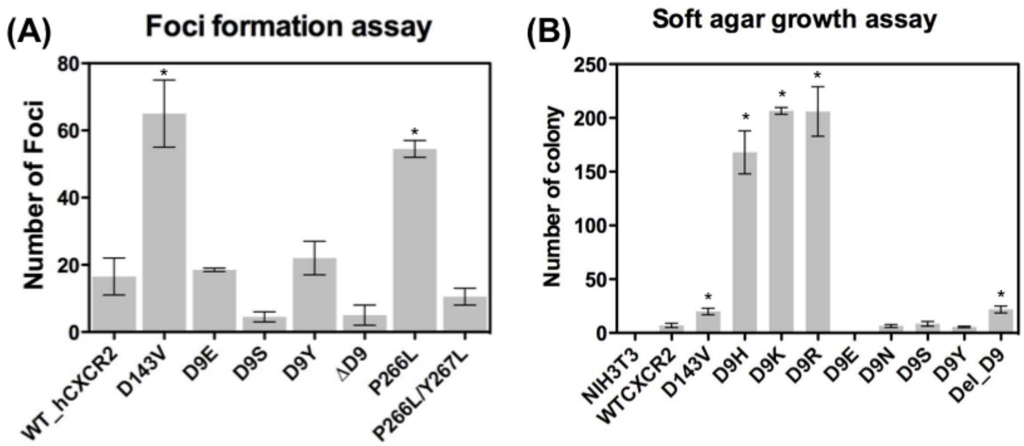

Figure 24. CXCR2s CAMs lead to differential foci formation and anchorage independent growth.

As a measure of their ability to transform cells, foci formation (A) and anchorage-independent growth (B) of stably transfected NIH3T3 cells expressing WT_CXCR2 or CXCR2 mutants in the presence of CXCR2 antagonist (SB225002, 1 μM) were measured. Bars represent the average of three independent experiments +/- standard deviation. Student's *t*-test (*PRISM (version 5.0b)* was used to determined statistical significance versus CXCR2_WT (*; $p<0.05$).

CXCR2 Mutants and Ligand Binding

Introduction

To address whether the mutations in CXCR2 eliminated ligand binding, a competition binding assay was performed to measure relative binding affinity.

Materials and Methods

Transiently transfected Cos-7 cells were seeded in a 48-well plate. At 48 hours post transfection, binding was performed on whole cells for 3 to 4 h at 4 ^{o}C with^{125}I-IL-8 in a binding buffer (50mM HEPES (pH7.4), 1mM CaCl2, 5mM MgCl2, 0.5% bovine serum albumin). After incubation, cells were washed four times with ice-cold binding buffer supplemented with 0.5M NaCl. Cells were collected and counted in a Wallac Compugamma counter.

Result

All mutants except for the E198A and the double mutants used for other experiments showed normal binding. This shows that the CXCR2 CAMs did not alter binding to ligands and the alteration in conformation that leads to constitutive activity does not affect the binding pocket. We have also carried out our transformation assays in presence of ligands and saw no increase in foci or colony formation (data not shown).

IL-8 Binding Assay

[radioligand] = 0.2-0.4 nM

Receptor	IC_{50} CXCL8	n
WT	8.92 ± 0.05	8
ΔD9	9.01 ± 0.06	4
D9A	no binding	2
D9E	no binding	4
D9H	8.73 ± 0.09	7
D9K	8.56 ± 0.05	2
D9N	8.75 ± 0.18	3
D9R	8.69 ± 0.21	3
D9S	8.71 ± 0.06	3
D9Y	8.81 ± 0.16	4
E198A	no binding	4
D199A	8.82 ± 0.20	4
E198A/D199A	no binding	4
D9K/E198A	no binding	1
D9K/D199A	no binding	1
D9K/E198A/D199A	no binding	1
D143V	9.28 ± 0.06	4
R144A	9.13 ± 0.11	4
$II^{250-251}_{ins}$	8.65 ± 0.14	3

CXCR2 CAM induction of Tumor Formation *in vivo*

Introduction

To address whether CXCR2_CAMs induce tumor formation *in vivo,* transfectants were injected into the hind flanks of mice and the size of the tumor was measured over time. Stable NIH3T3 transfectants were inoculated into *nu/nu* mice (Jackson Laboratory) and Melan-a transfectants into C57BL6 mice (Jackson Laboratory). The Melan-a cell line is a prototype of melanocytes and was originally derived from C57/BL6 mice [2]. These transfectants were generated to model melanoma development and allowed us to assess tumor development in the context of an immune competent mouse.

Materials and Methods

CXCR2 stable transfectants or untransfected controls (2×10^5/mice) were injected subcutaneously into the flanks of 6 to 8 wk old *nu/nu* mice (Jackson Laboratory) and C57BL6 mice (Jackson Laboratory). Tumor size was measured using a digital caliper. The protocol for animal experiment was reviewed and approved by the Institutional Animal Care and Concerns Committee of the University of Tennessee.

Results

Our data shows that even WT_CXCR2 can form tumors *in vivo*. This could be do to ligand engagement of the WT_CXCR2 receptor that contributes to tumor growth. The *in vivo* administration of the CXCR2 inhibitor SB225002 did not alter the growth of the tumors. There are multiple reasons for this. First, there is no information about the bioavailability of this small molecule inhibitor. Second, there is the possibility that once these cells have become transformed, they no longer need ligand stimulation. There are several other possibilities for this negative outcome. In the initial experiments using the Melan-A transfectants only the D9N transfectant consistently formed tumors (Figure 29). In the repeat experiment the D9N transfectants still showed significant tumor growth, but due to tumor growth in some of the mice inoculated with untransfected controls, these data are not significantly different (Figure 30). Although these experiments have led to confusing results, there is a definite trend towards D9N CXCR2 Melan-a transfectants leading to tumor growth. If we are able to definitively demonstrate this, it could mean that the D9N CXCR2 conformation stimulates signaling pathways that contribute to tumor growth in this cell line while the other CXCR2 CAMs do not. Only after further experimentation will we be able to make this conclusion.

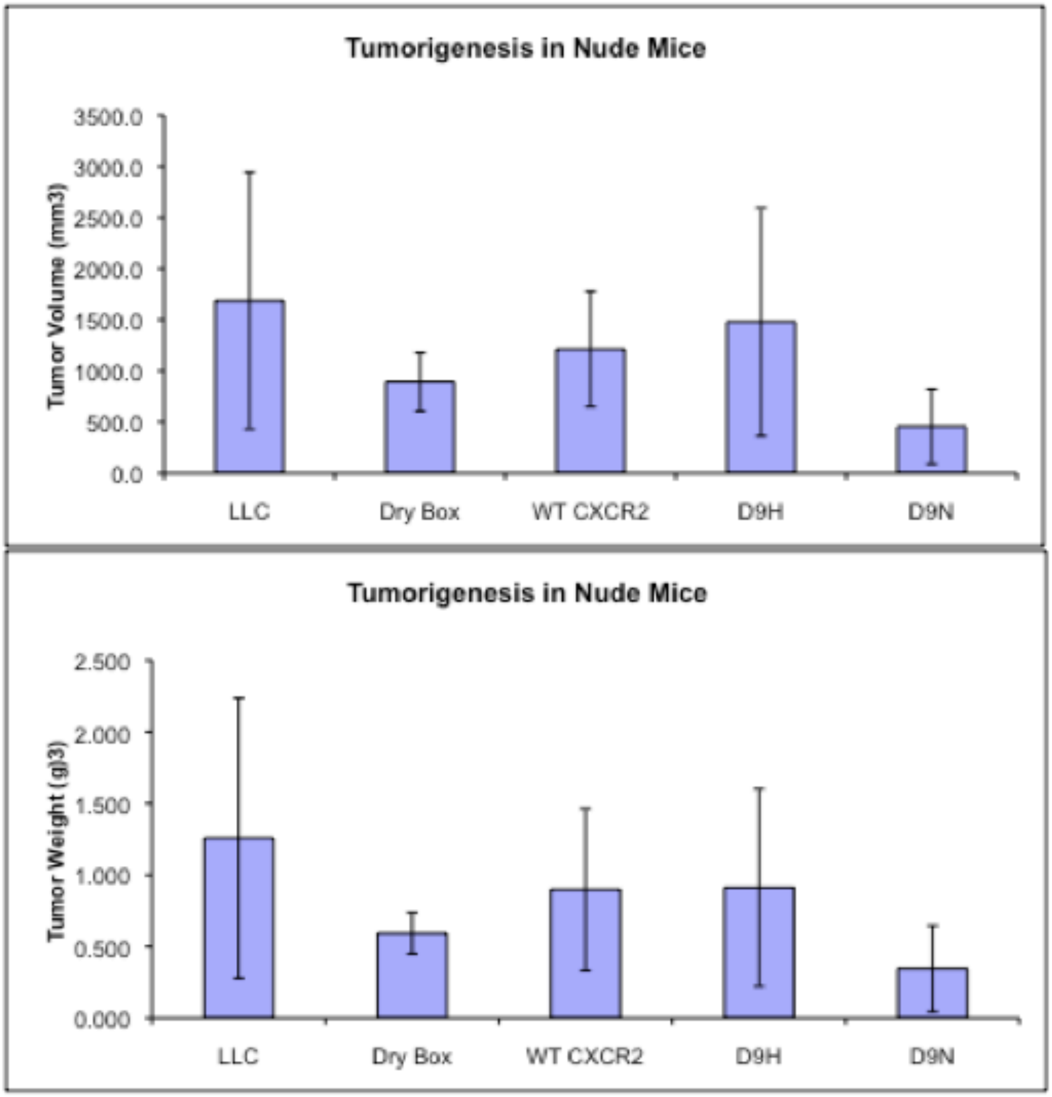

Figure 25. Differential tumor formation in *nu/nu* mouse.

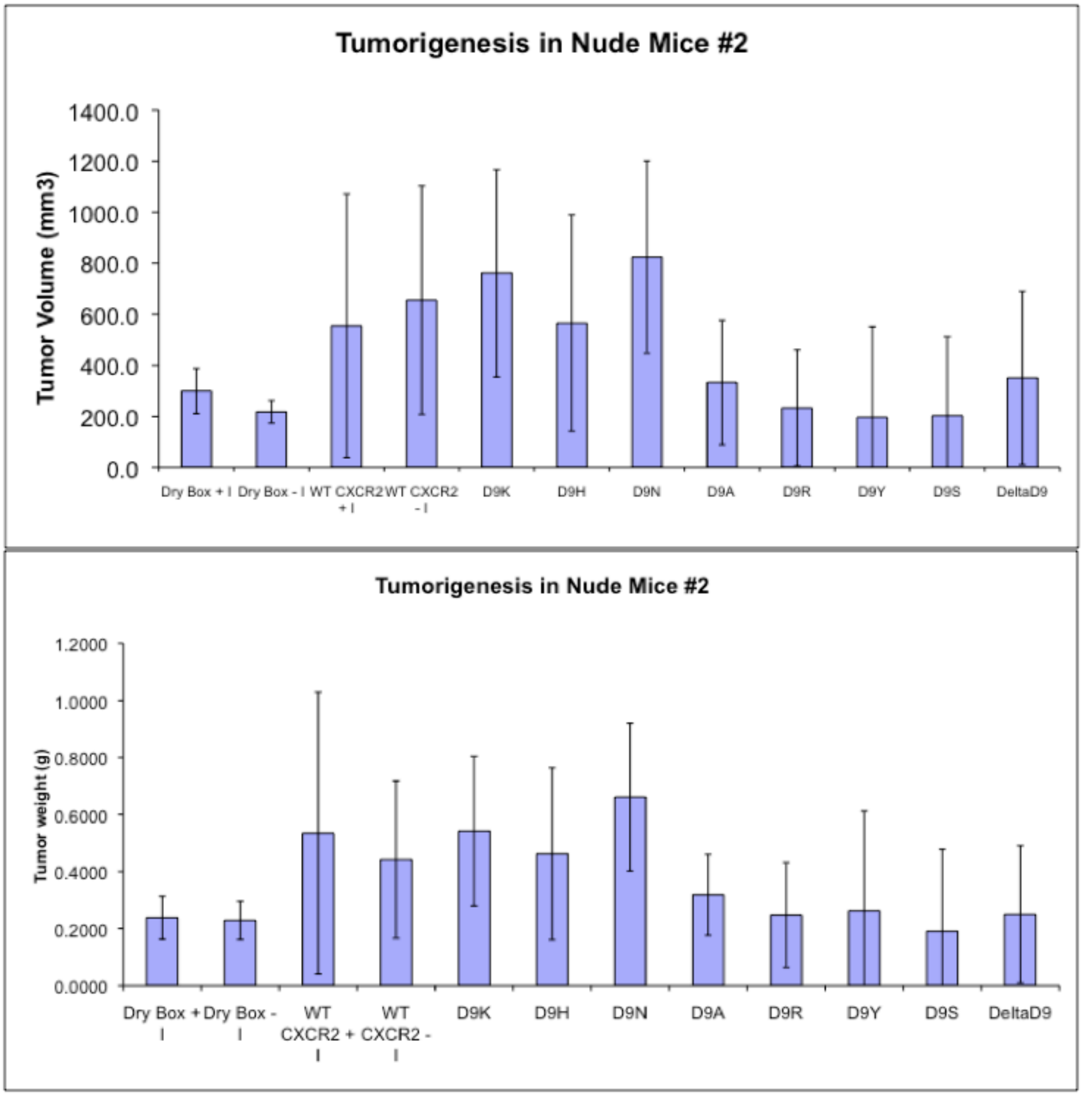

Figure 26. Differential tumor formation in *nu/nu* mouse.

In a similar experiment, nu/nu mice were injected and some of the mice were also injected with the CXCR2 inhibitor (I), SB225002, (1 mg/kg, i.p.) once per a week.

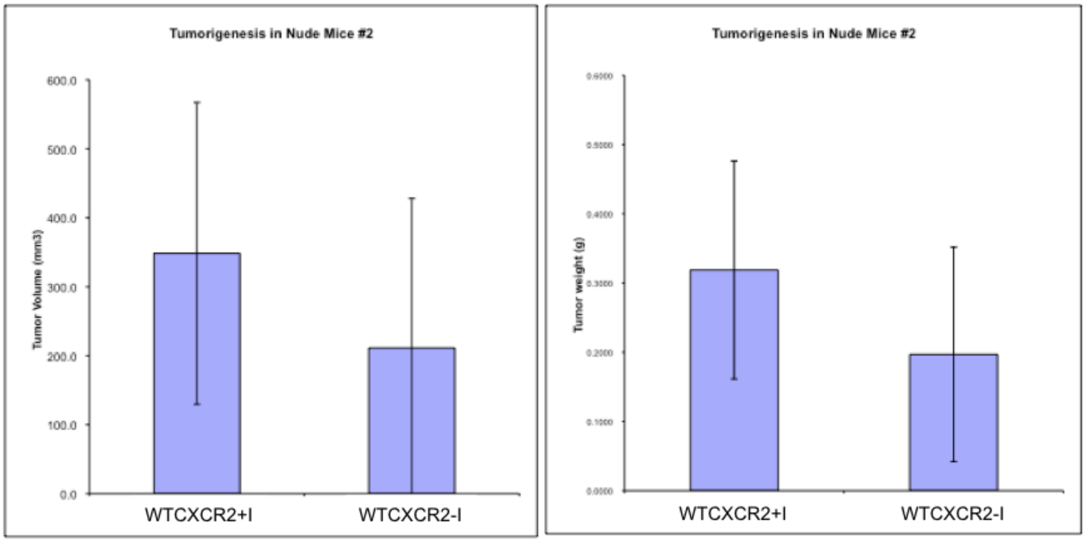

Figure 27. Effect of SB225002 for tumor formation in *nu/nu* mice

Note: WT CXCR2+I represents CXCR2 inhibitor, SB225002, injection into the mouse (1 mg/kg, i.p.) once per week for the duration of the experiment.

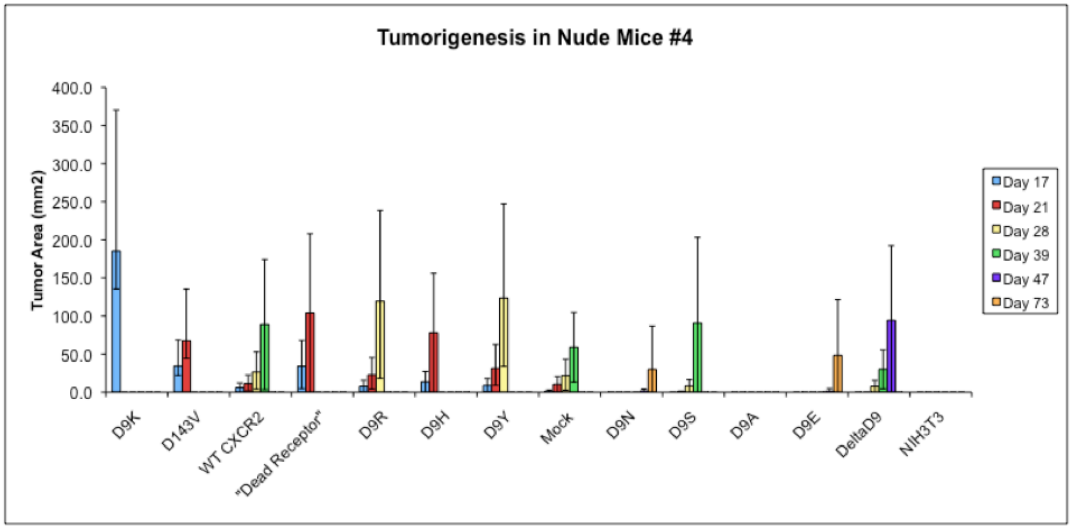

Figure 28. Differential tumor growth in *nu/nu* mice over time.

Weekly the size of the tumor (length x width) was measured. Bars represent the average size of the tumors +/- standard deviation. Note: A “Dead Receptor”, CXCR2_R144A, was used as an additional negative control. This receptor can not respond to ligand.

Transfectant	Number of mice with tumors	Days post inoculation
LLC	5/5	22
D9N	5/5	59
D9H	1/5	88
WTCXCR2	1/5	88
Untransfected	2/5	88

Figure 29. D9N_CXCR2 transfectant leads to a more robust and early tumor formation in BL6 mice.

After inoculation, whole groups of mice were removed from the study when one mouse in group had a tumor size greater than 1.5 cm. At the time of euthanization, the tumor size was measured.

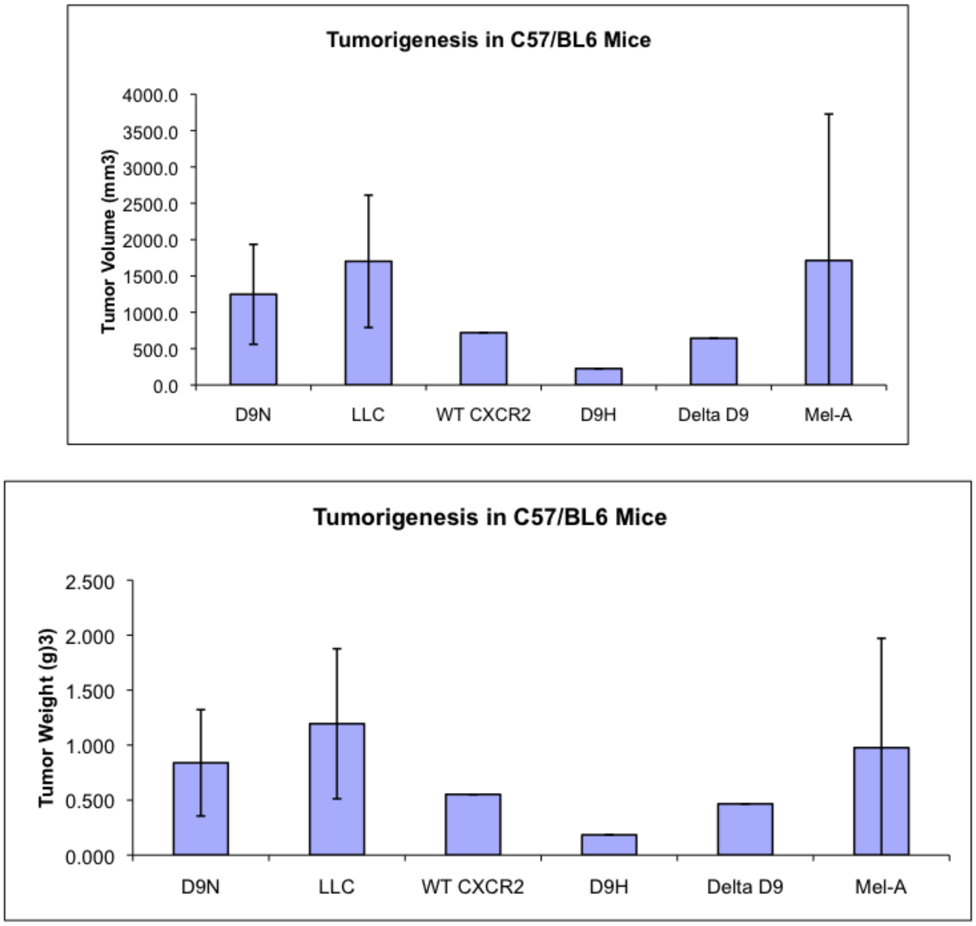

Figure 30. Differential tumor formation in *C57/BL6* mice.

In a repeat experiment, tumor volume was measured. Bars represent the average tumor volume +/- standard deviation.

Establishment of Stable Cancer Cell Lines Overexpressing wild type CXCR2 and CXCR2 Mutants

Introduction

As shown in part 4, mouse fibroblast cell line, NIH3T3, is a common cell line used to address the cellular transformation potential of a protein. Both foci formation and soft-agar growth assays show their relative transformed state. However, in order to assess the real potential of CXCR2 CAMs in cancer development, these proteins need to be analyzed in a real cancer environment. Therefore, we established stable cell lines that express WT_CXCR2 and CXCR2 CAMs in human adenocarcinoma cells, A549, and androgen independent and highly metastatic prostate cancer cell line, PC-3.

Materials and methods

The experimental procedures are same as described in part 4 of chapter 3.

Results

FACs analysis of stable cancer cell lines expressing WT_CXCR2 and CXCR2 CAMS shows equal expression in both lines (Figure 25). Clones were selected and used in our different assays.

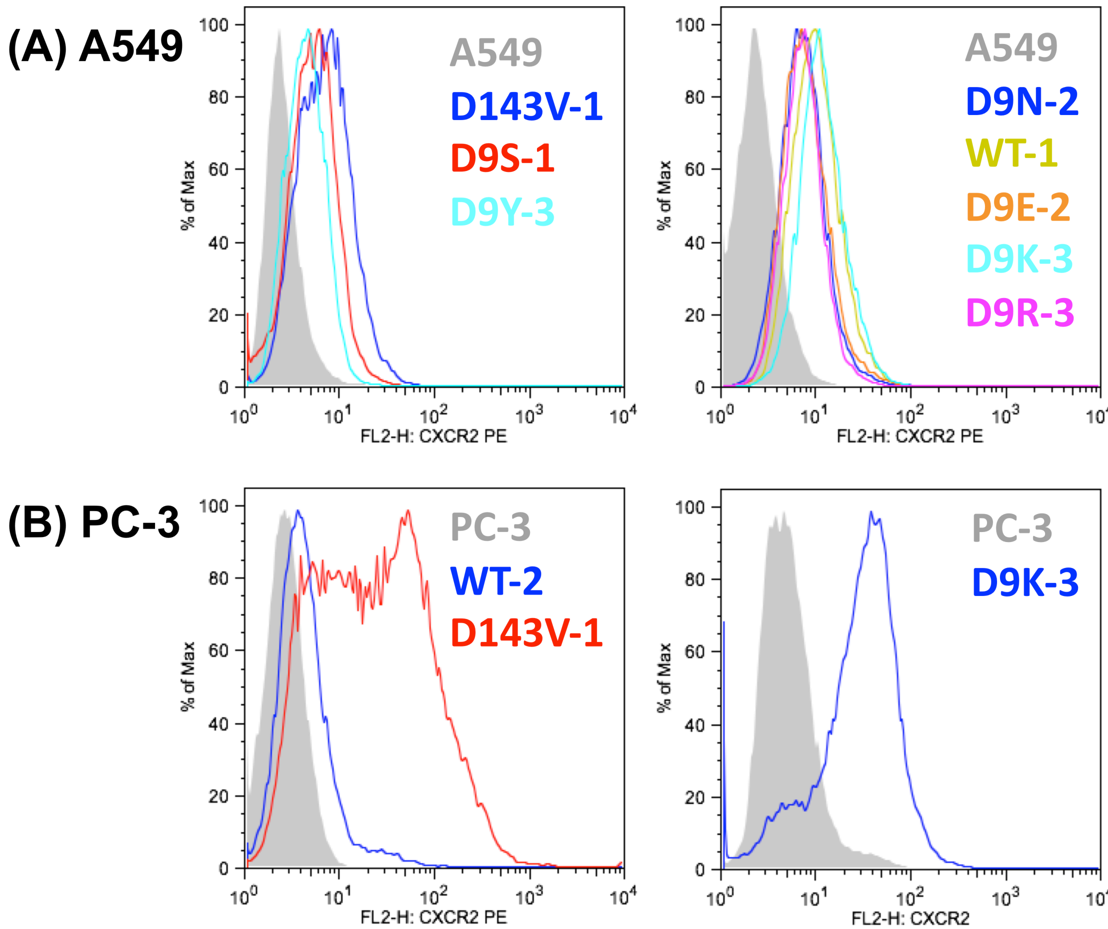

Figure 31. CXCR2 surface expression on stable transfectants.

Stable A549 and PC-3 transfectants were selected and stained with PE conjugated CXCR2 specific antibody (R&D Systems, Cat.No. FAB331P).

Differential Adhesion Molecule Expression in A549 stable lines

In order for cancers to metastasize, cancer cells may lose and/or gain adhesive interactions in order to spread throughout the body. Adhesion molecules, such as cadherins and cell adhesion molecules (CAMs), play an important role the metastatic process [248]. The cadherins are membrane glycoproteins that function in adherence in a calcium-dependent manner [249, 250]. One of the cadherins, E-cadherin, is expressed on epithelial cells and maintains intracellular adhesion, so E-cadherin reversely correlates with cancer cell metastasis [248]. Intercellular adhesion molecule-1 (ICAM-1) is the ligand for LFA-1, an integrin found on leukocytes [251]. Activation of ICAM-1 induces leukocyte binding to the endothelium through ICAM-1/LFA-1 interaction eventually leading to transmigration into tissues [252]. MCAM is a melanoma cell adhesion molecule and is used as a marker of the endothelial lineage [253]. MCAM is associated actin cytoskeletal rearrangements and plays a role in cell-cell adhesion [254-256]. In order to address the role of CXCR2 stimulation in cancer metastasis, our CXCR2 expressing A549 stable cell lines were stimulated with the CXCR2 ligand, Gro-α, and the levels of different adhesion molecules were measured.

Materials and Methods

To observe the changes in adhesion molecule expression, A549 and A549 transfectants expressing either WT_CXCR2 or CXCR2_D9N were either serum starved for 24 hours or starved and then stimulated with Gro-α (10nM) for the final four hours. Harvested cells were stained with specific antibodies for ICAM, MCAM, or N-cadherin (BD Biosciences). After staining, cells were washed, fixed and analyzed using a FACs Calibur (BD Biosciences).

Results

A549 cell lines express CXCR1 but not CXCR2 but expression (Dr. Masi, personal communication). Stable lines were stimulated with Gro-α as it only stimulates CXCR2. The levels of adhesion molecule expression was measured via flowcytometry as shown in Figure 26. ICAM is up regulated upon serum starvation but down regulated upon Gro-α stimulation. In contrast, MCAM is only upregulated in the CXCR2_D9N stimulated with Gro-α. E-Cadherin is upregulated equally throughout. This demonstrates that over-expression and stimulation of WT or D9N_CXCR2_ in adenocarcinomas can affect cellular adhesion molecule expression that could relate to their metastatic ability.

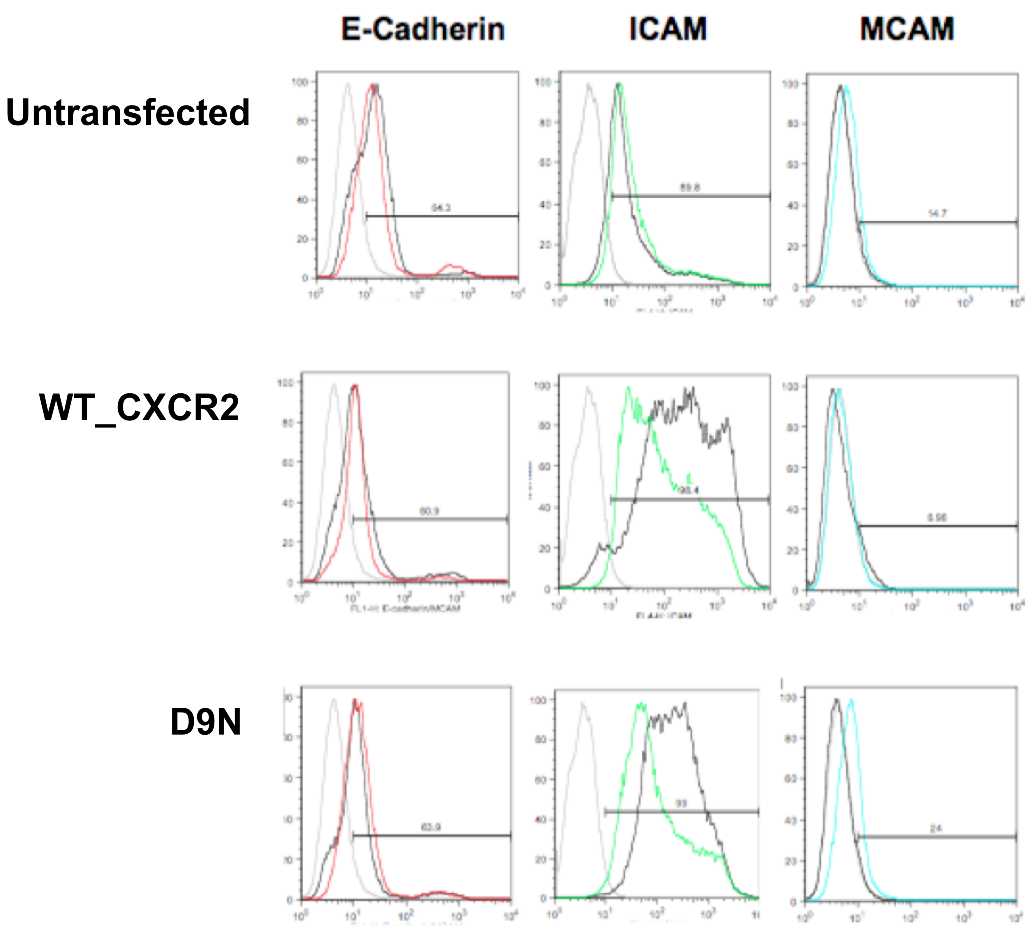

Figure 32. Alteration of adhesion molecule expression in CXCR2 expressing A549 stable lines upon exposure to Gro-α.

A549 lung cancer line transfectants were serum starved for 24 hours and then stimulated with Gro-α (10nM) or mock for the final four hours. Cells were then stained with the directly conjugated antibodies against the adhesion molecules listed above. Colored lines are Gro-α stimulated, black lines are serum starved alone, and gray lines are unstained controls.

VITA

Giljun Park was born in Seoul, Korea on January 22, 1975. He entered the Yonsei University, Seoul, Korea, in March 1993 and graduated with a Bachelor degree in Biology in February 2000. He started his graduate study at the Seoul National University in 1999 and graduated his master-thesis program in Oceanography in 2003. In January of 2004, he entered Graduate School at the University of Tennessee in Microbiology. Throughout the course of his time in this program, he served as a Graduate Teaching Assistant (2004-2007 and 2010) and as a Graduate Research Assistant (2008-2009). He officially received a Doctor of Philosophy degree in Microbiology in December 2010.